



**HAL**  
open science

# Role of vSNAREs in post-synaptic AMPAR trafficking, glutamatergic transmission and plasticity

May Bakr

► **To cite this version:**

May Bakr. Role of vSNAREs in post-synaptic AMPAR trafficking, glutamatergic transmission and plasticity. *Neurons and Cognition [q-bio.NC]*. Université de Bordeaux, 2020. English. NNT : 2020BORD0323 . tel-03229524

**HAL Id: tel-03229524**

**<https://theses.hal.science/tel-03229524>**

Submitted on 19 May 2021

**HAL** is a multi-disciplinary open access archive for the deposit and dissemination of scientific research documents, whether they are published or not. The documents may come from teaching and research institutions in France or abroad, or from public or private research centers.

L'archive ouverte pluridisciplinaire **HAL**, est destinée au dépôt et à la diffusion de documents scientifiques de niveau recherche, publiés ou non, émanant des établissements d'enseignement et de recherche français ou étrangers, des laboratoires publics ou privés.



THÈSE PRÉSENTÉE  
POUR OBTENIR LE GRADE DE

**DOCTEUR DE  
L'UNIVERSITÉ DE BORDEAUX**

ÉCOLE DOCTORALE DES SCIENCES DE LA VIE ET DE LA SANTÉ  
SPÉCIALITÉ NEUROSCIENCES

Par **May BAKR**

**Role of vSNAREs in post-synaptic AMPAR trafficking,  
glutamatergic transmission and plasticity**

Sous la direction de : Dr. David PERRAIS

Soutenu le 15 Décembre 2020

**Membres du jury**

Dr. Stéphane OLIET	Directeur de Recherche CNRS	Président
Dr. Gunnar GOURAS	Professeur, Lund University, Suède	Examineur
Dr. Sabine LEVI	Directrice de Recherche CNRS	Rapportrice
Dr. Marie-Claude POTIER	Directrice de Recherche CNRS	Rapportrice



**Interdisciplinary Institute for NeuroSciences (IINS)**

CNRS UMR 5297

Université de Bordeaux Centre Broca Nouvelle-Aquitaine

146 Rue Léo Saignat

33076 Bordeaux (France)



## Résumé

La plasticité synaptique, c'est-à-dire la modification de la force synaptique en fonction de l'activité, est une caractéristique remarquable du système nerveux et a longtemps été considérée comme la base cellulaire de l'apprentissage et de la mémoire. Une forme bien caractérisée de plasticité synaptique est la potentialisation à long terme (PLT) de la transmission synaptique excitatrice dans les neurones pyramidaux de la région CA1 de l'hippocampe. La PLT nécessite le recrutement et la stabilisation rapides des récepteurs  $\alpha$ -amino-3-hydroxy-5-méthyl-4-isoxazolepropionate (AMPA) sur les sites postsynaptiques par le biais du trafic régulé et de l'exocytose des endosomes de recyclage (RE). L'exocytose est médiée par une famille de protéines appelées récepteurs de la protéine soluble d'attachement à la NSF (N-ethylmaleimide-sensitive fusion protein) ou SNARE. Ces protéines servent de médiateurs à la fusion membranaire en formant un complexe composé d'une R-SNARE, généralement sur une membrane, et de deux ou trois Q-SNARE, généralement sur l'autre membrane. La formation du complexe SNARE fournit une spécificité pour une fusion contrôlable comme celle proposée pour la première fois par Rothman et al en 1993. Les protéines SNARE ont été bien caractérisées pour leur fonction dans la fusion des vésicules présynaptiques lors de la libération des neurotransmetteurs. Cependant, leur rôle dans le trafic membranaire post-synaptique dépendant de l'activité, et en particulier le trafic des AMPAR, est resté peu clair jusqu'à récemment. Étant donné l'importance du recyclage somato-dendritique dans la physiologie neuronale, notre objectif était d'identifier les principaux acteurs de l'exocytose des RE dendritiques. Dans cette étude, nous identifions VAMP4 comme la principale protéine vésiculaire SNARE qui intervient dans la majorité des cas d'exocytose des RE dans les dendritiques. En revanche, VAMP2 ne joue qu'un rôle mineur, même si elle a été précédemment identifiée comme critique pour l'expression post-synaptique de la PLT. Le knockdown (KD) de VAMP4 réduit la fréquence d'exocytose du récepteur de la transferrine (TfR), un marqueur des ERs et un marqueur de substitution des voies de trafic de l'AMPA. Étonnamment, l'expression de la neurotoxine tétanique (TeNT), qui clive VAMP2, n'affecte pas l'exocytose du TfR. De plus, VAMP4 KD augmente la fraction d'AMPA à la surface de la cellule et son recyclage. Conformément à ce résultat, dans les tranches organotypiques d'hippocampe, le VAMP4 KD augmente l'amplitude des courants excitateurs post-synaptiques (EPSC) médiés par les AMPAR sans affecter les EPSC médiés par les NMDAR dans les neurones pyramidaux CA1. Enfin, VAMP4 KD réduit la PLT alors que TeNT la bloque totalement. Nos données suggèrent un modèle dans lequel l'absence de VAMP4 conduit à un mauvais tri des AMPAR à l'état basal vers la membrane plasmique, ce qui affecte le PLT, vraisemblablement par un mécanisme d'occlusion. De plus, les changements opposés des niveaux de TfR et d'AMPA à la surface des cellules sur la KD du VAMP4 suggèrent que ces récepteurs peuvent être triés et faire l'objet d'un trafic indépendamment. Nous proposons donc que VAMP4 et VAMP2 servent de médiateurs à des voies de trafic fonctionnellement distinctes et complémentaires qui modulent la force et la plasticité synaptiques.

**Mots clés :** synapse, plasticité synaptique récepteur AMPA, exocytose, SNARE, endosome de recyclage.



## Abstract

Synaptic plasticity, the activity-dependent modifications in synaptic strength, is a remarkable feature of the nervous system and has long been postulated as the cellular basis of learning and memory. A well-characterized form of synaptic plasticity is long-term potentiation (LTP) of excitatory synaptic transmission in CA1 hippocampal pyramidal neurons. LTP requires the fast recruitment and stabilization of  $\alpha$ -amino-3-hydroxy-5-methyl-4-isoxazolepropionate receptors (AMPA receptors) at postsynaptic sites via the regulated trafficking and exocytosis of recycling endosomes (REs). Exocytosis is mediated by a family of proteins called soluble NSF (N-ethylmaleimide-sensitive fusion protein) attachment protein receptors or SNAREs. These proteins mediate membrane fusion by forming a complex composed of one R-SNARE, usually on one membrane, and two or three Q-SNAREs, usually on the other membrane. The formation of the SNARE complex provides specificity for a controllable fusion as first proposed by Rothman et al in 1993. SNARE proteins have been well characterized for their function in presynaptic vesicle fusion during neurotransmitter release. However, their role in activity-dependent post-synaptic membrane trafficking, and particularly AMPAR trafficking, remained elusive until recently. Given the importance of somato-dendritic recycling in neuronal physiology, our goal was to identify major players of dendritic RE exocytosis. In this study, we identify VAMP4 as the key vesicular SNARE protein that mediates the majority of RE exocytosis in dendrites. In contrast, VAMP2 plays only a minor role even though it was previously identified as critical for the post-synaptic expression of LTP. The knockdown (KD) of VAMP4 reduces the exocytosis frequency of transferrin receptor (TfR), a marker of REs, and a surrogate marker of AMPAR trafficking pathways. Surprisingly, the expression of tetanus neurotoxin (TeNT), which cleaves VAMP2, does not affect TfR exocytosis. Moreover, VAMP4 KD enhances the fraction of AMPARs at the cell surface and its recycling. Consistent with this result, in organotypic hippocampal slices, VAMP4 KD increases the amplitude of AMPAR mediated excitatory post-synaptic currents (EPSCs) without affecting NMDAR mediated EPSCs in CA1 pyramidal neurons. Finally, VAMP4 KD reduces LTP while TeNT totally blocks it. Our data suggest a model where the depletion of VAMP4 leads to a basal state missorting of AMPARs to the plasma membrane, which consequently impairs LTP possibly via an occlusion mechanism. Additionally, the opposing changes in the levels of both TfR and AMPAR on cell surface upon VAMP4 KD suggest that these receptors maybe sorted and trafficked independently. We therefore propose that VAMP4 and VAMP2 mediate functionally distinct and complementary trafficking pathways modulating synaptic strength and plasticity.

**Key words:** synapse, synaptic plasticity, AMPA receptor, exocytosis, SNARE, recycling endosome.



## ACKNOWLEDGEMENTS AND DEDICATION

First and foremost, I thank the Almighty God for guiding me to this path, for reminding me that I may perhaps dislike a thing though it is good for me, for placing so many beautiful people in my life who have held my hand every step of the way and made this journey a little easier for me. I feel extremely grateful for those people who have given me the strength and tenacity to complete this work, but more importantly, have given me a home away from home.

I hereby dedicate this manuscript to whom I consider my life's greatest blessing: my family. I also dedicate this work to my dear Venezuelan mother and friend, Virginia. Ich widme diese Arbeit auch meiner wunderbaren Venezolanische Mutter und Freundin, Virginia. Lastly, to my master thesis advisor: Dr. Inseon Song, for her kind words which I carry with me, always and endlessly.

I would like to express my deepest gratitude to my thesis supervisor, Dr. David Perrais for accepting me to his group and giving me the opportunity to work on this project. His invaluable guidance, dynamism, and discussions have inspired me to push my limits throughout the process of this research. I place on record, my sincere thank you to the IINS director: Dr. Daniel Choquet for his enthusiastic spirit, empathy, and knowledgeable scrutiny. Not only is he a phenomenal scientist, but he throws the best parties too! I feel extremely fortunate to start this PhD as part of Daniel's team and finish it in our new "TraMS" team, so I can be the team's official first graduate! It was indeed a great privilege and honor to work under both of their guidance.

I extend my heartfelt gratitude to the kindest heart of Magalie Martineau for her warm welcome during my first days in Bordeaux, for sharing her expertise, her attentive support and precious words of motivation, and above all her beautiful friendship without which the completion of this thesis would not have been possible. I am very much thankful as well to Lea Claverie for the great times we have shared in this lab, for always pushing me forward, and helping out in difficult times when the leaves were brown and the sky was grey i.e. my experiments were failing. Les mots ne suffisent pas pour exprimer ma profonde gratitude.

My sincere thanks similarly go to all my new DP team and office mates: the best PhD tutor of all times: Etienne Herzog, but also, Silvia Sposini, Marlene Pfeffer, Zehra Kazmi, Julie Angibaud, Paul Lapios, Vincent Paget-Blanc, and especially Lou Bouit for contributing to the experimental work of this thesis. Thank you all for your valued critique, constant help, and

support throughout this work and the thesis writing process. It has been a pleasure to do something I love alongside such remarkable team members.

A big thank you to my ex-colleague, but forever little sister, Florelle Domart for our fun cycling and city wandering days, for inviting me as the sole outlier to her CENBG team outings, and for forcing me to speak so much French, *Merci Beaucoup Flo!* I believe that I have become a little more French now. I would also like to thank Francesco Porcaro for his great friendship and all the good times the three of us had spent skating along the Garonne.

Needless to mention, the bright side of my PhD life, my first office friends/family members: my twin in rivalry: Valeria Pecoraro, ma deuxième Marmotte: Virginia Puente, my rich companion: Diogo Neto, Caroline Bonnet, Emeline Verdier, Angela Getz, and Charlotte Rimbault. Also, our beautiful neighbor: Hannah Zieger. I cannot express how amazing it has been going to work every day to such incredible colleagues, I really can't thank you enough for all the wonderful times. Our office slowly turned into a family living room filled with photos, a 6-language educational board, our country's flags, and so much food. It was sometimes impossible to work, but at least we could eat. Thank you for not removing my Egyptian flag after my parting. A special thank you to our cell culture Queen, Emeline Verdier, not only for her hippocampal neurons, but for being the sunshine of this office.

My beautiful sisters and lunchtime mates, Sarah Rahmati and Federica Quici, I am beyond grateful to have you two in my life. It is simply wonderful to have friends like you, thank you for your continuous support throughout this journey, thank you for being my comfort zone, and thank you for all our skype calls during the hard time of the lockdown, you have saved me from going mental. Your friendship is something I will cherish forever!

My very first and dearest friendships in Bordeaux: Nuria Miret Roig and Silvia Pagliarini, thank you for welcoming me to your homes in Barcelona and Verona, for all the fun we have had as travel partners and best buddies. Our little circle soon expanded to include Christina Vaghi, Laia Casamiquela, and Giuliano Carlino till I slowly felt adopted by the Italian and Spanish communities of Bordeaux. *Grazie mille* and *Muchas gracias* guys!

I would like to thank my dear friend Bhargav Teja Nallapu, for his delightful friendship, and all the Indian food that we have shared. Also, my world's favorite Argentinian: Miguel Lopez Cuina, thank you for tracking my writing progress word by word and line by line, and thank you for all the beautiful times, all the laughs, all the yoga, and all the support you have given me during the lockdown and beyond.

My gratitude extends to the rest of Daniel Choquet's team members for their constructive comments and guidance on this project: Agata Nowacka, Marie-lise Jobin, Tiago Campelo, Andrea Toledo, Justine Charpentier, Natacha Retailleau, Nicolas Chevrier, Ines Gonzalez-Calvo, Come Camus, Diogo Soares, Sophie Daburon, Cecile Lemoigne, Ellyn Renou, Mathieu Sainlos, Eric Hosy, Anna Brachet, Francoise Coussen. Also, to the BIC engineers: Christel Poujol, Sebastien Marais, Fabris Cordeliers, Magali Mondin, Mathieu Ducros, and Jeremie Teillon. Thank you for all the beautiful pictures that I have acquired with your microscopes.

My sincere thank you to all my colleagues at the IINS for their immense kindness, help, and encouragement: Dario Cupolillo, Remi Sterling, Krishna Inavalli, Ingrid Chamma, Mathieu Letellier, Agata Idziak, Konstantina Liouta, Zeynep Karatas, Filipe Nunes Vicente, Johannes Roos, Amine Mehdi, Hisham Forriere.

I take this opportunity to thank my IMN friends for sneaking me into their institute and for all their cakes that I have eaten: Silvia Pagliarini, Bhargav Teja Nallapu, Remya Sankar, Pramod Kaushik, Thalita Firmo-Drumond, Melody Labarchede, and the best baker of all times Anthony Strock.

I would like to thank my co-supervisor Dr. Gunnar Gouras for his support and encouragement over the years and my fellow "SynDegen" PhD network friends for the scientific exchange and the pleasurable times we have had all around Europe: Sabine Konings, Edoardo Brandi, Laura Torres Garcia, Joana Domingues, Diogo Neto, Ines Bras, Jose Medina Luque, Katrin Pratsch, Emma Kallstig, Roshni Das, Sarah Rahmati.

Last but not least, I acknowledge with gratitude all my loving family back home in Cairo: my mother, Azza El-berry, my father Salah Bakr, for their motivation and prayers, without which I would never be where I am today, and of course, my two brothers: Mohamed and Sherif, for not really doing much. Even though we are miles away from each other, my family has perpetual support and belief in me. They are my world and my words can never do them justice.

Finally, I would like to thank the French government for placing the country in confinement to avoid further spread of the COVID19 virus, forcing me to stay home and write down this thesis.



بِسْمِ اللَّهِ الرَّحْمَنِ الرَّحِيمِ

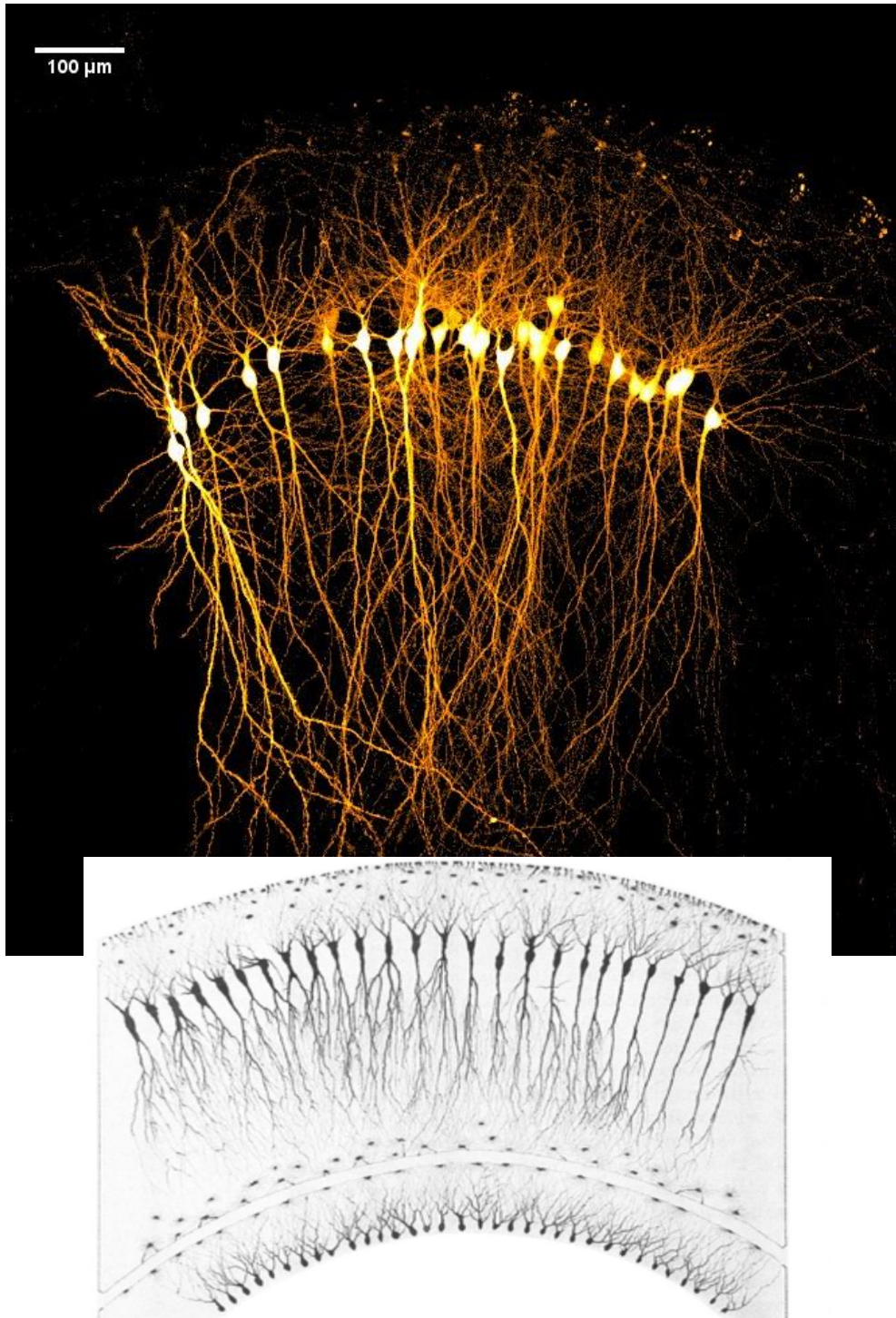
فَلْيَرْفَعْ لَكَ اللَّهُ بِإِيمَانِكَ وَالْإِيمَانُ بِمَا نَزَّلْنَا مِنَ الْقُرْآنِ وَإِنَّمَا يُرِيدُ اللَّهُ لِيُذْهِبَ عَنكُمُ الرِّجْسَ أَهْلَ الْبَيْتِ وَيُطَهِّرَ الصَّالِحِينَ

صَدَقَ اللَّهُ الْعَظِيمَ

*“Allah will exalt in degree those of you who believe, and those who have been granted knowledge” (The Quran, 58:11).*

*“Scientists are the inheritors of the prophets” (The Prophet Mohamed).*





*Between the past and the present.*

The resemblance between Camillo Golgi's early drawing of CA1 pyramidal neurons in the hippocampus that was published in 1903 and single-cell electroporated neurons of the same region.



## List of Abbreviations

**ABP:** AMPA receptor Binding Protein

**ACh:** Acetylcholine

**AD:** Alzheimer's Disease

**AIP1:** Actin interacting protein 1

**AMPA:**  $\alpha$ -amino-3-hydroxy-5-methyl-4-isoxazole propionic acid

**AP2:** Clathrin Adaptor Protein

**Arp:** Actin related protein

**ATD:** Amino Terminal Domain

**BoNT:** Botulinum NeuroToxin

**CA:** Cornu Ammonis

**CAMKII:** Calcium/calmodulin-dependent protein Kinase II

**cAMP:** Cyclic Adenosine MonoPhosphate

**CDK5:** Cyclin-Dependent Kinase 5

**CME:** Clathrin-mediated endocytosis

**CIE:** Clathrin-independent endocytosis

**CN:** Cyanogen Bromide

**CNT:** Clostridial NeuroToxin

**CTD:** C-Terminal Domain

**DG:** Dentate Gyrus

**EC:** Entorhinal Cortex

**EE:** Early Endosomes

**EPSP:** Excitatory Post Synaptic Potential

**ERC:** Early Recycling Compartment

**GABA:** Gamma-AminoButyricAcid

**GAP:** GTPase Activating Protein

**GDI:** GDP Dissociation Inhibitor

**GEF:** Guanine nucleotide Exchange Factor

**GPCR:** G-Protein Coupled Receptor

**GRIP:** Glutamate Receptor Interacting Protein  
**GSK3:** Glycogen Synthase Kinase-3  
**HC:** Heavy Chain  
**HFS:** High Frequency Stimulation  
**IPSP:** Inhibitory Post Synaptic Potential  
**KA:** Kainate  
**KD:** Knock Down  
**KO:** Knock Out  
**LBD:** Ligand Binding Domain  
**LC:** Light Chain  
**LE:** Late Endosomes  
**LFS:** Low Frequency Stimulation  
**LTD:** Long Term Depression  
**LTP:** Long Term Potentiation  
**MAPK:** Mitogen-Activated Protein Kinase  
**NCS:** Neuronal Calcium Sensor  
**NMDA:** N-Methyl-D-aspartate  
**NSF:** N-ethylmaleimide Sensitive Fusion protein  
**PICK1:** Protein Interacting with C-Kinase  
**PKA:** Protein Kinase A  
**PKC:** Protein Kinase C  
**PP1:** Protein Phosphatase 1  
**PP2B:** Protein Phosphatase 2B  
**Pr:** release Probability  
**PSD:** Post Synaptic Density  
**RA1BP1:** Ras-related protein (Ra1A)-binding protein 1  
**Rab:** Ras-related protein in brain  
**RabGGTase:** Rab GeranylGeranyl Trasnsferase  
**RE:** Recycling endosomes

**REP:** Rab Escort Protein

**RIM:** Rab3 Interacting Molecule

**RRP:** Readily Releasable Pool

**SEP:** pH-sensitive superEcliptic pHLuorin

**Ser/Thr:** Serine/Threonine

**SM:** Sec1/Munc18

**SNAP:** Synaptosomal Associated Protein

**SNARE:** Soluble N-ethylmaleimide-sensitive factor attachment protein receptors

**STP:** Short Term Potentiation

**SV:** Synaptic Vesicles

**Syb:** Synaptobrevin

**Syt:** Synaptotagmin

**TBS:** Theta Burst Stimulation

**TeNT:** Tetanus NeuroToxin

**TGN:** Trans-Golgi Network

**TMD:** Trans Membrane Domain

**tSNARE:** Target SNARE

**VAMP:** Vesicle Associated Membrane Protein

**VGCC:** Voltage Gated Calcium Channels

**vSNARE:** Vesicular SNARE

**Vti1a:** Vesicle Transport Through Interaction with T-SNARE homolog 1A

## List of Figures

Figure 1. Neuronal diversity.	33
Figure 2. Action potentials and synapses.	34
Figure 3. The general structures of a chemical and an electrical synapse.	35
Figure 4. Synchronous vs asynchronous neurotransmitter release.	38
Figure 5. Architecture of glutamatergic synapses.	40
Figure 6. Structural and domain organization of iGluRs.	42
Figure 7. Molecular organization of the Glutamatergic excitatory synapse.	42
Figure 8. Hippocampus compared to the sea horse.	44
Figure 9. Basic anatomy of the hippocampus.	44
Figure 10. Model for LTP induction in the hippocampal CA1 region.	48
Figure 11. Trafficking of AMPA receptors during LTP.	48
Figure 12. The two major forms of LTD.	51
Figure 13. Model of AMPA receptor trafficking during synaptic plasticity.	52
Figure 14. The morphology of dendritic spines.	53
Figure 15. Morphological changes in dendritic spines after LTP or learning.	55
Figure 16. Spine remodeling is dependent on actin cytoskeleton.	56
Figure 17. Local trafficking at the post-synapse.	58
Figure 18. Structural organization of the synaptic fusion complex embedded in a lipid bilayer.	62
Figure 19. The SNARE cycle.	63
Figure 20. SNARE complexes subcellular localization.	66
Figure 21. Ribbon representation of BoNT/A.	67
Figure 22. SNARE cleavage by CNTs.	69
Figure 23. Localization of Rab Proteins.	71
Figure 24. The Rab proteins cycle.	72
Figure 25. Dynamicity of synaptic vesicles.	74
Figure 26. A classical model for the localization of three distinct synaptic vesicle pools.	75
Figure 27. Spatial organization of presynaptic release machinery.	78

Figure 28. Schematic of SNARE proteins mediating the regulated AMPAR exocytosis during LTP.	81
Figure 29. ScrambleRNA-mscarlet infected CA1 pyramidal neurons.	90
Figure 30. ScrambleRNA-mscarlet electroporated CA1 pyramidal neurons.	91
Figure 31. A schematic of the optical configuration of a spinning disk confocal microscope.	93
Figure 32. Schematic of SEP fluorophore fused to transferrin receptor.	94
Figure 33. Analysis of exocytic events in somatodendritic compartments using Matlab.	96
Figure 34. Dual whole-cell recording configuration.	101



# INTRODUCTION

<b>A. Neural signaling and plasticity</b> .....	29
<b>1. The neuronal cells</b> .....	29
1.1 Morphological properties of neurons .....	29
1.2 Electrical properties of neurons .....	29
<b>2. The Synapse</b> .....	31
2.1 Synaptic Transmission .....	31
2.1.1 The chemical synapse.....	31
2.1.2 The electrical synapse .....	32
2.2 Neurotransmitter release .....	35
2.2.1 Different modes of neurotransmitter release .....	36
2.2.2 Vesicular mechanism of neurotransmitter release .....	37
2.3 Glutamatergic Excitatory Synapses .....	39
2.3.1 Ionotropic glutamate receptors .....	39
2.3.2 Metabotropic glutamate receptors .....	41
<b>3. Synaptic Plasticity</b> .....	43
3.1 The hippocampal formation and memory .....	43
3.2 Long term potentiation.....	46
3.3 Long term depression.....	49
3.4 Structural plasticity .....	53
<b>B. Membrane trafficking and exocytosis machinery</b> .....	57
<b>1. The endosomal system</b> .....	57
<b>2. SNARE-mediated membrane fusions</b> .....	59
2.1 The SNARE complex structure and function .....	59
2.1.1 SNARE structure and classification .....	59
2.1.2 Main SNARE proteins .....	60
2.1.3 The SNARE cycle .....	61
2.2 SNARE specificity.....	64
2.3 SNARE cleavage by neurotoxins.....	67
<b>3. Regulators of membrane trafficking: Rab proteins</b> .....	70
3.1 Localization of Rab proteins .....	70
3.2 The Rab cycle .....	71

<b>4. SNAREs at the synapse</b> .....	73
4.1 SNARE proteins in synaptic vesicle exocytosis .....	73
4.2 Post-synaptic SNARE fusion machinery .....	79
<b>C. Membrane trafficking in synaptic plasticity</b> .....	82
<b>1. Endosomal recycling and LTP</b> .....	82
1.1 TfR in constitutive recycling.....	82
1.2 Activity-dependent recycling.....	83

## **MATERIALS AND METHODS**

1. Primary hippocampal Banker cultures .....	87
2. Organotypic hippocampal culture .....	88
3. Expression of exogenous proteins and shRNA .....	88
3.1 Plasmid constructs .....	88
3.2 Calcium phosphate transfection .....	89
3.3 Transduction with lentivirus .....	90
3.4 Single cell electroporation .....	91
4. Live cell imaging.....	92
4.1 Spinning disk confocal microscopy .....	92
4.2 Visualization of single exocytic events.....	94
a. SuperEcliptic pHLuorin (SEP).....	94
b. Fusion events, imaging and analysis .....	94
4.3 Glycine treatment on live cells after photobleaching.....	96
a. Chemical Long-term potentiation protocol .....	96
b. Fluorescence Recovery after Photobleaching .....	97
4.4 pH change for quantification of surface expression.....	97
5. Immunocytochemistry and Transferrin recycling assay .....	98
6. Electron Microscopy .....	99
7. In- vitro electrophysiology .....	100
7.1 Whole-cell patch-clamp recordings .....	100
7.2 Long term potentiation induction.....	101
8. Statistical tests.....	101

## RESULTS

VAMP4 controls constitutive recycling and sorting of post-synaptic receptors in neuronal dendrites.....	105
ABSTRACT.....	106
INTRODUCTION .....	107
RESULTS .....	109
VAMP4 is a marker of recycling endosome exocytosis in neuronal dendrites.....	109
Downregulation of VAMP4 but not cleavage of VAMP2 reduces TfR exocytosis and recycling .....	111
VAMP4 exocytosis increases after chemical induction of LTP .....	112
VAMP4 KD does not impair the increase in RE exocytosis during cLTP induction .	113
VAMP4 KD accelerates AMPAR recycling and impairs its modulation during LTP induction.....	114
Effect of VAMP4 KD on synaptic transmission and plasticity .....	114
DISCUSSION .....	125
Involvement of VAMP4 in dendritic exocytosis.....	125
VAMP4 is necessary for endosomal sorting of AMPAR .....	126
A sequence of fusion events for the expression of LTP.....	128
REFERENCES .....	129

## GENERAL DISCUSSION AND PERSPECTIVES

Further comments on the diversity of the endosomal system in dendrites.....	137
Implications for neuropathology .....	140
References .....	143



# **INTRODUCTION**



## **A. Neural signaling and plasticity**

### **1. The neuronal cells**

The basic unit of the nervous system is the nerve cell or the neuron. Neurons within the central and peripheral nervous system process information by generating sophisticated electrical and chemical signals across synapses. Signaling between interconnected neurons forms the circuitry which provides higher-level brain functions. The human brain with 100 billion neurons is the most cognitively able despite not being the largest among mammalian brains (Herculano-Houzel, 2009).

This introductory section is mainly from neuroscience books: The hippocampus book, Theoretical Neuroscience (Dayan, Abbott), Purves (3<sup>rd</sup> edition), Principles of neural science (4<sup>th</sup> edition), Molecular cell biology (7<sup>th</sup> edition).

#### **1.1 Morphological properties of neurons**

Neurons are highly specialized cells that generate electrical signals and transmit them to other cells via specialized morphological nerve fibers, the dendrites and the axons. Neurons connect and transmit information across junctions called synapses. The dendrites allow a neuron to receive inputs from multiple other neurons through synaptic connections. The structure of the dendrites or dendritic trees is very diverse (Figure1), likely reflecting diversity in the functional properties and the types of computations performed by different types of neurons (Sprutson, Hausser, & Stuart, 2013). Axons from a single neuron can traverse large brain fractions and carry the integrated neuronal output to other cells. In the mouse brain, cortical neurons typically send out an estimated 40 mm of axon which makes on average 180 synaptic connections with other neurons per mm of length. They have a total dendritic cable of approximately 10 mm and the dendritic tree receives 2 synaptic inputs per  $\mu\text{m}$  on average. The cell body or soma of a typical cortical neuron ranges in diameter from about 10 to 50  $\mu\text{m}$ . It houses the nucleus and other structures that support the metabolic activity of the neuron.

#### **1.2 Electrical properties of neurons**

Neurons also have physiological specializations besides their morphological features. Most prominently, they harbor a wide variety of membrane-spanning ion channels that allow ions, mainly sodium ( $\text{Na}^+$ ), potassium ( $\text{K}^+$ ), calcium ( $\text{Ca}^{2+}$ ), and chloride ( $\text{Cl}^-$ ) to move across the

cell membrane. These ion channels open and close in response to voltage changes and other internal and external signals. The electric charges of these ions are important for many aspects of neuronal function, mainly the maintenance of the cell's resting membrane potential and the generation of an action potential.

In quiescent cells, there are relatively more sodium and chloride ions outside the cell, whereas potassium and organic anions are typically found at higher concentrations within the cell than outside. This difference in concentrations provides a concentration gradient for ions to flow down their concentration gradients when their channels are open. As such, sodium and chloride ions will move into the cell, whereas potassium ion will flow out of the cell. However, of the three ions, the cell is most permeable to potassium, allowing it to have the greatest influence on the cell resting membrane potential. Thus, the resting membrane potential of neurons typically sits between -50 and -75 mV, a value that is closest to the equilibrium potential of potassium ions, and the cell is said to be polarized.

Ion pumps located in the cell membrane maintain concentration gradients that support this membrane potential difference. A change in voltage or concentration gradients across the membrane will allow the flow of ions into and out of a cell. Current in the form of positively charged ions flowing out of the cell (or negatively charged ions flowing into the cell) through open channels makes the membrane potential more negative, and the cell is hyperpolarized. In contrast, the current flowing into the cell changes the membrane potential to less negative or positive values leading to cell depolarization.

If a neuron is depolarized above a certain threshold, a positive feedback is initiated, and the neuron generates an action potential. An action potential is a 100 mV fluctuation in the electrical potential across the cell membrane lasting for about 1 ms (Figure 2A). A few milliseconds after the action potential, there is a hyperpolarization phase during which it may be impossible to initiate another spike, and the cell is said to be in the absolute refractory period.

Action potentials generated along axon processes can propagate rapidly over large distances. Axons terminate at synapses where the voltage transient of the action potential opens ion channels and calcium influx into the cell leading to neurotransmitter release (Figure 2B). The neurotransmitter binds to receptors at the post-synaptic membrane causing ion-conducting channels to open. Depending on the nature of the neurotransmitter release and the ion flow, the synapses can have an excitatory or an inhibitory effect on the post-synaptic neuron (discussed later in detail).

## **2. The Synapse**

A Synapse is a term introduced by Charles Sherrington in 1897 and is derived from the Greek word Sinapsis meaning to “hold together”. It represents the precise location that transmits information from a pre- to a post-synaptic neuron allowing neuronal communication. Hence, the synapse consists of the pre-synaptic component; axonal bouton, the synaptic cleft of ~20 nm, and a post-synaptic component of a neighboring neuron (Figure 2B).

Large neurons are generally connected by thousands of boutons. The boutons may be opposed to dendrites of the receptor neuron (axodendritic synapses), to small projections of dendritic membrane or spines (axospinous synapses), to the perikaryon (axosomatic synapses), or the initial segment of the axon (axoaxonal synapses).

### **2.1 Synaptic Transmission**

Synaptic transmission is the biological process by which a neuron communicates with a target cell across a synapse. There exist two main modalities of synaptic transmission: chemical and electrical, which coexist in most organisms and brain structures. At chemical synapses, a neurotransmitter is released from one neuron and detected by another, whereas in electrical synapses, adjacent cells are directly connected via gap junctions. The majority of the CNS synapses are chemical, while electrical synapses are much less common (Pereda, 2015).

#### **2.1.1 The chemical synapse**

The discovery of the chemical synapse was one of the most crucial in the history of neuroscience in the 20th century. It came from detailed studies on the functioning of the autonomic nervous system by T.R. Elliott, H. H. Dale, and O. Loewi (Tansey, 1991; Todman, 2008). The culmination of this work has led H. H. Dale together with O. Lowe to the Nobel prize in physiology or medicine in 1936 for the ‘discovery of chemical synaptic transmission’.

The chemical synaptic transmission requires the release of neurotransmitter molecules from presynaptic axon terminals that are detected by the adjacent postsynaptic cell. The process is initiated when an action potential invades the terminal of a presynaptic neuron, which triggers the influx of calcium into the cell. Elevation of presynaptic calcium ion concentration, in turn, allows synaptic vesicles (SV) to fuse with the presynaptic plasma membrane and the release of neurotransmitters into the synaptic cleft. Following exocytosis, transmitters diffuse across the synaptic cleft and bind to their specific post-synaptic receptors (Figure3). This process plays

crucial functions in neuronal growth and development, synapse formation, and signal transduction.

One way of classifying synapses is whether the action of the neurotransmitter released tends to promote or inhibit the generation of an action potential in the postsynaptic cell. Therefore, neurotransmitters can either have excitatory or inhibitory effects on post-synaptic membrane. Excitatory postsynaptic potentials (EPSPs) are associated with a transmitter-induced increase in  $\text{Na}^+$  and  $\text{K}^+$  conductance of the synaptic membrane, resulting in net entry of positive charge carried by  $\text{Na}^+$  and membrane depolarization. Inhibitory postsynaptic potentials (IPSPs) are associated with a transmitter-activated influx of  $\text{Cl}^-$  and membrane hyperpolarization. The majority of the excitatory synapses are found at dendrites, at the heads of spines, whereas the inhibitory synapses are found at the soma or the axon hillock, where excitation is generated and can be most effectively suppressed. Therefore, a single neuron receives a wealth of excitatory and inhibitory inputs through their synapses, which results in complex spatiotemporal signal integration involving current flow that ultimately converges in the axon until a fixed threshold for action potential firing is reached (Sprutson, Hausser, & Stuart, 2013).

### **2.1.2 The electrical synapse**

The electrical synaptic transmission is mediated by clusters of intracellular channels called gap junctions that directly communicate the interior of two adjacent cells, enabling the bidirectional passage of electrical currents and small molecules, for example, calcium, cyclic AMP and inositol-1,4,5-triphosphate). Gap junctions have a large internal diameter of  $\sim 1.2$  nm and are formed by the docking of two hexameric connexin ‘hemichannels’ or ‘connexons’, one from each adjacent cell (figure3). Their bi-directionality enables them to coordinate the activity of a large group of interconnected neurons. Although they are a distinct minority, electrical synapses are found in all nervous systems, permitting direct, passive, and low resistance flow of electrical current from one neuron to another. Because gap junction communication occurs without the involvement of any intermediate messenger, they provide a fast mechanism for intercellular synaptic transmission (Curti and O’Brien, 2016). Electrical synapses are known to occur in the retina, inferior olive, and olfactory bulb (Pereda, 2014).

Gap junctions are highly dynamic structures, and their levels are maintained by a constant insertion and removal of channels providing a continuous and reliable conductance. By contrast, chemical synaptic communication is episodic given that it relies on the intermittent presence of an action potential at the presynaptic terminal which generates a transient increase in

intracellular calcium levels. Moreover, the neuro-transmitter release is probabilistic, and failures in trans-mission will occasionally occur despite the presence of an action potential in the presynaptic terminal (Alcami and Perada, 2019).

Electrical and chemical synapses can mutually co-regulate each other's formation. Therefore, normal brain development and function relies on the interaction between these two forms of interneuronal communication (Jabeen and Thirumalai, 2018).

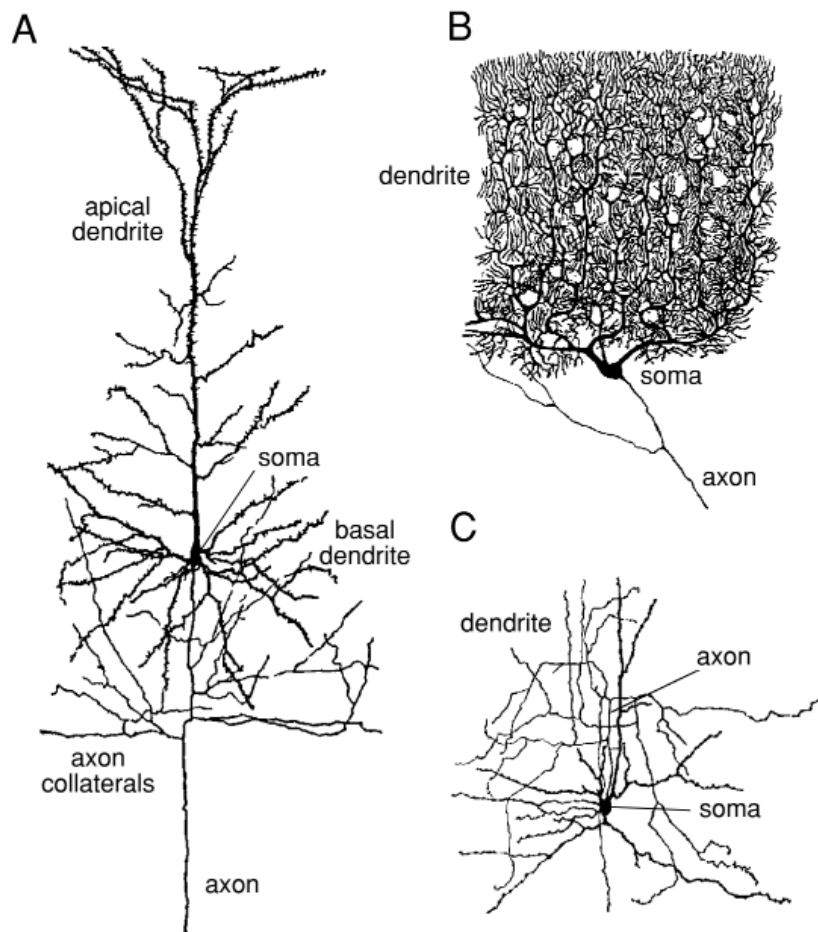


**Figure 1. Neuronal diversity.** (A) A cortical pyramidal cell: the primary excitatory neuron of the cerebral cortex. (B) A Purkinje cell: present the most striking histological feature of the cerebellum and are the sole output of the cerebellar cortex. (C) A stellate cell of the cerebral cortex: they send inhibitory signals to the dendritic arbors of Purkinje cells. These figures are magnified about 150-fold. (Drawings from Cajal, 1911; figure from Dowling, 1992). Theoretical neuroscience book (Dayan, Abbott).

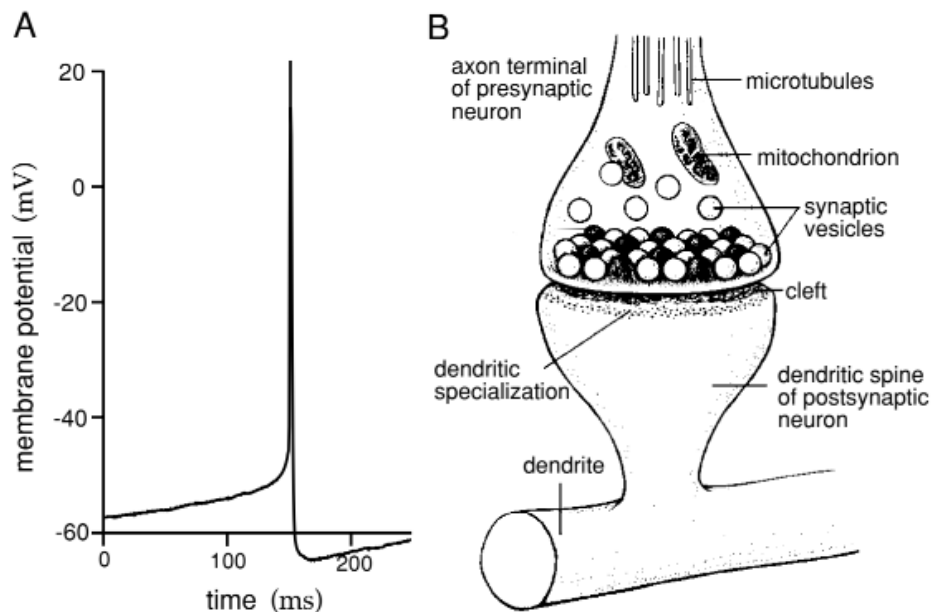


**Figure 2. Action potentials and synapses.** Intracellular recording of an action potential from a cultural rat neo-cortical pyramidal cell. (B) Diagram of a chemical synapse. The synapse consists of the pre-synaptic component (bouton), the synaptic cleft, and the post-synaptic component (dendritic spine) of the next neuron. The axonal boutons contains mitochondria and small synaptic vesicles carrying neurotransmitter molecules that are released at the active zone. The presynaptic active zone is opposing the postsynaptic membrane containing a protein dense specialization called the postsynaptic density (PSD). Membrane fusion and exocytosis is triggered by a rise in intracellular calcium. Theoretical neuroscience book (Dayan, Abbott).

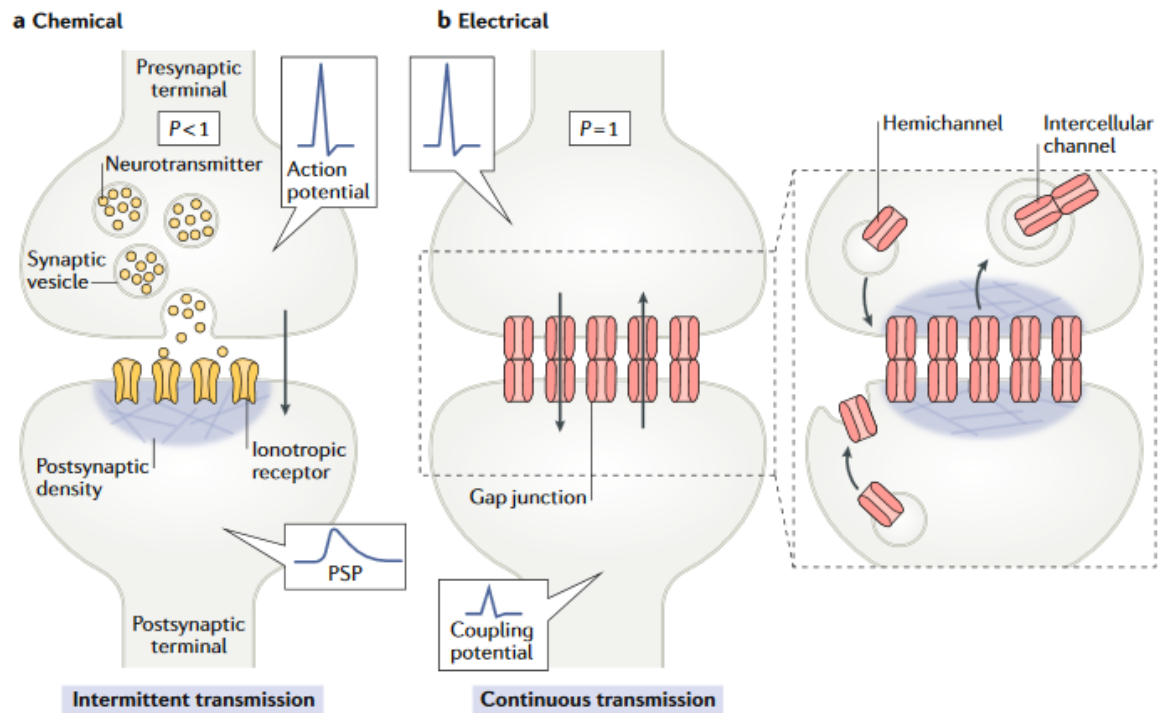


**Figure 3. The general structures of a chemical and an electrical synapse.** (A) The chemical synapse requires transmitter release evoked by presynaptic action potentials, which activate calcium influx, and trigger synaptic vesicles exocytosis. Neurotransmitters released activate specific postsynaptic gated channels, eliciting a transient change in membrane permeability to cations or anions. Transmission at most chemical synapses is intermittent, as transmitter release is probabilistic ( $P < 1$ ) and depends on the presence of an action potential in the presynaptic terminal. (B) Electrical synapse transmission involves the transfer of electrical signals through gap junctions, that could be bidirectional. Continuous electrical communication is a highly regulated process that is maintained by a delicate balance between insertion and removal of gap junction channels. Electrical transmission is continuous in nature ( $P = 1$ ). Electrical currents underlying an action potential can directly spread to the postsynaptic cell, generating an electrical or a coupling potential. Figure from Alcami & Perada, 2019.

## 2.2 Neurotransmitter release

Neurotransmitters are endogenous molecules responsible for information transmission across chemical synapses. Over the years, several formal criteria have emerged that identify a substance as a neurotransmitter. The compound must be synthesized by the neuron; it must be released by the neuron in sufficient amounts to exhibit an effect on another neuron or effector organ; exogenous application in appropriate quantities must mimic the action of the endogenously released compound; and a mechanism must exist to remove the neurotransmitter from the site of action (Veca and Dreisbach, 1988). These criteria have led to the identification of more than 100 different neurotransmitter substances.

This large number of transmitters allows for tremendous diversity in chemical signaling between neurons. It is therefore useful to classify them into two major groups: (i) classic, such as amino acid derivatives, and (ii) neuropeptides. The most widely distributed classic transmitter substances in the nervous system are acetylcholine (ACh), glutamate, gamma-aminobutyric acid (GABA), dopamine, serotonin, norepinephrine, and glycine. The first substance identified as a neurotransmitter was ACh in 1914. The most abundant neurotransmitter in the CNS is glutamate, which is present in more than 80% of synapses and is the major excitatory neurotransmitter in the brain. In contrast, most inhibitory synapses use either GABA or glycine as neurotransmitters.

### **2.2.1 Different modes of neurotransmitter release**

Most neuronal communication requires rapid information transfer within the CNS and relies upon the fast, synchronous release of neurotransmitters, which occurs within several milliseconds after an action potential invades a presynaptic bouton. However, neurotransmitter release could persist for tens or hundreds of msec after an action potential (asynchronous release), or in the absence of presynaptic depolarization stimulus (spontaneous release) (Rozov, Bolshakov, & Valiullina-Rakhmatullina, 2019; Kaeser and Regehr, 2014). The asynchronous release can influence network parameters including the efficacy of neurotransmission, synchronicity, and plasticity, whereas spontaneous release potentially affects synapse formation and connection strength (Chanaday et al., 2019).

Both synchronous and asynchronous releases are  $\text{Ca}^{2+}$  dependent, but the source of  $\text{Ca}^{2+}$  ions, and the  $\text{Ca}^{2+}$  sensors involved in both modes are different and have different binding kinetics. There is a general consensus that synchronous release is mainly triggered in the active zones by  $\text{Ca}^{2+}$  influx through presynaptic VGCC. Opening of these channels leads to a short-lasting and spatially restricted elevation of intraterminal  $\text{Ca}^{2+}$  at channel clusters known as nano- or microdomains. Furthermore,  $\text{Ca}^{2+}$  channels are closely associated with low-affinity vesicular synaptotagmines, usually, Syt1 and Syt2 at presynaptic release sites, which are suitable for triggering highly synchronized phasic release during the short-lived  $\text{Ca}^{2+}$  elevation within the microdomain (figure4) (Rozov, Bolshakov, & Valiullina-Rakhmatullina, 2019; Bukharaeva, 2015).

On the other hand, delayed asynchronous release requires a long-lasting elevation of free intraterminal  $\text{Ca}^{2+}$ , but the source remains poorly identified. It has been proposed that VGCC may also provide a longer-lasting phase of  $\text{Ca}^{2+}$  influx that may contribute to asynchronous

release (figure4). In addition, it was hypothesized that synaptic activation may liberate sufficient ATP that activates presynaptic  $\text{Ca}^{2+}$  permeable P2X receptors. Intracellular  $\text{Ca}^{2+}$  is suggested to bind to Syt7, which is a high-affinity calcium sensor mediating asynchronous release. However, the mechanism of its recruitment is not identified. Syt7 is also required for synaptic facilitation. It is found on the presynaptic plasma membrane and other internal membranes, but not on synaptic vesicles suggesting a non-canonical mechanism of vesicle exocytosis. (Rozov, Bolshakov, & Valiullina-Rakhmatullina, 2019; Kaeser and Regehr, 2014; Jackman et al., 2016).

### **2.2.2 Vesicular mechanism of neurotransmitter release**

The foundations of presynaptic physiology were first established by the Nobel prize winner Bernard Katz and Ricardo Miledi during the 1950s and 1960s. Their pioneering work demonstrated the importance of presynaptic depolarization and  $\text{Ca}^{2+}$  influx for triggering the fast, synchronous transmitter release at nerve terminals. They have also shown that the synaptic transmitter is released in discrete packages called quanta. The discovery of the quantal release immediately raised the question of how such quanta are formed and discharged into the synaptic cleft. Later, Katz and colleagues revealed with electron microscopy the presence of synaptic vesicles in presynaptic terminals, which were then proposed to be loaded with the transmitter, and were thought to be the source of the quanta. These early findings are the basis for much of our current understanding of neurotransmitter release.

The ‘classical’ neurotransmitters are held in membrane-bound vesicles 40-50 nm in diameter near the synapse at the presynaptic cell. The exocytic release of neurotransmitters is triggered when electrical impulses in the form of an action potential invade the axon terminal. The transducers of electrical signals are voltage-gated  $\text{Ca}^{2+}$  channels (VGCC) localized at a region adjacent to the synaptic vesicles. The arrival of an action potential depolarizes the membrane and permits the influx of  $\text{Ca}^{2+}$  ions into the cytosol from the extracellular medium. This leads to a highly localized, transient increase in intracellular levels of  $\text{Ca}^{2+}$  ions in the region near the synaptic vesicles from  $<0.1\ \mu\text{M}$ , characteristic of a resting state, to 1-100  $\mu\text{M}$  (Figure 4B). The increase in  $\text{Ca}^{2+}$  triggers the exocytosis of synaptic vesicles and thus the release of neurotransmitters.  $\text{Ca}^{2+}$  ions bind to a protein in the synaptic vesicle membrane called synaptotagmin (Syt), which is considered the key  $\text{Ca}^{2+}$  sensing protein that triggers vesicle fusion, initiating synaptic transmission (Lodish, Berk, & Zipursky, 2000; Sudhof, 2012). Syts do not act alone but require a cofactor called complexin, which is a small protein that binds to

SNARE complexes (soluble N-ethylmaleimide-sensitive factor attachment protein receptor), proteins that catalyze membrane fusion, triggering exocytosis (Sudhof, 2012). However, the mechanism by which  $\text{Ca}^{2+}$ -Syt catalyzes the exocytic release of neurotransmitter remains largely unknown (Gundersen, 2019).

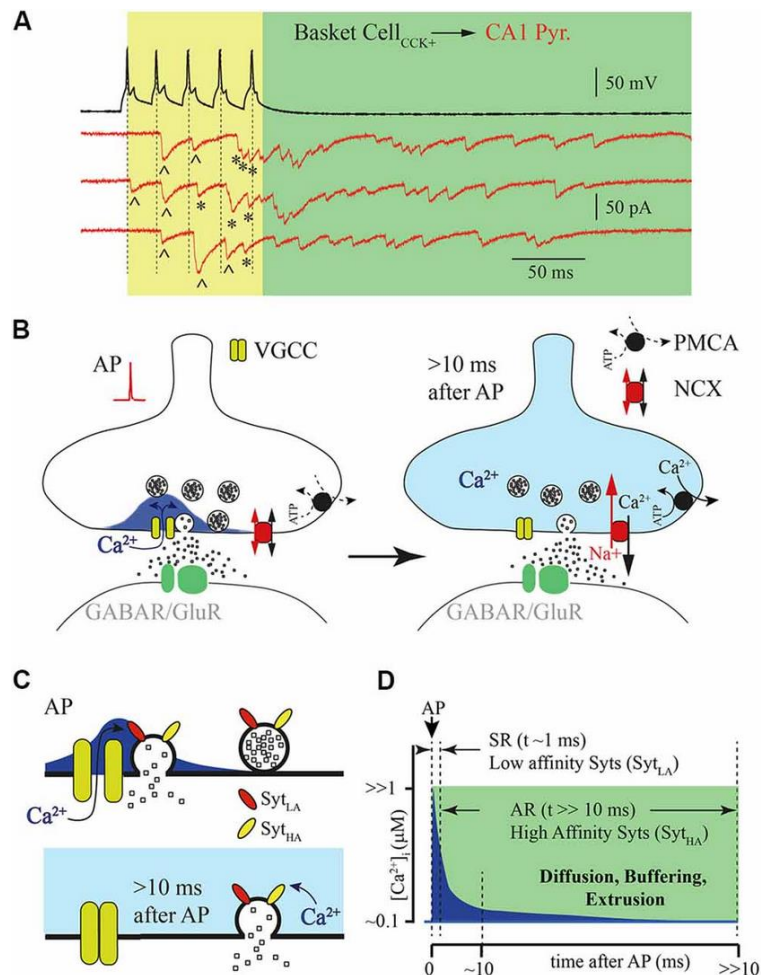


**Figure 4. Synchronous vs asynchronous neurotransmitter release.** (A) Example traces of responses recorded from a presynaptic hippocampal cholecystokinin (CCK)+ basket cell shown in black and a postsynaptic CA1 pyramidal neuron shown in red (three traces recorded subsequently). Five action potentials triggered synchronized phasic IPSC (labeled with ^) and delayed responses (labeled with \*). (B) Schematic drawing of a synapse after a single action potential. VGCC open transiently leading to an influx of calcium ions triggering phasic release (left panel). After closure of VGCC,  $\text{Ca}^{2+}$  concentration declines due to radial diffusion and binding to endogenous buffers (right panel). Two membrane transport proteins are responsible for maintaining pre-synaptic  $\text{Ca}^{2+}$  homeostasis: plasma membrane calcium-ATPase (PMCA) and the sodium/calcium exchanger (NCX). (C) Schematic drawing of vesicle fusion by  $\text{Ca}^{2+}$  micro/nano evoked by an action potential (upper panel). Phasic synchronous release arises from low affinity Syt (Syt<sub>LA</sub>). The lower panel shows delayed vesicle fusion mediated by high affinity Syt (Syt<sub>HA</sub>). (D) Schematic representation of  $\text{Ca}^{2+}$  time course at release site (blue) after an action potential. Dotted lines show time courses for synchronous and asynchronous release. Figure from Rozov, Bolshakov, & Valiullina-Rakhmatullina, 2019.

## **2.3 Glutamatergic Excitatory Synapses**

Glutamatergic neurotransmission has been drawing substantial scientific interest owing to its implication in higher-order cognitive functions including learning and memory. Glutamate is a nonessential amino acid that was first speculated to have a metabolic function in the CNS. Then during the 1950s, it has been known that glutamate has an excitatory action in the mammalian brain and spinal cord (Meldrum, 2000). However, it was not until 1984 that it was acknowledged as fulfilling the criteria of a neurotransmitter and became widely recognized as the main excitatory transmitter within the vertebrate nervous system (Niciu, Kelmendi, & Sanacora, 2012). Glutamatergic excitatory synapses are now one of the best-understood synapses in the mammalian CNS (Siddoway, Hou, & Xia, 2011).

Glutamatergic synapses are excitatory relay points between presynaptic nerve terminals and postsynaptic spines. They are easily recognized via electron microscopy due to the appearance of the electron-dense region of the postsynaptic density (PSD) (Figure5). PSDs correspond to disks which are ~50 nm thick and 200-500 nm wide and may contain up to 100 types of proteins including membrane receptors, second messengers signaling molecules, anchoring and scaffolding proteins, and cytoskeletal components that provide structural and functional support to the synapse. The presynaptic terminal contains glutamatergic synaptic vesicles, which once released, targets its postsynaptic glutamate receptors (Siddoway, Hou, & Xia, 2011; Niciu, Kelmendi, & Sanacora, 2012).

### **2.3.1 Ionotropic glutamate receptors**

Postsynaptic glutamate receptors can be divided into two broad categories: ionotropic and metabotropic receptors. The ionotropic receptor or iGluR family can be grouped into three subtypes that can all bind glutamate and are named based on their agonist selectivity: N-methyl-D-aspartate (NMDA),  $\alpha$ -amino-3-hydroxy-5-methyl-4-isoxazole propionic acid (AMPA), and kainate (KA).

Ionotropic glutamate receptors are integral membrane proteins that assemble as tetramers of four intertwined subunits (>900 residues) that form an ion channel. Each subunit comprises an extracellular amino-terminal domain (ATD), a ligand-binding domain (LBD), a common pore-forming transmembrane domain (TMD), and an intracellular C-terminal domain (CTD) (Figure6). Assembly of subunits within the same functional class leads to the formation of a functional receptor. The AMPAR subunits (GluA1-GluA4) can form both homo- and

heteromers. Kainate receptors have five subunits (GluK1-GluK5), the subunits GluK1-GluK3 can also form both homo- and heteromers, but GluK4 and GluK5 are only functional when co-expressed with GluK1-GluK3. In addition, functional NMDA receptors require the assembly of two GluN1 subunits together with either two GluN2 subunits or a combination of GluN2 and GluN3 subunits. Different subunits are expressed in distinct brain regions and may serve different functions (Traynelis et al., 2010).

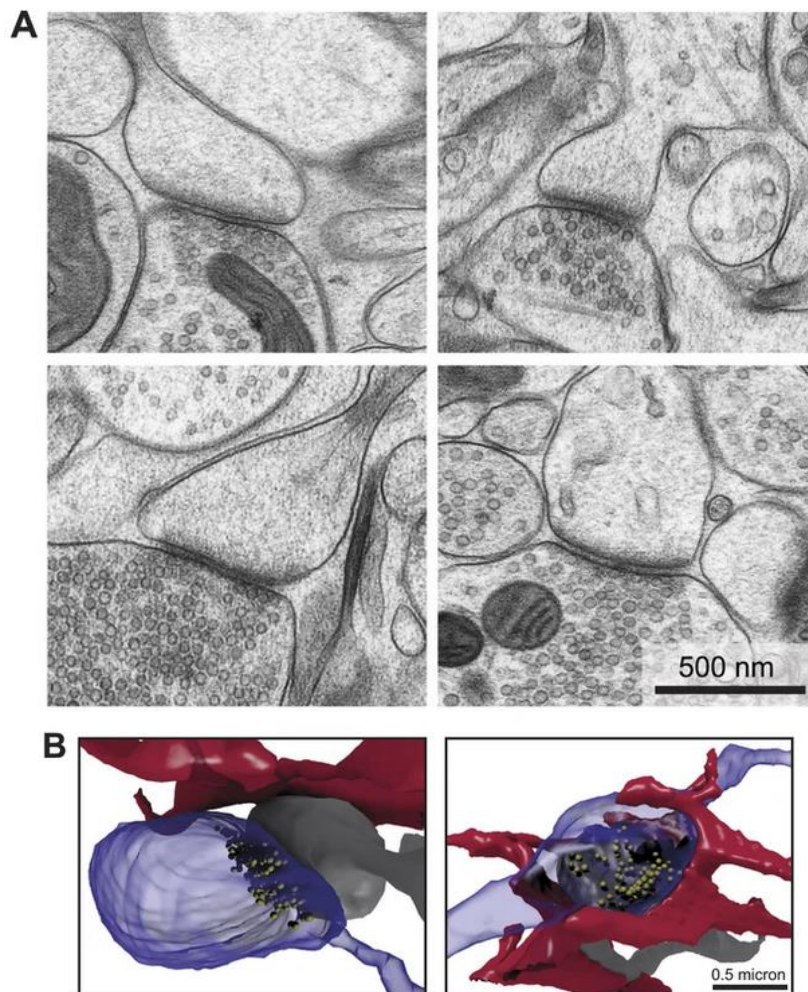


**Figure 5. Architecture of glutamatergic synapses.** (A) Two dimensional EM images of synapses, showing presynaptic terminal containing vesicles, and postsynaptic electron-dense region of the PSD. (B) Reconstructed serial EM images, of axonal boutons (blue), dendritic spines (grey), and the astrocytic processes nearby (red). Image from Korogod et al., 2015.

The function of iGluRs is exhibited through ligand-gated, non-selective cation channels, which allow the passage of  $\text{Na}^+$ ,  $\text{K}^+$ , and in some cases  $\text{Ca}^{2+}$ . The neuronal excitatory postsynaptic potential (EPSP) is mediated additively by AMPA and NMDA receptors (Figure 7), whereas KA receptors do not contribute significantly to synaptic transmission, except in specific synapses such as mossy fiber synapses in CA3 pyramidal cells (Siddoway, Hou, & Xia, 2011).

AMPA receptors have a lower glutamate affinity than NMDA receptors, but they have faster kinetics (millisecond timescale) and are responsible for the fast initial component of the EPSP (Meldrum, 2000). The rapid kinetics of AMPARs allows for fast depolarization of the postsynaptic membrane and high-fidelity basal synaptic transmission. In contrast, NMDA receptors have slower kinetics, use glycine as a co-agonist (which bind on the GluN1 subunits), and elicit relatively slow and long-lasting EPSPs. NMDAR is also considered a molecular coincidence detector that requires for activation both presynaptic release of glutamate and a sufficiently strong postsynaptic depolarization. The reason is that under basal conditions, magnesium ions block NMDAR pore, which can be removed upon adequate membrane depolarization allowing postsynaptic Ca<sup>2+</sup> entry, activating downstream calcium-dependent signaling cascades. Therefore, NMDARs are not critical for basal transmission, but rather initiates changes in synaptic strength and plasticity as a result of their calcium permeability (Siddoway, Hou, & Xia, 2011). At some synapses, however, a minority of AMPARs (GluA2 subunit-lacking) are calcium-permeable and can trigger or contribute to various forms of synaptic plasticity (Greger, Watson, & Cull-Candy, 2017). Synaptic AMPA and NMDA receptors are clustered at the PSD, anchored by F-actin and other scaffolding and signaling proteins underneath (Figure 7) (Siddoway, Hou, & Xia, 2011).

### **2.3.2 Metabotropic glutamate receptors**

Eight metabotropic glutamate receptors or mGluRs have been identified (mGlu1-8), and subdivided into three functional groups (Group I, II, or III) based on amino acid sequence homology, agonist binding, and activated downstream G protein signaling partners (Kim et al., 2008; Niciu, Kelmendi, & Sanacora, 2012). Group I mGluRs consist of mGlu1 and mGlu5, Group II is mGlu2 and mGlu3, Group III is mGlu4,6,7. Both receptor families provide functional diversity and are widely expressed throughout the nervous system (Reiner and Levitz, 2018).

mGluRs are present on both sides of the synapse but tend to be located perisynaptically and not within the synaptic zone (Sherman, 2014). They are members of the G-protein coupled receptors (GPCRs) superfamily which are constitutive dimers. Glutamate binding leads to activation of G protein signaling cascades that can modulate cell excitability and synaptic transmission. Group I mGluRs are primarily G<sub>q</sub>-coupled, and elicit their downstream effects by Ca<sup>2+</sup> mobilization and activation of protein kinase C. Group II and III are G<sub>i/o</sub>-coupled that are negatively coupled to adenylyl cyclase/protein kinase leading to a decrease in intracellular

cyclic adenosine monophosphate (cAMP), and inhibition of glutamatergic transmission (Niswender and Conn, 2010; Crupi et al., 2019).

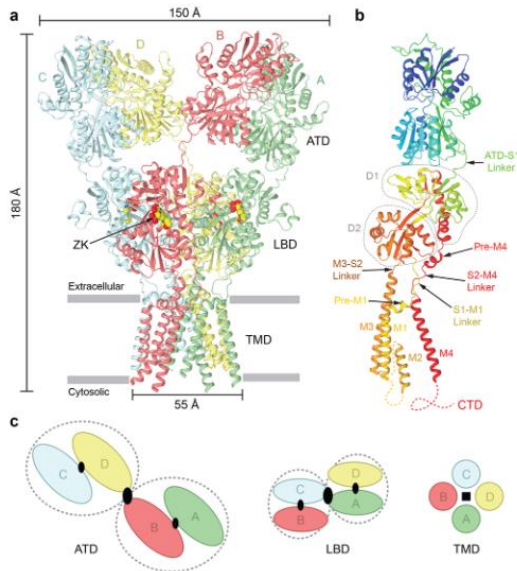


**Figure 6. Structural and domain organization of iGluRs.** (A) crystal structure of AMPARs composed of homotetrameric GluA2 subunits shown in four different colours. (B) Structure of a single GluA2 subunit. (C) Representations of each iGluR domain layer (ATD, LBD, and TMD) viewed extracellularly. Image from Twomey and Sobolevsky, 2017.

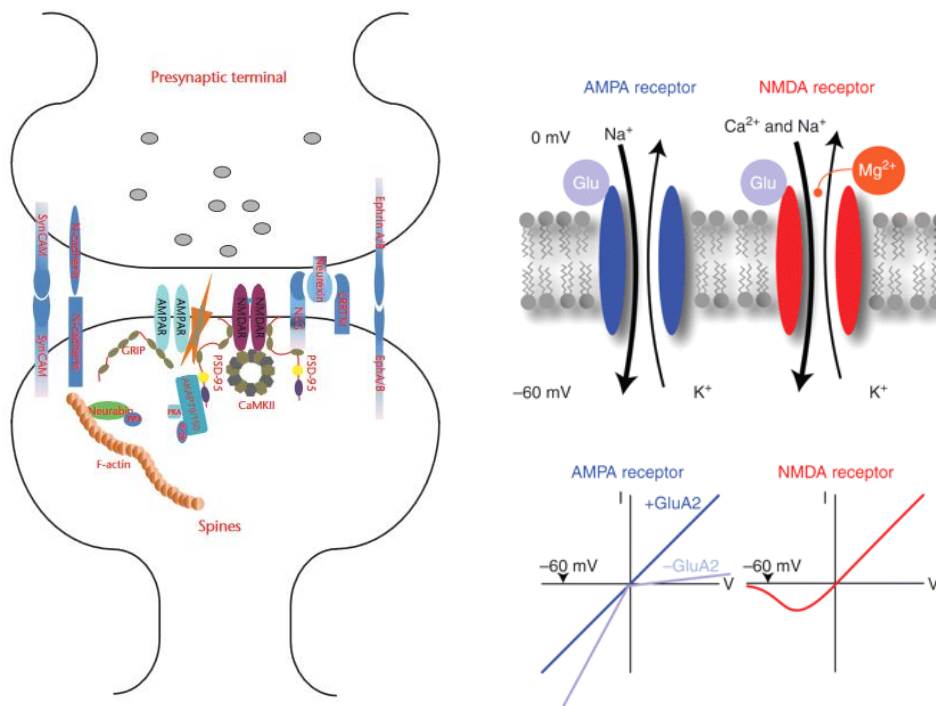


**Figure 7.** To the left, a schematic of the molecular organization of a glutamatergic excitatory synapse showing AMPA and NMDA receptors localization at the PSD, and other anchoring and scaffolding proteins. Figure from Siddoway et al., 2011. To the right, major ionotropic glutamate receptors and their current voltage relationships (I-V) that is considered a biophysical signature for different receptors. AMPARs containing GluA2 show a linear I-V relationship, but are inward rectifying without GluA2. NMDARs have a more complex I-V curve because of the  $Mg^{2+}$  block at resting potentials. Figure from Luscher & Malenka, 2012.

### **3. Synaptic Plasticity**

One of the most fascinating brain features is its capacity to adapt and modify neural synapses in response to ever-changing intrinsic and extrinsic stimuli. The idea that synapses could undergo dynamic changes in their activity was first proposed by the Canadian psychologist Donald Hebb, who postulated in 1949 that:

*“When an axon of cell A is near enough to excite a cell B and repeatedly or persistently takes part in firing it, some growth process or metabolic change takes place in one or both cells such that A’s efficiency, as one of the cells firing B, is increased.”* (Hebb, 1949).

These activity-dependent changes in synaptic transmission are the basis of synaptic plasticity (Langille & Brown, 2018). Synaptic transmission can be either enhanced or depressed, and the time span of such changes can be quite variable. Understanding the cellular and molecular mechanisms underlying synaptic plasticity is imperative given that it is the leading candidate for memory formation and storage (Citri & Malenka, 2008). And since the hippocampus is considered the brain’s memory hub, it has become one of the most extensively studied brain regions for synaptic plasticity to date.

#### **3.1 The hippocampal formation and memory**

The striking appearance of a distinct group of millions of neurons, buried deep within the medial temporal lobe of the human brain forming into an elegant, curved structure has captivated anatomists since the first dissections that took place at the Alexandrian school of medicine in classical Egypt. The structure resembles the coiled horns of a ram. Hence, the ancient scholars named the hippocampus cornu ammonis (CA), or the horns of Amun, an ancient Egyptian God, who is often represented as having a ram’s head. Later, the Bolognese anatomist Giulio Cesare Aranzi was the first to introduce the name ‘‘Hippocampus’’ which comes from the greek hippokampos meaning sea horse (Figure 8) (The hippocampus book).

The emergence of microscopy has revealed the neatly organized cellular arrangement of the hippocampus that is condensed into single layers. Thus, the hippocampus was anatomically and functionally divided into four distinct subfields named CA1, CA2, CA3, and CA4, which

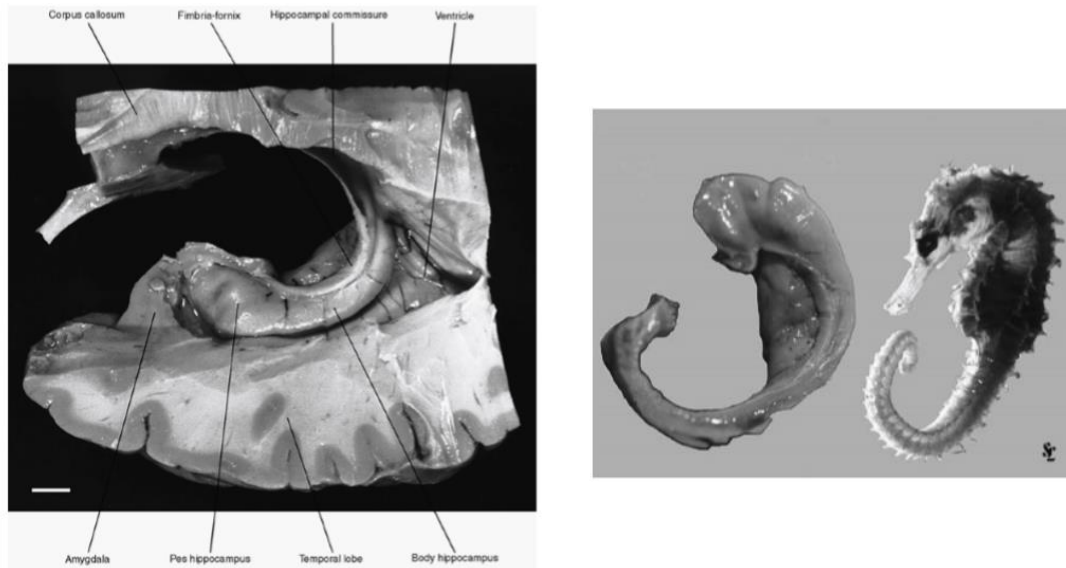


**Figure 8.** Dorsolateral view of the human hippocampus (left). Dissected and isolated human hippocampus compared to the sea horse (Right). (The hippocampus book).

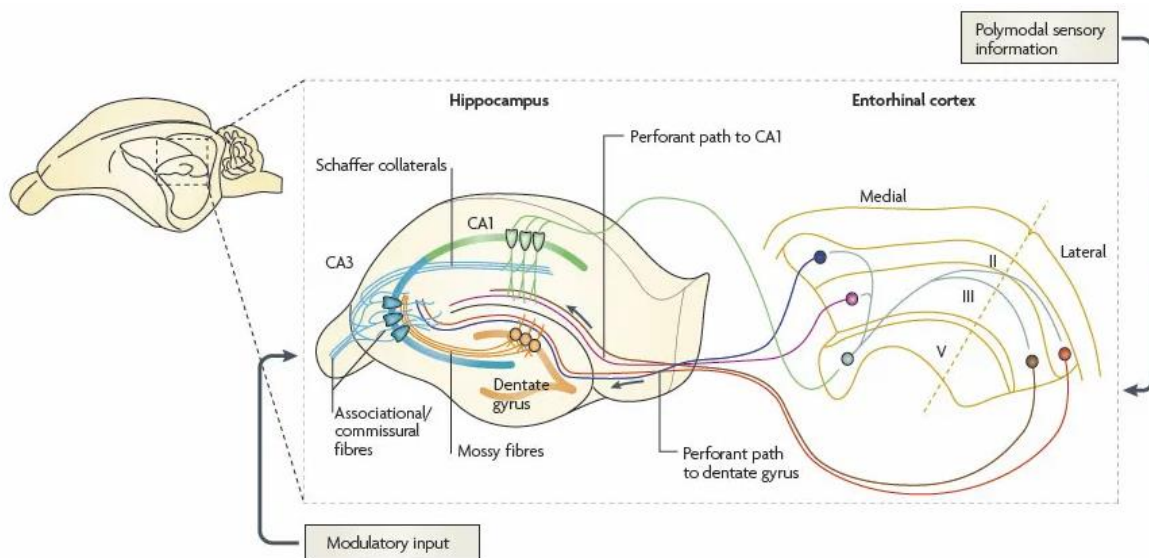


**Figure 9. Basic anatomy of the hippocampus showing the EC-DG-CA3-CA1 circuitry.** The term hippocampal formation is a compound structure that refers to the DG, the hippocampus proper (cornu ammonis), and the subicular cortex. The entorhinal cortex sends projections from layers II, III, V, VI. Figure from Neves et al., 2008.

connect serially to form what is called a ‘trisynaptic loop’ (Figure 9). The major input to the hippocampus is provided by the entorhinal cortex (EC) which projects to the dentate gyrus (DG) granule cells via the perforant path (synapse1). The DG projects mossy fibers to the CA3 region (synapse2). CA3 pyramidal neurons project to the CA1 region via the Schaffer collateral

pathway (synapse3). Finally, CA1 pyramidal neurons project back to the entorhinal cortex, closing the loop. In addition, CA3 neurons provide feedback projections to the DG and make extensive recurrent connections onto other CA3 neurons. The EC also projects directly to the CA3 and CA1 regions (Knierim, 2015). Area CA2 is often excluded from circuit diagrams showing information flow through the hippocampus and has been seen as a transition zone between area CA1 and CA3. However, recent evidence indicates that area CA2 also receives direct excitatory inputs from both layers II and III of the EC (Chevalyere and Siegelbaum 2010), and axons of CA2 pyramidal neurons project to both area CA1 and CA3 (Mercer et al. 2007).

The hippocampus receives direct inputs from the olfactory bulb, and it was historically believed to function solely as an olfactory structure. The first link between the hippocampus and memory formation came from the observation of a case study of H.M. patient who had surgical removal of the medial temporal lobe including large parts of both hippocampi to cure epilepsy, which left him with profound global amnesia. Later, animal studies have confirmed the role of the hippocampus in various forms of memory including episodic memory; the memory of a particular single event, semantic memory; recall of general facts, spatial navigation, short-term memory. Given its crucial role in learning and memory, the hippocampus is indeed one of the earliest and most severely affected brain regions in Alzheimer's disease (AD), the most common cause of dementia. Other roles include the regulation of emotional behavior, motor behavior and hypothalamic functions. (Anand & Dhikav, 2012; Bird & Burgess, 2008).

The memory function of the hippocampus has been correlated to the fact that activity-dependent synaptic plasticity is a prominent feature of hippocampal synapses. Therefore, the hypothesis that synaptic plasticity is the neural basis of information storage in the brain has remained to this day, an inference to the best explanation that has been accepted but yet difficult to prove in practice (Neves et al., 2008). Depending on the specific pattern of activation, synapses can either strengthen or weaken their connections, phenomena that are commonly known as long-term potentiation (LTP) or long-term depression (LTD) respectively. Synaptic plasticity has been studied and well-characterized extensively in the hippocampus due to its simple, laminar neuronal organization that enables the use of electrophysiological techniques to record synaptic events (Edelmann et al., 2017; Neves et al., 2008). However, it is now evident that synaptic plasticity is a property of many excitatory and inhibitory synapses across the brain (Castillo et al., 2011).

### 3.2 Long term potentiation

The first experimental evidence of LTP was performed by Bliss and Lomo in 1973 (Bliss and Lomo, 1973), who demonstrated a long-lasting activity-dependent increase in synaptic efficacy, in a paper that is considered a breakthrough in the field of neuroscience. The broad definition of LTP is the long-lasting enhancement of synaptic strength in response to a brief high-frequency stimulation (Nicoll, 2017). Certainly, LTP exists in many mechanistically distinct forms, at different types of synapses, or even at the same synapse (Edelmann et al., 2017). Adding to the complexity, there are currently more than 100 proteins that have been claimed to be involved in LTP (Granger & Nicoll, 2014).

The classical form of LTP, or the Hebbian form of synaptic plasticity, is exhibited by the perforant path projection to granule cells of the dentate gyrus and by the Schaffer-collateral afferents to the CA1 pyramidal cells of the hippocampus. These synapses express a robust NMDAR-dependent LTP, which is blocked by D-AP5 (D (-)-2-amino-5-phosphonovaleric acid) or other NMDAR-antagonists. It is now generally accepted that LTP is induced by binding of glutamate to AMPA and NMDA receptors, depolarization of the postsynaptic membrane, Ca<sup>2+</sup> influx through NMDARs, transient elevation of postsynaptic Ca<sup>2+</sup> concentration, the release of Ca<sup>2+</sup> from intracellular stores, and the subsequent activation of calcium/calmodulin-dependent protein kinase II (CaMKII) (Figure 10) (Nicoll, 2017). Activated CaMKII is necessary and sufficient for the induction of LTP (Lisman et al., 2012).

The exact mechanisms underlying LTP expression remain debated. A wide variety of induction protocols exist, each with potentially distinct expression mechanisms including high-frequency stimulation (HFS) or tetanus-induced LTP, theta-burst stimulation (TBS), pairing-induced LTP, spike-timing-dependent LTP, and chemically induced LTP (Bliss & Collingridge, 2013). Several key studies demonstrated a primarily postsynaptic locus of LTP expression, where the major contribution comes from increased current through postsynaptic AMPARs. Advances have been made in understanding the role of CaMKII in LTP expression. CaMKII diffuses to the synapse and interacts with the NMDA receptor (NR2B) forming a complex. CaMKII-NMDA receptor complex is believed to act as a molecular memory at the synapse, and is also a mechanism for LTP saturation. The use of Cyanogen bromide (CN) peptides that inhibit CaMKII binding to NMDARs can allow additional LTP induction by reversing saturated LTP (Sanhueza et al., 2011). In addition, activated CaMKII translocates to the PSD and enhances AMPAR-mediated transmission in two ways: phosphorylation of GluA1 (at serine 831),

increasing single-channel conductance, and phosphorylation of extrasynaptic stargazin (an AMPAR auxiliary protein), leading to AMPAR immobilization and trapping at the PSD (Lisman et al., 2012; Hayashi et al., 2000; Opazo et al., 2010).

In addition, strong evidence supports the idea that trafficking and exocytosis of new AMPARs lead to an increase in receptors number at the synapse and is involved in LTP expression. For instance, the use of neurotoxin which blocks exocytosis by cleaving some vesicular SNARE proteins blocks tetanus-induced LTP (Lledo et al., 1998) and HFS-induced LTP, but not short-term potentiation (STP) in the CA1 region of the hippocampus (Penn et al., 2017). Direct visualization of postsynaptic AMPARs exocytosis in dendritic shaft and spines during LTP is possible using pH-sensitive superecliptic pHluorin (SEP)-tagged AMPARs (Kopec et al., 2006, 2007a; Yudowski et al., 2007; Lin et al., 2009; Makino and Malinow, 2009; Petrini et al., 2009; Araki et al., 2010; Kennedy et al., 2010; Patterson et al., 2010; Cho et al., 2015; Tanaka and Hirano, 2012). Additionally, chemically induced LTP using glycine increases SEP-GluA1 exocytosis in dendrites and dendritic spines (Yudowski et al., 2007; Cho et al., 2015). Recent evidence from Choquet's lab shows that surface cross-linking of exocytosed AMPARs blocks both HFS and TBS-induced LTP expression in the CA1 region of the hippocampus (Penn et al., 2017).

Surface AMPARs tune synaptic transmission via a constant exchange between synaptic and extrasynaptic sites (Heine et al., 2008). Accordingly, several studies accentuate the role of AMPAR lateral diffusion for the incorporation of the receptor at the synapse during LTP (Makino and Malinow, 2009; Penn et al., 2017). Given the fact that AMPAR exocytosis during LTP occurs at sites adjacent to the PSD, it would require these exocytosed receptors to be relocated via lateral mobility to synapses for synaptic potentiation. It is therefore proposed that pre-existing extrasynaptic AMPARs at the surface provide the reservoir for the initial phase of potentiation, whereas newly exocytosed AMPARs from the recycling endosomes are required for LTP maintenance (Figure 11) (Choquet, 2018).

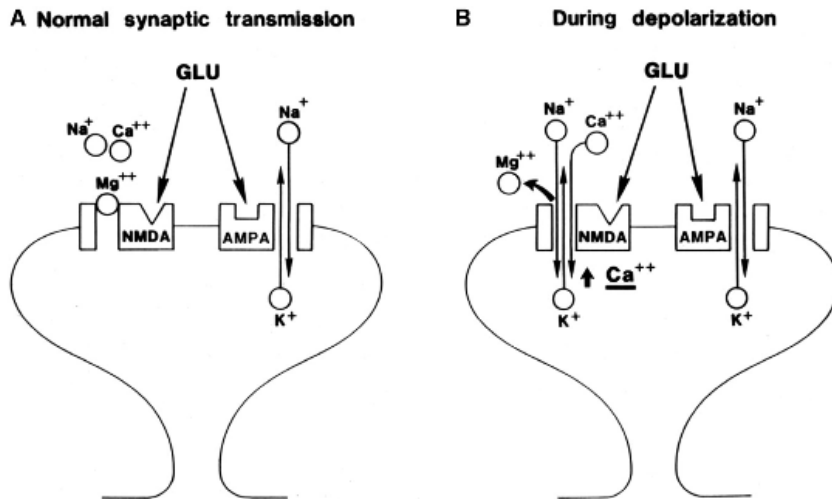


**Figure 10. Model for LTP induction in the hippocampal CA1 region.** Under basal conditions, glutamate could bind to both AMPA and NMDA receptors, but mainly AMPARs mediate basal synaptic transmission. Upon adequate depolarization of postsynaptic membrane,  $Mg^{2+}$  blockade is expelled, NMDA receptors are activated allowing the influx of cations, mainly calcium mediating downstream calcium-calmodulin signaling events. Figure from Nicoll, 2017

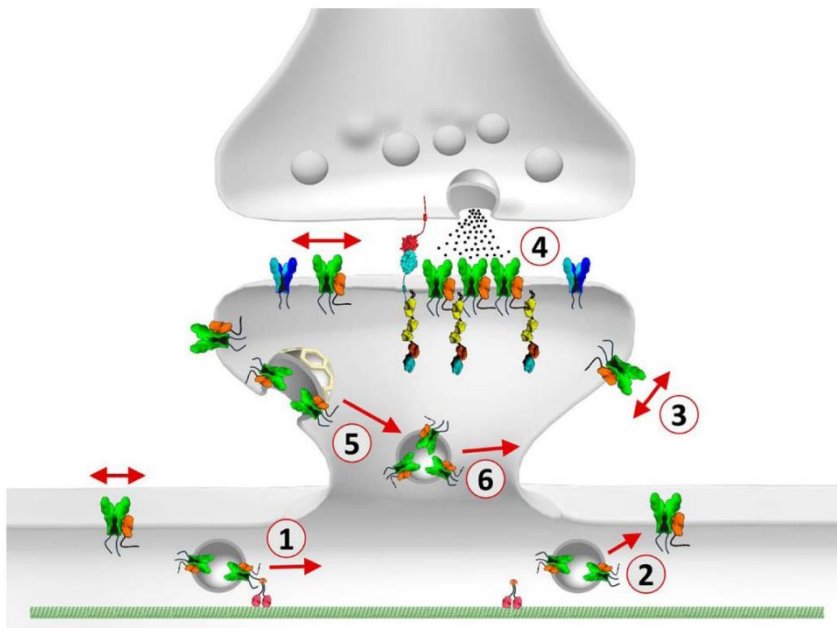


**Figure 11. Trafficking of AMPA receptors during LTP.** 1- AMPA receptors are trafficked along microtubules to reach the target synapse. 2- Vesicles are exocytosed mainly at extrasynaptic sites in the dendritic shaft. 3- Receptors reach the synapse via lateral mobility. 4- They are stabilized at the PSD via interaction with scaffold proteins. 5- Receptors are endocytosed and can be recycled back to the plasma membrane. Figure from Choquet, 2018.

### 3.3 Long term depression

Long-term depression or LTD is the contrasting phenomenon of LTP, which is the persistent, use-dependent decrease in synaptic efficacy or strength. Two broad forms of LTD exist, heterosynaptic and homosynaptic. Heterosynaptic LTD occurs at inactive synapses, or in a non-conditioned input, whereas, homosynaptic LTD is usually induced in the conditioned input, thus is known to be input-specific (Figure 12). Homosynaptic LTD can be further divided into two main types: depotentiation, which is the depression of a potentiated response observed after LTP induction or *de novo* LTD which is observed from baseline conditions. These different forms of LTD have different molecular mechanisms and probably serve different functions. Generally, LTD is involved in some types of learning and memory, cognitive flexibility, acute stress-induced cognitive defects, drug addiction, and neurodegeneration (Collingridge et al., 2010).

The discovery of LTD came from Dunwiddie and Lynch in 1978, who first reported that LTD could be induced with low-frequency stimulation (LFS) (100 stimuli at 1Hz) (Dunwiddie and Lynch, 1978). However, interest in LTD began to accelerate later in 1992 when Dudek and Bear showed that prolonged trains of low-frequency stimulation (LFS) (900 stimuli at 1 Hz) induced reliable homosynaptic LTD in hippocampal slices. LTD induced with this protocol is long-lasting, input specific, and NMDAR-dependent (Dudek and Bear, 1992). Nevertheless, it was not clear at that time whether the induction of LTD in the hippocampal area CA1 was solely NMDAR-dependent or if the process can be triggered by mGluRs (Dudek and Bear, 1992; Bashir et al., 1993). In 1997, Oliet et al. confirmed the existence of both types of homosynaptic LTD and showed that it was possible to induce both types by changing the induction protocol.

LTD can be induced by LFS (typically 900 stimuli at 1-3 Hz), by pairing baseline stimulation with depolarization (to -40 mV), appropriately timed back-propagating action potential (a form of spike-timing-dependent plasticity or STDP), or chemically induced using an NMDAR agonist, such as 3,5-dihydroxyphenylglycine (DHPG) or NMDA. Most synapses that undergo LTD are glutamatergic, and like LTP require NMDAR activation. The determinant of the synaptic modification polarity is widely assumed to be the kinetics, subunit composition, and the magnitude of activation of NMDARs. For example, the NR2A-containing NMDARs are important for LTP, whereas *de novo* LTD requires NR2B-containing receptors (Collingridge et al., 2004).

NMDAR-dependent LTD at CA1 synapses is usually induced by LFS. It is dependent mainly on postsynaptic alterations that lead to AMPARs removal from the synapse or alteration in the conductance properties of the receptors (Collingridge et al., 2004). However, evidence exists that this form of LTD can also involve a reduction in the probability of glutamate release through either direct changes in presynaptic terminals or by postsynaptic changes that are communicated via a retrograde messenger including nitric oxide (NO) (Stanton et al., 2003). The expression mechanism depends on the type of synapse and the developmental stage of the animal among possible other factors (Collingridge et al., 2010).

The postsynaptic expression of NMDAR-dependent LTD requires a modest increase in  $\text{Ca}^{2+}$  influx through NMDARs and the subsequent activation of two phosphatases. Intracellular  $\text{Ca}^{2+}$  binds to calmodulin and activates the calcium/calmodulin-dependent protein phosphatase 2B (PP2B), also known as calcineurin, which dephosphorylates inhibitor 1 leading to the activation of protein phosphatase 1 (PP1) (Lisman, 1989; Milkey et al., 1993, 1994; Carroll et al., 2001). The modest increase in calcium will preferentially activate calcineurin, which has a higher affinity for calcium/calmodulin than does CaMKII, and is therefore a preferential trigger for LTD and not LTP. In addition,  $\text{Ca}^{2+}$  entry through NMDARs triggers the release of  $\text{Ca}^{2+}$  from intracellular stores, which may initiate endocytosis via activation of  $\text{Ca}^{2+}$  sensitive enzymes away from the PSD (Collingridge et al., 2010).

In support of the role of AMPAR endocytosis during NMDAR-LTD, several proteins that regulate clathrin-mediated endocytosis are involved in this process. For instance, AMPARs are stabilized at the membrane by an N-ethylmaleimide-sensitive factor (NSF; an ATPase involved in membrane fusion events), which interact with GluA2 subunits. During LTD, a small rise in  $\text{Ca}^{2+}$  ( $10^{-7}$  to  $10^{-5}\text{M}$ ) is sensed by hippocalcin; a member of the neuronal calcium sensor (NCS) family. Hippocalcin then translocates to the plasma membrane and forms a complex with AP2 (clathrin adaptor protein), that replaces NSF binding site on GluA2 and initiates clathrin-mediated AMPAR endocytosis (Palmer et al., 2005). Another molecule that help dissociate synapse-tethered AMPARs is PICK1 (protein interacting with C-kinase), which is a low-affinity  $\text{Ca}^{2+}$  sensor that targets activated  $\text{PKC}\alpha$  (protein kinase C) to dendritic spines and phosphorylates serine 880 of GluR2. Once phosphorylated, AMPARs can be released from synaptic anchoring proteins GRIP (glutamate receptor-interacting protein) and ABP (AMPA receptor-binding protein), where they are free for lateral diffusion and internalization (Perez et al., 2001; Kim et al., 2001). In addition, the endocytic adaptor RAI1BP1 (Ras-related protein (Ra1A)-binding protein 1); an AP2 targeting molecule is involved in NMDAR-dependent LTD.

NMDAR activation stimulates the small GTPase Ra1A which binds and translocates RA1BP1 to dendritic spines. Also, NMDAR activation dephosphorylates Ra1BP1 allowing its interaction with PSD-95. These two interactions are necessary and sufficient for the induction of AMPAR endocytosis during NMDAR-dependent LTD (Han et al., 2009). Furthermore, several serine/threonine protein kinases are implicated in NMDAR-LTD including protein kinase A (PKA) (Brandon et al., 1995), cyclin-dependent kinase 5 (CDK5) (Oshima et al., 2005), P38 mitogen-activated protein kinase (p38MAPK) (Zhu et al., 2005) and glycogen synthase kinase-3 (GSK-3) (Peineau et al., 2007; Peineau et al., 2009; Bradley et al., 2012).

In conclusion, long-lasting changes in synaptic efficacy can bi-directionally affect synaptic strength and is underlying many forms of experience-dependent plasticity including learning and memory. Such synaptic plasticity is mainly dependent on the trafficking of AMPARs to and away from the synapse. LTD requires the removal of AMPARs from the synapse and their trafficking to endocytic zones. Contrary to this process is LTP, which is dependent on the exocytosis and delivery of intracellular AMPARs to synaptic sites (Figure 13) (Malenka, 2003; Choquet, 2018).

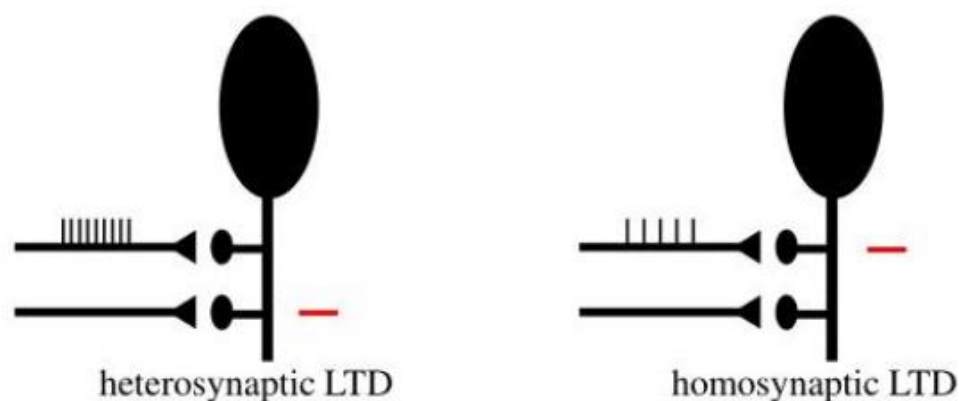


**Figure 12. The two major forms of LTD.** Heterosynaptic LTD is induced in a test pathway (2) when a conditioning pathway (1) is stimulated by a tetanic pulse for example. Homosynaptic LTD is confined to the stimulated synapse and is typically induced by prolonged low-frequency stimulation (1 Hz for 10 min) of afferent fibers (1). Figure from Linden and Connor, 1995.

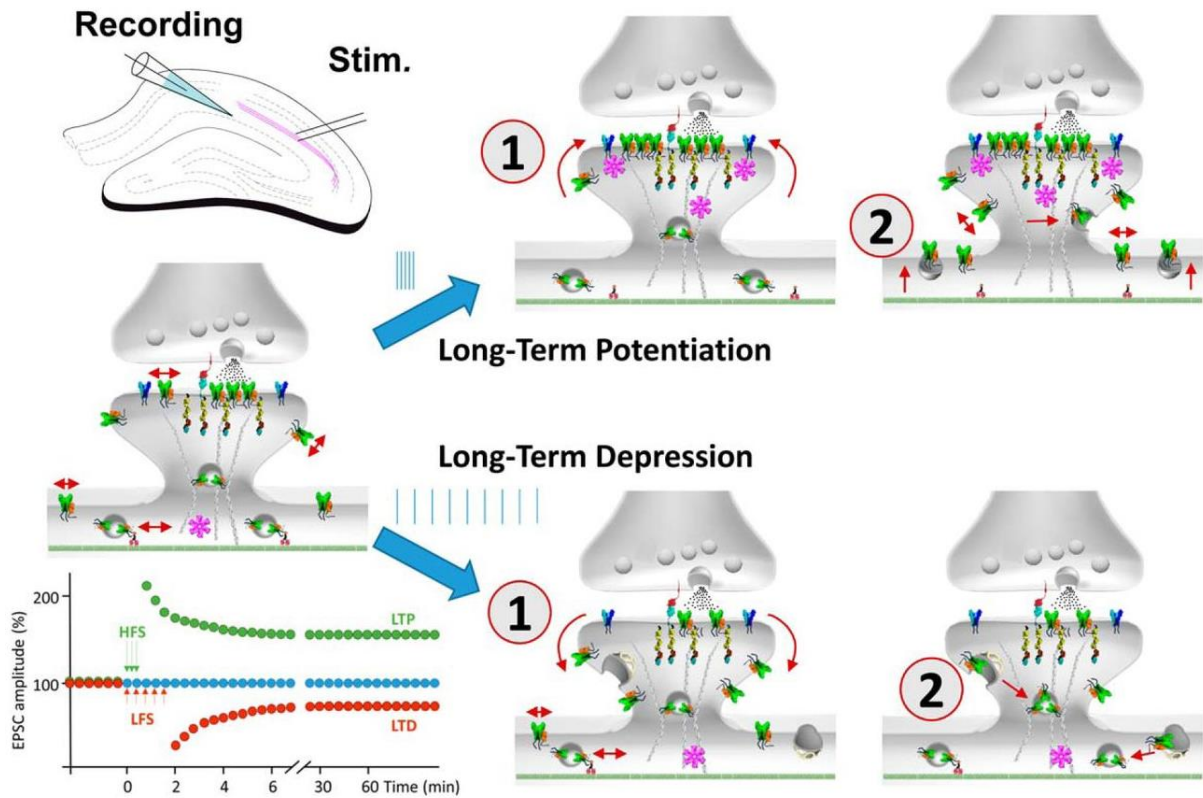


**Figure 13. Model of AMPA receptor trafficking during synaptic plasticity.** The molecular mechanisms of LTP and LTD have been best characterized at the Schaffer collateral-CA1 synapse of the hippocampus. High-frequency stimulation of Schaffer collateral afferents induces LTP in CA1 pyramidal cells that can last for hours. 1- Activation of CAMKII (pink) leads to AMPARs trapping and stabilization at the PSD. 2- Exocytosis of intracellular receptors mainly at the dendritic shaft but also directly into the spine replenishes the extrasynaptic pool of receptors. In contrast, low-frequency stimulation induces LTD. 1- AMPA receptors are released from PSD. 2- They diffuse and endocytose in the spine or at the dendritic shaft. Figure from Choquet, 2018.

### 3.4 Structural plasticity

Besides the functional aspects of synaptic plasticity, synaptic modifications are associated with structural rearrangements in dendritic spines; the characteristic morphological feature of excitatory synaptic transmission. Structural plasticity is also tightly controlled by activity, NMDAR dependent, and affects the organization and development of neuronal networks in the brain (Bernardinelli et al., 2014). However, the intrinsic relationship between the functional and the structural plasticity is not fully understood (Bosch & Hayashi, 2012).

Dendritic spines were first described by Santiago Ramon y Cajal and were proposed to be the contact sites between axons and dendrites. A hypothesis that was later confirmed with the advent of electron microscopy. Rather than having an immutable structure, spines have a unique and highly heterogeneous morphological organization that serves as electrical and biochemical confined compartments allowing each spine to function independently. They can exhibit thin, elongated filopodia-like protrusions (longer than  $4\mu\text{m}$ ), which lack distinctive heads and are thought to be spine precursors that appear during cortical development and diminish with adulthood. Dendritic filopodia are highly motile and exploratory in nature, which when in contact with an axon, can gradually develop into more mature thin, stubby, or mushroom-like structures with a prominent head and thin neck ( $0.2\mu\text{m}$  in width) (Figure 14) (Harris et al., 1992; Friedman et al., 2000; Li & Sheng, 2003; Noguchi et al., 2005). Time-lapse imaging studies have shown the dynamic picture of spines, where they can form, enlarge, shrink, and retract throughout the animal's life. Their morphology and dynamics vary with neuronal types, in response to different sensory experiences, across developmental stages, and in various learning paradigms. The rapid alterations in spine formation and elimination are thought to be the structural substrate for memory encoding in the mammalian brain (Chen et al., 2014).

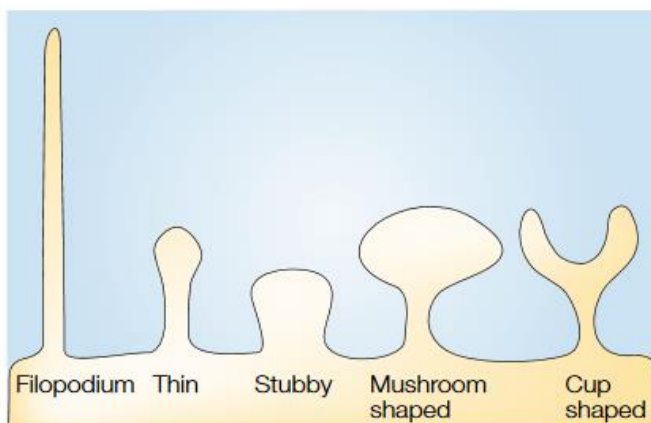


**Figure 14. The morphology of dendritic spines.** Spines are typically  $<2\mu\text{m}$  in length. Filopodia are elongated dendritic protrusions that are longer than  $4\mu\text{m}$ . The thin spine contains a small head and a thin long neck. Stubby spine lacks an apparent neck. Mushroom spine contains a large mushroom-shaped head. Cup-shaped spines are less common. Image from Hering & Sheng, 2001.

Despite early speculations that memory is associated with structural changes in the brain, the very first reports that morphological changes in dendritic spines are activity-dependent came from studies by Fifkova and colleagues. They showed that tetanic stimulation of the perforant path induced long-lasting enlargement of dendritic spines in the dentate granular cells compared to a control pathway (Harrevelde & Fifkova, 1975), and these spines had wider and shorter spine necks (Fifkova & Harrevelde, 1977; Fifkova & Anderson, 1981). Later, evidence accumulated that the induction of synaptic plasticity causes changes in the number or shape of spines (Figure 15). For example, it has been shown that new spines are formed in hippocampal slice cultures upon LTP induction, which was prevented by the use of the NMDA receptor antagonist AP5 (Engert & Bonhoeffer, 1999; Maletic-Savatic & Svoboda, 1999). Chemically induced LTP in dissociated hippocampal neurons is also associated with the rapid formation of new spines (Lin et al., 2004; Park et al., 2006). These alterations could last for many hours and might have a key role in maintaining molecular changes in synaptic transmission during memory formation (Lamprecht & LeDoux, 2004).

In addition, *in vivo* changes in spine density persisting for weeks or months have been found in various brain regions following a learning paradigm (Figure 15) (Leuner et al., 2003; Geinisman et al., 2001; Kleim et al., 2002; Knafo et al., 2004; Xu et al., 2009; Yang et al., 2009). Better behavioral performance of the animal during training was correlated with the degree of spine enlargement and a greater amount of spine AMPARs (Yang et al., 2009; Roth et al., 2019). Furthermore, NMDAR dependent enlargement of single dendritic spines is seen with two-photon glutamate uncaging which is associated with an increase in AMPAR mediated currents, calmodulin, and actin polymerization (Matsuzaki et al., 2004). The enlargement of single spines was also dependent on brain-derived neurotrophic factor (BDNF) and protein synthesis when two-photon uncaging was paired with spike-timing-dependent protocol in rat brain slices (Tanaka et al., 2008). Remarkably, LTP induced by glutamate uncaging, besides forming new spines, also increased the stability of individual newly formed spines (Hill & Zito, 2013). In contrast, LTD inducing stimulus causes a synapse-specific spine shrinkage and retraction that is dependent on both NMDARs and mGluRs (Oh et al., 2013).

Taken together, these studies suggest that NMDAR dependent LTP induction modulates dendritic spines through the enlargement of preexisting spines, the formation of new spines, and the stabilization of newly formed spines (Lai & Ip, 2013). Notably, LTP might be preferentially induced in small spines, whereas larger spines are the physical traces for long term memory formation (Matsuzaki et al., 2004).

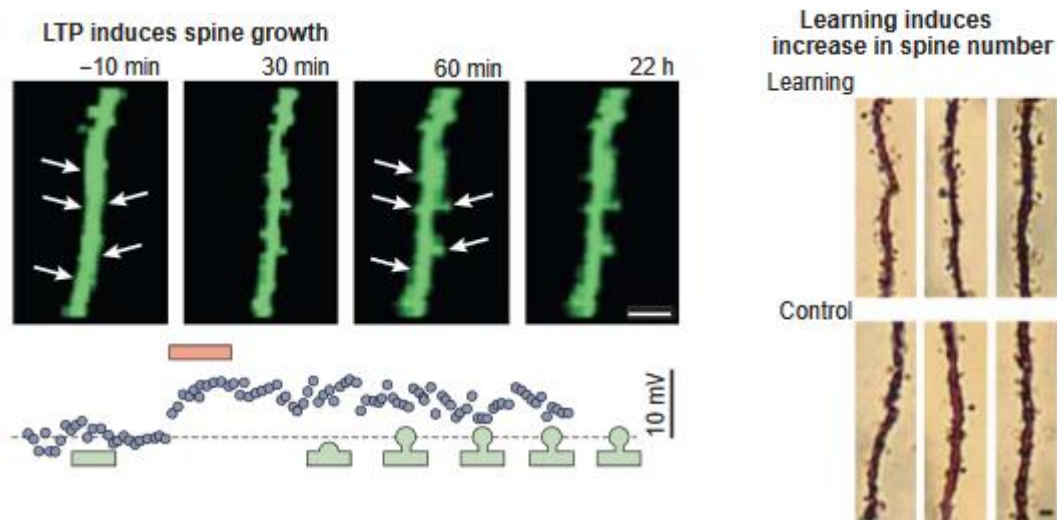


**Figure 15. Morphological changes in dendritic spines after LTP or learning.** The left panel shows new spine growth after LTP induction using two-photon microscopy (Engert & Bonhoeffer, 1999). The right panel shows an increase in spine density 24 hours after learning (trace eyeblink conditioning) using Golgi staining (Leuner et al., 2003). Figure from Lamprecht & LeDoux, 2004.

The molecular mechanisms responsible for structural plasticity of spines involve actin filaments that are enriched at the PSD in the dendritic spines forming a lattice structure within the spine head and neck (Figure 16) (Lai & Ip, 2013; Bosch & Hayashi, 2012). The postsynaptic actin is a highly dynamic structure that undergoes constant treadmilling by an equilibrated rate of F-actin (filamentous actin) polymerization and depolymerization. Over 80% of F-actin turns over per minute in spines (Star et al., 2002). At the basal state, F-actin binds to CAMKII $\beta$  which prevents the binding of other actin-binding molecules. Upon NMDAR-dependent LTP induction, CAMKII $\beta$  is activated ( $\sim$ 1min) and is detached from F-actin leading to an initial phase of rapid actin remodeling. F-actin disassembly or unbundling is followed by a period of F-actin assembly through polymerization and branching (as fast as  $\sim$ 20 sec after LTP induction). Then, there is a net increase in actin and F-actin polymerization rate leading to the long-term stabilization of the dendritic spine and consolidated spine expansion (Bosch et al., 2014; Borovac et al., 2018). Such changes are mainly controlled by the rapid recruitment of several actin-binding proteins (ABPs) such as cofilin, actin interacting protein 1 (Aip1), actin-related proteins 2 and 3 complexes (Arp2/3). These proteins function to modify F-actin where Arp2/3 works in synergy with cofilin (severing) and Aip1 (capping) and generates a dense network of branched actin within the dendritic spine. The new set of branched actin filaments are involved in spine expansion, maintenance, and delivery of proteins to the PSD, especially GluA1-containing AMPARs. Other proteins include profilin, drebrin, and  $\alpha$ -actinin which are

F-actin stabilizers that are transiently depleted upon LTP induction allowing actin remodeling (Bosch et al., 2014; Ackermann & Matus, 2003). The stabilization of the newly reorganized F-actin cytoskeleton can support the long-term maintenance of structural changes and spine enlargement (Borovac et al., 2018; Lee et al., 2015).

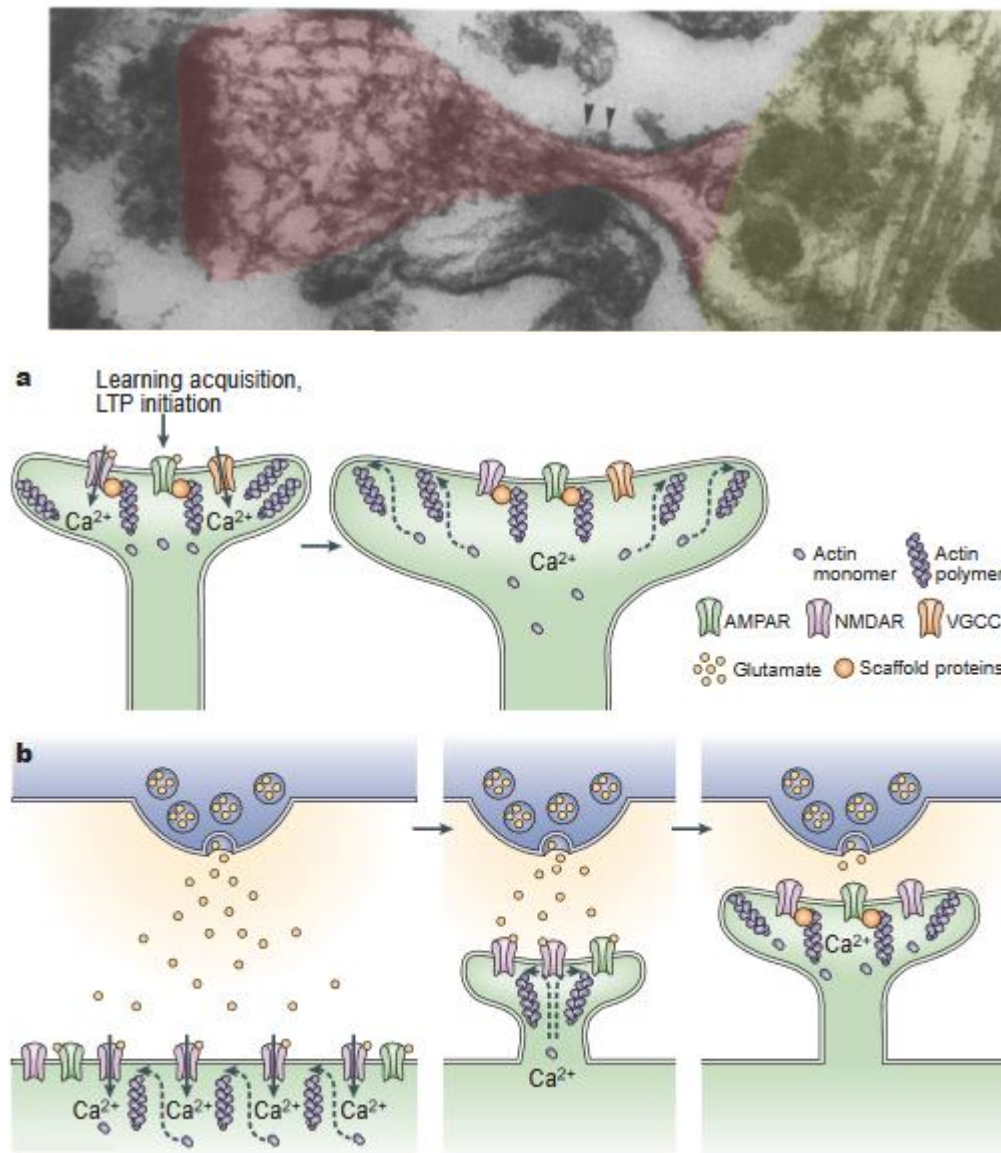


**Figure 16. Spine remodeling is dependent on the actin cytoskeleton.** (Upper panel) An electron microscopic image of a dendritic spine showing actin filaments. Arrows point to S1-fragment labeled F-actin. Shown in red is the spine head, and in yellow is the dendritic shaft. (Bosch & Hayashi, 2012). (Lower panel) LTP induction causes rapid actin polymerization which leads to spine enlargement (a) or formation of new spines (b). Figure from Lamprecht et al., 2004.

## B. Membrane trafficking and exocytosis machinery

### 1. The endosomal system

The endosomal system plays multiple roles in cellular functions including establishing and maintaining neuronal polarity, neuronal development, migration, axonal growth, and guidance. Notably, for neurons to accommodate their unique morphology, they need to accurately sort and traffic newly synthesized integral membrane proteins over long distances from the cell body to dendritic spines. Importantly, the local trafficking at the post-synaptic membrane underlies various forms of synaptic plasticity via regulating the number and availability of plasma membrane receptors and other cargo molecules (Kennedy & Ehlers, 2006).

Newly synthesized proteins are delivered from the endoplasmic reticulum (ER) via the Golgi and trans-Golgi network (TGN) to the plasma membrane. The endocytic pathway starts with the internalization of cargo molecules at the plasma membrane by endocytosis. Different modes of endocytosis exist, but the most widely studied is clathrin-mediated endocytosis (CME). Clathrin is a triskelion composed of three heavy chains and three light chains, which forms lattice-like structures on the interior face of the plasma membrane (Kirchhausen, 2000). Membrane invagination is initiated by the adaptor protein AP-2 which nucleate the formation of the clathrin lattice. The large GTPase dynamin is required to pinch off clathrin-coated invaginations forming intracellular vesicles. Other forms of endocytosis include clathrin-independent, pinocytosis, and phagocytosis (Lisiecka & Winckler, 2011; Kennedy & Ehlers, 2006).

The endosomal network is composed of several distinct types of compartments including early/sorting endosomes (EE), recycling endosomes (RE), late endosomes (LE), and lysosomes (Figure 17). The distinction is established by different functional criteria, phospholipid content, and molecular markers. Most endocytosed cargoes enter in endocytic vesicles which can either fuse with the EEs or with each other to create the EEs. From the EE, molecules can be trafficked to the LEs and lysosomes via multivesicular bodies (MVBs), to TGN, or traffic back to the plasma membrane directly or via REs. The direct recycling from the EEs is fast and returns cargo to the same site of their original endocytosis. Recycling from the RE is slower and usually returns cargo to multiple locations on the cell surface. Along the endosomal pathway, luminal pH gradually acidifies from ~7.0 to ~6.0 of the EEs with the lowest pH found in lysosomes (pH

< 5). Acidification affects the activity of luminal enzymes and allows ligands to dissociate from their receptors (Yap & Winckler, 2012; Schmidt & Haucke, 2007).

The regulated trafficking finely tunes receptor distribution and signaling (Huotari and Helenius, 2011) and trafficking defects have been linked to neurodegenerative diseases. For example, AD neurons have defective trafficking which leads to the abnormal physical proximity between the amyloid precursor protein (APP) and its  $\gamma$ -secretase  $\beta$ -site APP cleaving enzyme 1 (BACE1) in endosomes. This results in an increased generation of the  $\beta$ -amyloid peptide, the main constituent of senile plaques in AD brains (Sun and Roy, 2017).

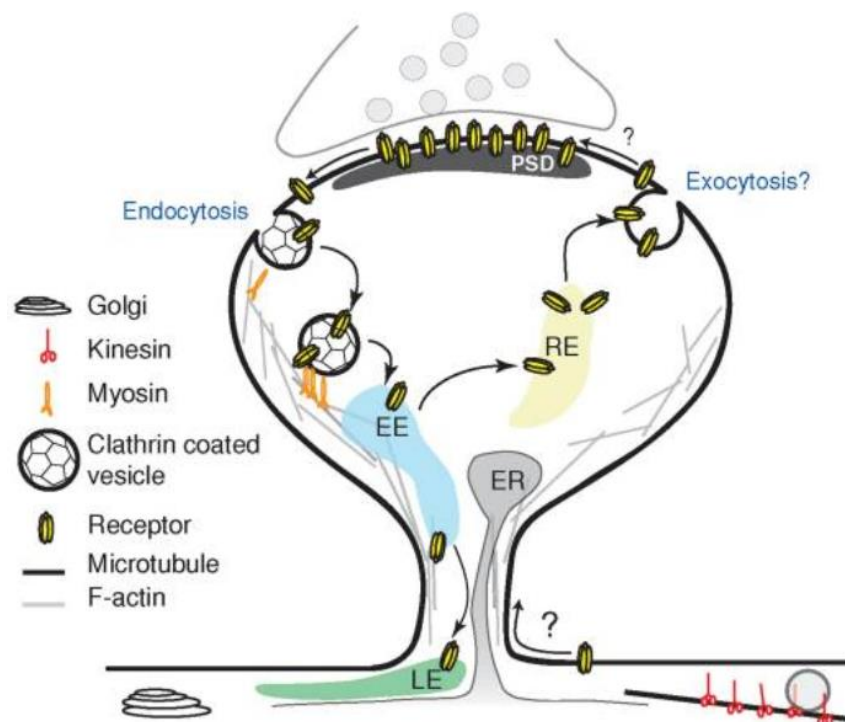


**Figure 17. Local trafficking at the post-synapse.** Cell surface receptors diffuse from the synapse where they are internalized at endocytic zones surrounding the PSD. They traffic to EEs and are either sorted to LE for degradation or REs to return to the plasma membrane. Receptors reach cell surface by exocytosis at the dendritic shaft where they can diffuse to the spine, or directly at the spine head. Figure from Kennedy & Ehlers, 2006.

## **2. SNARE-mediated membrane fusions**

The compartmentalization of biological membranes within eukaryotic cells renders the processes of membrane trafficking and fusion an absolute necessity for maintaining the vital functions of the cells. The end step of such membrane vesicle trafficking is the fusion of two lipid bilayers. A process that is normally energetically unfavorable to the cells, and is therefore catalyzed by specialized machinery of fusion proteins called soluble NSF-attachment protein (SNAP) receptors or SNAREs. SNAREs have become the most intensively studied proteins involved in intracellular trafficking pathways since their discovery (Ungar & Hughson, 2003; Wang et al., 2017; Han et al., 2017).

### **2.1 The SNARE complex structure and function**

#### **2.1.1 SNARE structure and classification**

The SNARE proteins are a large superfamily of 20 to 30 kDa proteins comprising more than 60 members in mammalian and yeast cells. They harbor a conserved coiled-coil stretch of 60-70 amino acid residues called the SNARE motif which has an intrinsic  $\alpha$ -helical configuration that binds SNARE proteins to each other (Weimbs et al. 1997; Fasshauer et al., 1998; Kloepper et al., 2007). Most SNAREs are integral membrane proteins that are anchored via their carboxy-terminal transmembrane domains. The pairing of a distinctively localized v-SNARE (vesicular SNARE) with a cognate pair of t-SNARE (target SNARE) forms a trans-SNARE complex. This has led to the SNARE hypothesis by Rothman in 1993 who proposed that SNARE proteins provide specificity for a controllable fusion of membranes, a role that is now no longer a hypothesis (Söllner et al., 1993; Südhof & Rizo, 2011; Jahn & Scheller, 2006). The first SNARE complex identified is located at the presynaptic neuron and contains 3 SNAREs, the vesicle-associated membrane protein 1 (VAMP1), the plasma membrane-associated protein 1 (syntaxin1), along with the synaptosomal-associated protein of 25 kDa (SNAP25) (Figure 17) (Trimble et al., 1988; Bennett et al., 1992). Generally, the SNARE complex consists of 1 v-SNARE and 2 or 3 t-SNAREs which form an extremely stable four-helix bundle of SNARE proteins that interact via their amphipathic  $\alpha$ -helical domains. The parallel arrangement of the SNARE motifs within the SNARE complex brings the two membranes into close apposition and provides enough energy for the fusion process (Scales et al., 2000; Fasshauer et al., 1998; Sutton et al., 1998).

Although SNAREs are functionally classified as t-SNAREs or v-SNAREs, this classification scheme is sensible for reactions that involve fusion between a vesicle and an organelle or a plasma membrane such as in neurotransmitter release. However, the scheme might not be applicable for other types of reactions that are not inherently asymmetric such as homotypic fusion of yeast vacuoles. Therefore, another nomenclature has been developed that structurally classifies SNARE proteins into glutamine Q-SNARE or arginine R-SNAREs. This nomenclature describes the interior of the four-helix bundle of the SNARE complex which is highly conserved, mostly hydrophobic residues, but has a hydrophilic ionic layer in the center. This ionic layer (also called '0' layer) is formed from an arginine residue contributed by the SNARE motif of synaptobrevin and three glutamine residues contributed by each of the three SNARE motifs of syntaxin and SNAP25, respectively (Figure 18). These residues make hydrogen bonds inside the hydrophobic core. The Q SNAREs can be further subdivided into Qa-, Qb-, and Qc-SNAREs based on the amino acid sequence of the SNARE domain. Both naming schemes are still in common use and in many cases, the R-SNARE is contributed by the transport vesicle (the v-SNARE), and three Q-SNAREs are contributed by the target acceptor membrane (the t-SNAREs) (Weimbs et al., 1997; Fasshauer et al., 1998; Ungar & Hughson, 2003; Hong, 2005; Jahn & Südhof, 1999).

### **2.1.2 Main SNARE proteins**

VAMPs are a group of small transmembrane R-SNARE proteins. There exist seven genes of the VAMP family (1, 2, 3, 4, 5, 7, 8), all of which are reported to form functional SNARE complexes except VAMP5 (Hasan et al., 2010). Sec22 and Ykt6 are additional R-SNAREs in mammals (Jahn & Scheller, 2006). VAMP1 and 2 (synaptobrevins) are brain-specific SNAREs that consist of a short NH<sub>2</sub>-terminal sequence, a SNARE motif, and a COOH-terminal transmembrane region (Schoch et al., 2001). VAMP1 is highly expressed in the spinal cord and neuromuscular junctions and less in the brain. VAMP2 is the most abundant and widely distributed throughout the brain (Madrigal et al., 2019; Hoogstraaten et al., 2020). Both VAMP1 and VAMP2 are highly enriched in synaptic vesicles. VAMP3 (cellubrevin) is highly expressed in glial cells but is undetectable in neurons (Schoch et al., 2001). VAMP4 is enriched in TGN and EEs. VAMP5 is mainly expressed in the skeletal muscle and heart. VAMP7 is enriched in late endosomal compartments and the lysosomes and is also involved in neurite outgrowth. VAMP8 (endobrevin) has low expression in the brain and may function in regulated exocytosis of the exocrine system (Wang et al., 2004). Sec22b is enriched in the transport between the ER and the cis-Golgi, whereas Ykt6 is enriched in the cis-Golgi and Golgi stack (Tran et al., 2007).

Syntaxins are small transmembrane proteins that contain an NH<sub>2</sub>-terminal three-helical domain that interacts with multiple other proteins in addition to a SNARE motif and a membrane anchor. They comprise 15 members, four of which (Stx 1-4) localize to the plasma membrane and mediate fusion events (Teng et al., 2001).

SNAP proteins are Q-SNAREs which contribute two SNARE motifs to the SNARE complex (Sutton et al., 1998). There are four isoforms: SNAP 23, 25, 29, and 47 that are named based on their molecular weight. SNAP-25 has been extensively studied for its role in neurotransmitter release (Kádková et al., 2019).

### **2.1.3 The SNARE cycle**

It is generally accepted that the SNARE complexes directly mediate membrane fusions, however, this does not rule out the involvement of other regulatory proteins (Ungar & Hughson, 2003). The SNARE complex pairing, assembly, and disassembly are highly regulated by a variety of auxiliary machinery including tethering factors, SM (Sec1/Munc18 family) proteins, NSF, and  $\alpha$ -SNAP (Wang et al., 2017). SNARE proteins undergo a fusion cycle of the assembly into complexes that catalyze fusion, and disassembly of the complexes by the AAA ATPase NSF and SNAPs which make SNARE proteins available for another cycle of fusion.

SNARE proteins are usually maintained in inactive conformations in the cellular milieu via an amino-terminal three-helix domain in the syntaxin Q-SNARE protein, called the Habc domain (Figure 18). This domain folds on the SNARE motif forming a closed conformation. The opening of the Habc domain switches the SNARE protein to the active conformation making it accessible for association with two other Q-SNARE motifs (e.g. SNAP25). This activation step is regulated by the Sec/Munc18 (SM) and tethering proteins. Syntaxin binding to SM proteins promotes conformational change that frees the SNARE motif allowing interaction with the rest of the SNARE proteins (Jahn & Scheller, 2006). The SNARE complex is finally formed by the association with the R-SNARE protein to form the four-helix structure. The SNARE complex formation starts with the amino- (the distal end of the membrane) to carboxy- (proximal end of the membrane) terminal zippering that brings the two fusing membranes in nanometer proximity and the vesicle is in a "docked state". The full zippering of the trans-SNARE complex possibly produces fusion pore opening per se, or the fusion occurs subsequently mediated by the SM protein. A point contact, called the fusion stalk between two fusing membranes initiates membrane fusion. This fusion stalk expands to form a hemifusion structure, where only the outer membrane leaflets are merged but not the inner leaflets. This

hemifusion structure is observed with optical super-resolution microscopy during several cellular fusion processes such as dense-core vesicle fusion (Zhao et al., 2016; Kweon et al., 2017). Then, pore formation and expansion marks the final connection between the membrane contents and completes the cycle of membrane fusion. After the membranes completely merge, the trans-SNARE complexes are converted into cis-SNARE complexes on a single membrane, which are then dissociated into monomers by the ATPase NSF in conjunction with its adaptors SNAPs. Finally, the vesicles recycle and are ready to start another round of the fusion cycle (Figure 19) (Südhof & Rizo, 2011; Yoon & Munson, 2018).

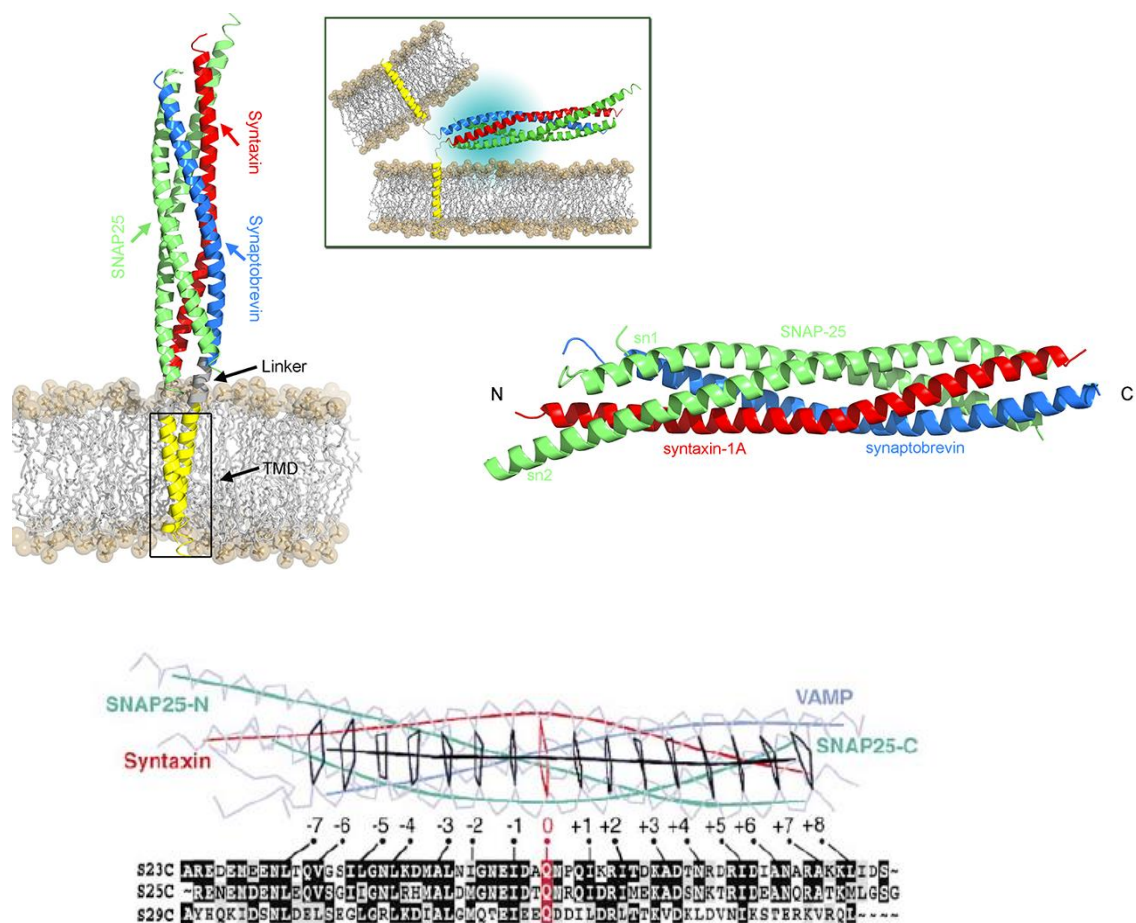


**Figure 18. Structural organization of the synaptic fusion complex embedded in a lipid bilayer.** The cis-SNARE complex consists of one syntaxin, one synaptobrevin, and two SNAP-25. Synaptobrevin and syntaxin have a cytoplasmic domain (SNARE motifs), a short linker domain, and a transmembrane domain (TMD). The top right panel shows the SNARE complex in the prefusion state. At the bottom is the structure of the four-helix bundle showing the 15 hydrophobic layers numbered from -7 to +8 and are outlined in black. In red is the central ionic layer (0) with the conserved amino acid glutamine. Figure from Sutton et al., 1998; Stein et al., 2009; Scales et al., 2000.

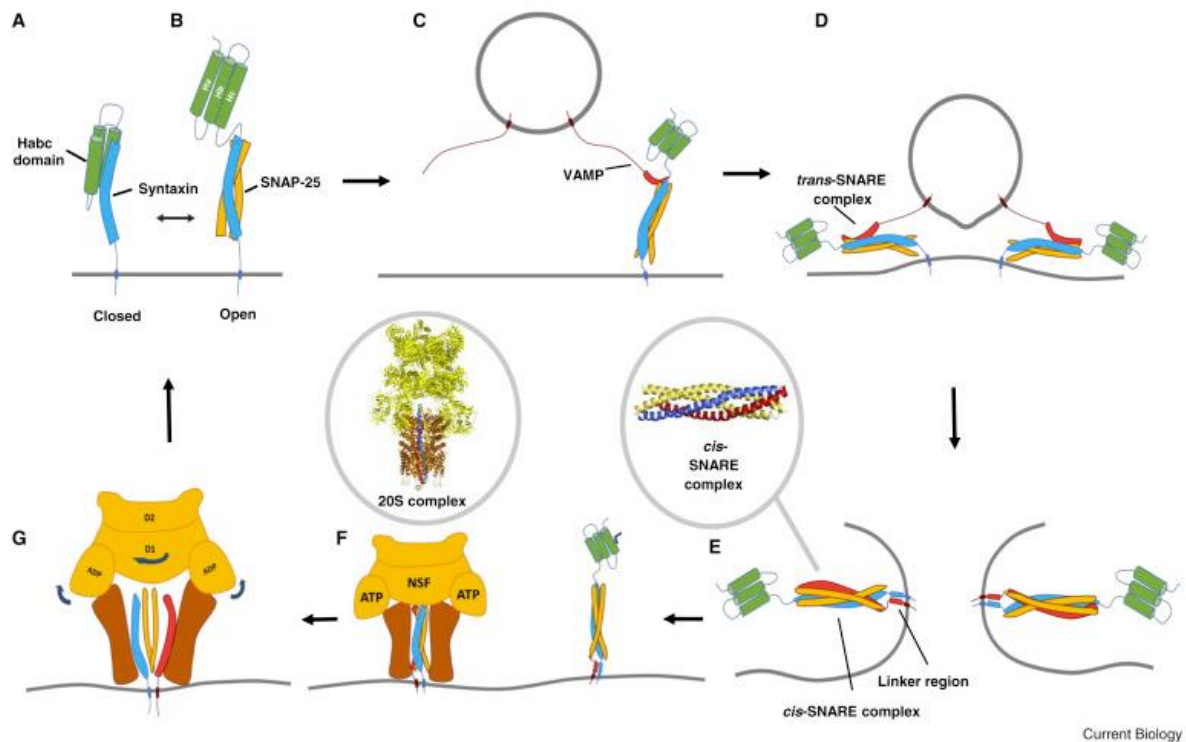


**Figure 19. The SNARE cycle.** (A, B) Habc domain allows syntaxin to change conformation from a closed to an open state where it can associate with two more Q-SNARE motifs forming a pre-complex of Q-SNARE proteins. (C, D) The pre-complex interacts with the vesicular R-SNARE starting from the N-terminal end of the SNARE motif and zippering towards the transmembrane domains initiating the SNARE complex formation. The SNARE complex assembly provides energy to overcome the repulsion as the fusing membranes approach each other. (E) SNARE complex formation is followed by the opening of the fusion pore and the complete merging of the two fusing membranes. (F) The trans SNARE complex is relaxed into a cis-configuration which is disassembled by SNAPS (brown) and NSF (yellow/orange) to form the 20S complex (20 S particles are named for their sedimentation coefficient of 20 Svedberg units). (G) ATP hydrolysis via NSF generates large conformational changes that lead to the disassembly of the SNARE complex. After recycling and sorting, SNARE proteins are ready again for another fusion cycle. Figure from Yoon & Munson, 2018

## 2.2 SNARE specificity

It was originally formulated based on the SNARE hypothesis that SNARE proteins not only drive membrane fusions but account for the specificity of intracellular membrane trafficking. Different SNAREs are distinctively localized and participate in discrete fusion reactions along the secretory pathway. This view has therefore been the main motive for the identification and characterization of SNARE complexes in various subcellular compartments mediating different transport pathways and diverse functional properties (Figure 20) (Wang et al., 2017; Ungar & Hughson, 2003; Scales et al., 2000; Hong, 2005; Yoon & Munson, 2018; Jahn & Scheller, 2006).

For example, VAMP4 localizes to the trans-Golgi network (TGN), and plays a role in retrograde trafficking from the plasma membrane via early and recycling endosomes (EE/RE) to the TGN (Steehmaier et al., 1999; Tran et al., 2007). It exists in a complex with its cognate partners syntaxin-6, syntaxin-16, and Vti1a (Vesicle Transport Through Interaction with T-SNAREs 1A), which were recently found to be required for maintaining the Golgi apparatus ribbon structure by balancing the endosome-TGN membrane transport (Shitara et al., 2013; Shitara et al., 2017). At the presynapse, VAMP4 is required for the bulk  $\text{Ca}^{2+}$ -dependent asynchronous release of synaptic vesicles by forming a complex with syntaxin-1 and SNAP25 (Raingo et al., 2012). On the other hand, the structurally homologous VAMP2 (also known as synaptobrevin 2/syb2) is also present on synaptic vesicles and mediates fast synchronous neurotransmitter release when in a complex with the same t-SNAREs. This complex interacts with complexin and synaptotagmin 1 which are required for synchronous release, in contrast to VAMP4-containing complexes that do not (Raingo et al., 2012).

Such cognate interaction of a specific set of SNAREs is not, however, absolute and the mechanisms ensuring such specificity remain unclear. Thus, whether SNAREs encode fusion specificity or not remains debatable. It is now generally accepted that SNAREs do not provide complete specificity for different compartments and other regulators remain essential. But why would there be so many SNAREs if their interactions are not specific? Indeed, distinct SNAREs could function to regulate the extreme dynamicity of membrane trafficking pathways (Yang et al., 1999). Notably, SNAREs can associate *in vitro* in non-cognate pairs with similar biophysical properties to the cognate ones as long as a member of each subclass is present (Jahn et al., 2006; Bethani et al., 2007). Moreover, some SNAREs are known to function in multiple fusion steps, some do not strictly localize to their site of action, and others are even able to

functionally substitute for the loss of one another (Ungar & Hughson, 2003; Yoon & Munson, 2018).

Biochemical studies have shown that SNARE proteins that do not reside normally in the same membrane compartment when used in various combinations, were able to readily form stable complexes *in vitro*. Hence, they suggest that SNARE complex formation is not inherently specific and the possible contribution of other mechanisms for the organization of the secretory pathway (Yang et al., 1999; Fasshauer et al., 1999). However, the functionality of such formed complexes in driving membrane fusion remains questionable. It has been shown that the exocytosis of norepinephrine from PC12 (pheochromocytoma) cells is rescued or inhibited by specific SNAREs (e.g. VAMP2 and VAMP4) but not others (e.g. VAMP7 and VAMP8) (Scales et al., 2000). Therefore, it is possible that the specificity of SNARE pairing is determined, not only by the ability to form a stable complex but rather by interactions with other proteins including Rab (Ras-related protein in brain) effector proteins and sec1 family (Scales et al., 2000). Additionally, a series of studies have shown that only a few pairs of SNAREs among hundreds were able to mediate vesicle fusion in an *in vitro* fusion assay (McNew et al., 2000; Parlati et al., 2000; Fukuda et al., 2000; Parlati et al., 2002). However, the fact remains that *in vitro* assays are not a faithful reflection of vesicle fusion *in vivo* where a large number of regulatory proteins exist that modulate SNARE complex formation. For example, the cytosolic proteins Munc-13, Munc-18 and complexin are known to initiate SNARE complex assembly and vesicle fusion (Lai et al., 2017; Shu et al., 2019; Wang et al., 2019; Brunger et al., 2019).

Furthermore, it has been shown that in drosophila, the two characterized v-SNAREs, a ubiquitous synaptobrevin (syb) essential for cell viability and a neuron-specific synaptobrevin (n-syb) required only for synaptic vesicle secretion, can functionally replace each other *in vivo* (Bhattacharya et al., 2002). Consistent with this finding, two Qa-SNAREs (Vam3p and Pep12p) in yeast vacuolar transport pathways can functionally rescue each other's loss when overexpressed (Götte & Gallwitz et al., 1997; Darsow et al., 1997). In neurons, VAMP3 can substitute for VAMP2 and rescue synaptic vesicle exocytosis in cultured neurons from VAMP2<sup>-/-</sup> mice (Deak et al., 2006). Also, evidence exists on the functional redundancy of SNARE proteins in vesicle trafficking. SNAP-25 null mutants in the drosophila larval stage exhibit normal neurotransmitter release at the neuromuscular junction due to substitution by SNAP-24, which normally does not take part in neurotransmitter release (Vilinsky et al., 2002). The yeast R-SNARE Ykt6p that functions at the late stages of the secretory pathway is upregulated in the absence of its homolog Sec22 which is required for the ER-Golgi trafficking

pathway (Liu & Barlowe, 2002). Altogether, these studies collectively argue against the sufficiency of SNARE pairing to confer fusion specificity (Xue and Zhang, 2002). Finally, a recent study shows that targeting specificity of trafficking vesicles requires tethering factors that are recruited by small GTPases (Rabs) and phosphoinositides. Such recruitment is dependent on the type of vesicular SNAREs, suggesting that specificity, in this case, is exhibited via a SNARE combinatorial code rather than the SNARE pairing during fusion (Koike & Jahn, 2019).

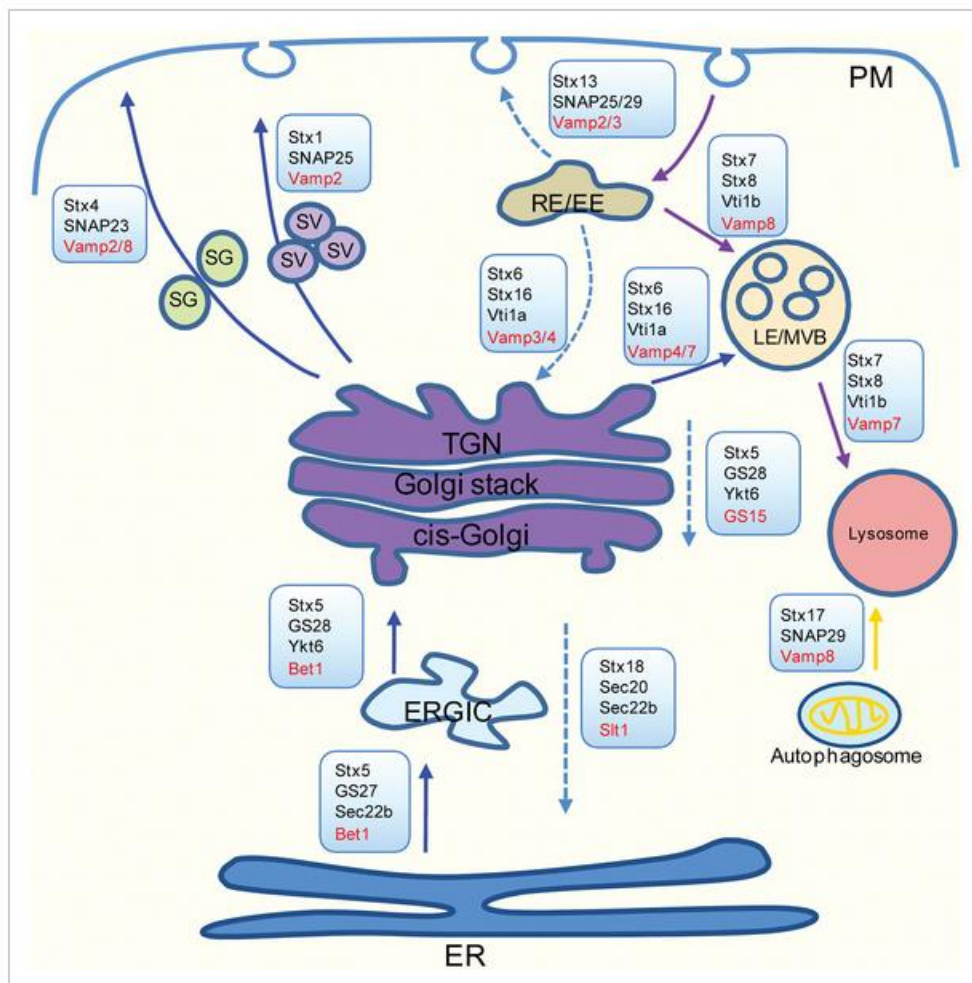


**Figure 20. SNARE complexes subcellular localization.** Summary of known SNARE complexes in different vesicle transport pathways and their sites of action. Vesicular SNAREs are shown in red. PM, plasma membrane; ER, endoplasmic reticulum; TGN, trans-Golgi network; ERGIC, ER-Golgi intermediate compartment; SG, secretory granule; SV, synaptic vesicle; RE/EE, recycling endosome/early endosome; LE/MVB, late endosome/multivesicular body. Figure from Wang et al., 2017.

### 2.3 SNARE cleavage by neurotoxins

Several species of gram-positive, spore-forming, anaerobic bacteria of genus *Clostridia* produce the most lethal natural protein toxins known to humans: tetanus and botulinum toxins. Clostridial neurotoxins (CNT) cause the neuromuscular syndromes of tetanus and botulism, respectively. The 50% lethal dose for mammals is approximately one nanogram per kg of body weight (Gill, 1982). They exert their toxicity by cleaving the fusion SNARE proteins in neuronal cells, thus inhibiting neurotransmitter release at synapses (Rossetto et al., 1994; Singh et al., 2014; Gardner & Barbieri, 2018). Each CNT is synthesized as an inactive single-chain protein of 150 kDa and is subsequently cleaved by the specific host or clostridial proteases. Cleavage results in the formation of the active di-chain molecule of ~50 kDa N-terminal light chain (LC) and 100 kDa C-terminal heavy chain (HC) that remain linked by a single disulfide bond (Figure 20). The HC consists of two subunits, a largely  $\alpha$ -helical domain of 50 kDa at the N-terminus HN, and a ~50 kDa fragment at the C-terminus HC, which is composed of two ~25 kDa domains, lectin like jelly roll domain HCN and a  $\beta$ -trefoil domain HCC (Figure 21) (Binz et al., 2010).

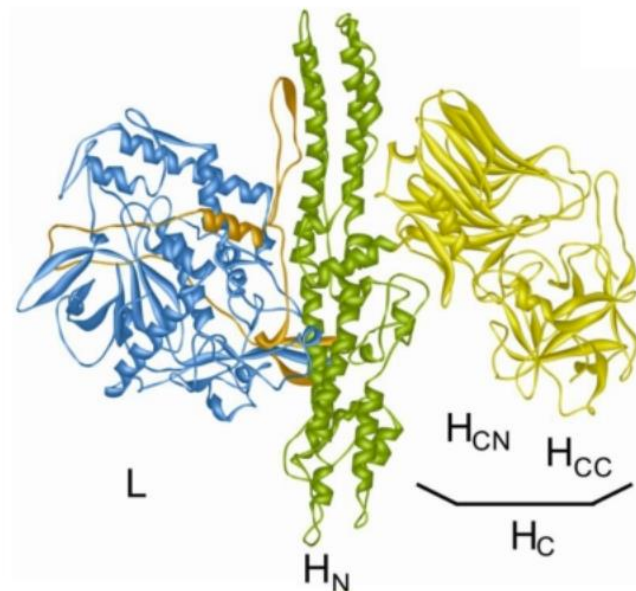


**Figure 21. Ribbon representation of BoNT/A.** The catalytic (L), translocation (HN), and binding domains (HC; consisting of HCC and HCN) are shown. In orange is the HN domain derived loop wrapping around the LC (L). Figure from Binz et al., 2010

Botulinum neurotoxins (BoNTs) are produced by several species of *Clostridium*, including *botulinum*, *baratii*, and *butyricum* (Schiavo et al., 2000; Johnson & Bradshaw, 2001). They are composed of seven immunologically different serotypes named BoNT (A-G) (Niemann et al., 1994). In addition, several new BoNT serotypes have been identified using bioinformatics tools, including BoNT/FA, BoNT/en (eBoNT/J) (Zhang et al., 2018; Brunt et al., 2018), BoNT/Wo (Zornetta et al., 2016), and BoNT/X (Zhang et al., 2017). BoNTs poisoning mainly occurs via oral ingestion and eventually reaches motor neurons causing flaccid paralysis that may lead to respiratory failure and death. They also represent a major bioweapon due to the lack of immunization in the population (Arnon et al., 2001; Bigalke et al., 2005). Conversely, BoNT/A and B are widely used as therapeutics for the treatment of a variety of neurological disorders such as strabismus (Scott, 1981), blepharospasm (involuntary blinking), and hemifacial spasm (Münchau & Bhatia, 2000; Turton et al., 2002). On the contrary, Tetanus neurotoxin (TeNT) is released into the circulation by bacteria in infected tissue lesions and poisons the inhibitory interneurons causing spastic paralysis (Binz et al., 2010).

Each subunit of the CNTs has a role in the mechanism of action of neurotoxicity which is a four-step process. First, intoxication starts with the interaction with surface gangliosides and a protein receptor of non-myelinated nerve terminals (via the HCC domain) (Dolly et al., 1984; Turton et al., 2002). It has been shown that protein receptors for BoNT/B and G are Syt-I and Syt-II (Dong et al., 2003; Dong et al., 2007; Nishiki et al., 1994; Rummel et al., 2004). Also, synaptic vesicle protein 2 (SV2) is a receptor for BoNT/A and E (Dong et al., 2008; Dong et al., 2006; Mahrhold et al., 2006), and possibly BoNT/F (Fu et al., 2009; Rummel et al., 2009). Whereas, protein receptors for BoNT/C and D, and TeNT have not been yet determined. Then, the toxin receptor complex is internalized into an intracellular vesicle. BoNT is targeted to a synaptic vesicle recycling pathway in a cholinergic neuron, and TeNT is translocated to the spinal cord. The third stage is the release of the LC of the toxin from the HC when exposed to the acidic environment of the endocytosed vesicle via the reduction of the disulfide bond. Acidification also triggers structural rearrangements in the HN chain and pore formation (cation-selective channel). These channels might be the paths by which the LC enters the cytosol (Koriazova et al., 2003). Once liberated, the LCs are zinc proteases which exert intoxication through a highly specific proteolytic cleavage of the SNARE complex (Schiavo et al., 1992; Rossetto et al., 1994).

BoNTs recognize and interact with a specific nine-residue motif (the SNARE secondary recognition motif; SSR motif) within the SNARE protein. SNARE cleavage by BoNTs is highly

specific; no two toxin serotypes cleave the same peptide bond of the same SNARE protein. Generally, BoNTs/A and E act on SNAP-25, BoNTs/B, /D, /F and /G cleave VAMP1 and 2, and BoNT/C can act on both SNAP-25 and syntaxins 2 and 3 (and not syntaxin 4), whereas, TeNT cleaves VAMP 1, 2 and 3 (Figure 22) (Rossetto et al., 1994; Gardner et al., 2018). Given the highly stable structure of the SNARE complex bundle, most CNTs can only act on free and not complexed SNAREs (Hayashi et al., 1994). However, some SNARE proteins are insensitive to cleavage by specific toxins. For example, VAMP7, a v-SNARE with a broad neuronal and non-neuronal expression, is found to be insensitive to TeNT and is thus named tetanus insensitive VAMP or TI-VAMP. VAMP4 is also insensitive to TeNT and BoNT/B but is cleaved by a recently identified isoform BoNT/X (Zhang et al. 2017). Murine SNAP-23 (Syndet) is cleaved by BoNT/E and /A, unlike human SNAP-23 that is resistant to both toxins due to a single amino acid substitution. Also, VAMP8 (endobrevin) is insensitive to BoNT/B, /D, /F and /G (Humeau et al., 2000; Turton et al., 2002). Such target specificity has allowed CNTs to be a valuable research tool for studying the function of different SNARE proteins both *in vitro* and *in vivo*.

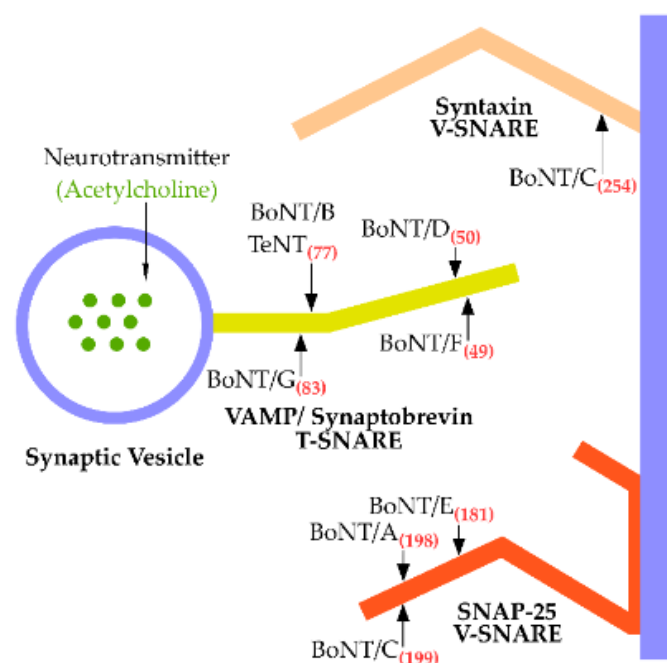


**Figure 22. SNARE cleavage by CNTs.** BoNT/A and /E cleave SNAP-25, BoNT/C cleaves SNAP-25, and Syntaxin. BoNT/B, /D, /F, /G, and TeNT cleave VAMP/Synaptobrevin. All toxins cleave their targets at a specific site except for BoNT/B and TeNT which attack the same peptide bond in the VAMP. Toxins cleavage prevents the interaction of v and t-SNAREs and the subsequent vesicle fusion and neurotransmitter release. Figure from Gardner & Barbieri, 2018.

### **3. Regulators of membrane trafficking: Rab proteins**

Another key player in the complex intracellular membrane trafficking system are Rab proteins (Ras-related protein in brain) which have been implicated in regulating the formation, transport, tethering, and fusion of transport vesicles together with SNAREs (Hutagalung & Novick, 2011; Ohya et al., 2009; Stenmark, 2009). Rab proteins are small monomeric GTP-binding proteins (21-25kDa) which belong to the Ras GTPase superfamily and represent the largest small GTPase family. All Rabs contain a conserved globular G-domain of about 180 residues that is related to other Ras-superfamily members. In humans, there are approximately 70 Rabs that belong to 44 subfamilies, five of which are found in all eukaryotic genomes (Rab1, Rab5, Rab6, Rab7, Rab11) (Diekmann et al., 2011; Klöpper et al., 2012; Pereira-Leal & Seabra, 2001). The first Rab gene was identified in yeast *Saccharomyces cerevisiae* and named Sec4/Ypt (Yeast protein transcript) that is required for vesicle trafficking from Golgi to the plasma membrane (Gallwitz et al., 1983; Salminen & Novick, 1987).

#### **3.1 Localization of Rab proteins**

Rab proteins have distinct subcellular localization and seem to mediate specific membrane trafficking pathways (Figure 22) (Ferro-Novick & Novick, 1993; Novick & Zerial, 1997; Zerial & Stenmark, 1993). They act by recruiting diverse tethering factors and other Rab-interacting proteins (Rab effectors) bringing together two compatible membranes for fusion (Stenmark, 2009; Hutagalung & Novick 2011; Grosshans et al. 2006; Wandinger-Ness & Zerial 2014). In steady-state, Rab proteins accumulate at their target compartments and are accordingly used as markers for different intracellular membrane-bound organelles (Figure 23). Rabs occupy distinct microdomains on endosomes and therefore function to determine membrane identity across the recycling pathway (Sönnichsen et al., 2000; Barbero et al., 2002; Pfeffer, 2013).

For example, both Rab5 and Rab4 are associated with early endosomes (EEs). Rab5 regulates the trafficking from the plasma membrane to the EE and is therefore considered as a marker for EE (Bucci et al., 1992). Rab4 and Rab35 control the fast recycling from the EEs and recycling endosomes (REs) back to the plasma membrane (Van der Sluijs et al., 1992; Daro et al., 1996; Kouranti et al., 2006). Rab11 is localized to RE and TGN, and mediates the transport between plasma membrane, the endosomal recycling compartments (ERC), and the TGN (Ullrich et al., 1996; Wilcke et al., 2000). Rab9 is involved in transport from late endosomes (LEs) to the TGN and lysosomes (Diaz et al., 1997; Ganley et al., 2004). Rab24 is involved in the transport from LE to the lysosomes (Munafò & Colombo, 2002). Rab7 is a marker of LEs and mediates the

transport from EE to LE (Feng et al., 1995). Rab1 and Rab2 are localized to the ER and regulate the ER to Golgi transport (Tisdale et al., 1992). The precise localization of Rabs and the spatiotemporal control of their activity require diverse cellular partners that regulate the Rab functional cycle (Figure 24) (Pylypenko et al., 2018).

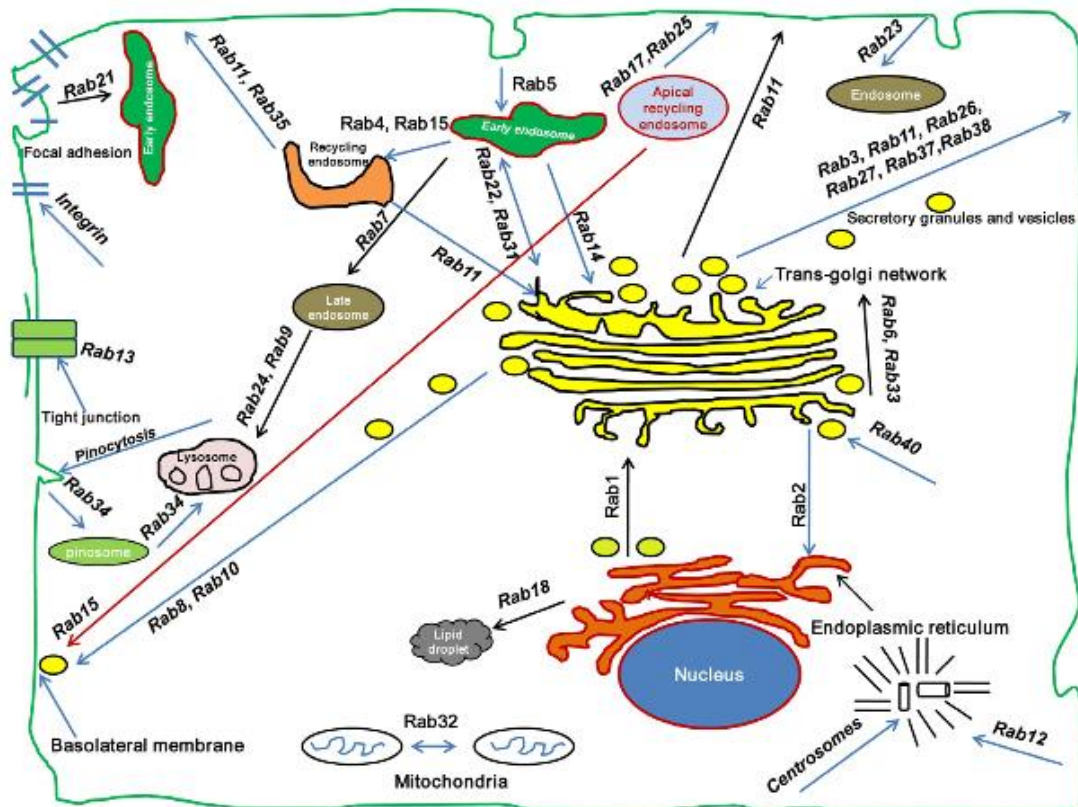


**Figure 23. Localization of Rab Proteins.** Image from Bhui & Roy, 2014.

### 3.2 The Rab cycle

Rab proteins cycle between the cytosol and the membrane of their respective compartments. Like other protein GTPases, Rabs are nucleotide-dependent molecular switches that are active in GTP-bound form and are inactive in GDP-bound form (Pfeffer, 2005). Synthesized Rab protein associates with the Rab escort protein (REP) forming a stable complex (Andres et al., 1993). The complex is presented to the RabGGT (Rab geranylgeranyl transferase) which geranylgeranylates (covalent addition of a 20-carbon group) the Rab at the C-terminal cysteine residues. This post-translational modification makes the Rab protein hydrophobic which allows the reversible association with the membrane (Wilson et al., 1996; Alexandrov et al., 1994). The REP-associated Rab is then delivered to the membrane of a specific organelle or vesicle,

GDP is replaced by GTP by the action of a guanine nucleotide exchange factor (GEF) and the Rab dissociates from the REP (Wilson et al., 1996). The active membrane-bound Rab-GTP is stabilized on the membrane by interacting with effectors and tethering complexes that regulate the activity of downstream proteins such as molecular motors or SNARE complexes for membrane fusion (McBride et al., 1999; Wurmser et al., 2000). After fusion of the target membranes, Rab is inactivated by GTPase activating protein (GAP) via GTP hydrolysis where it is converted back to the GDP-bound form. Then, membrane-bound Rab-GDP is released from the membrane by a GDP dissociation inhibitor (GDI) to the cytosol as a Rab-GDI complex in preparation for another cycle (Figure 24) (Ullrich et al., 1993; Bhui & Roy, 2014; Goody et al., 2017; Hutagalung & Novick, 2011).

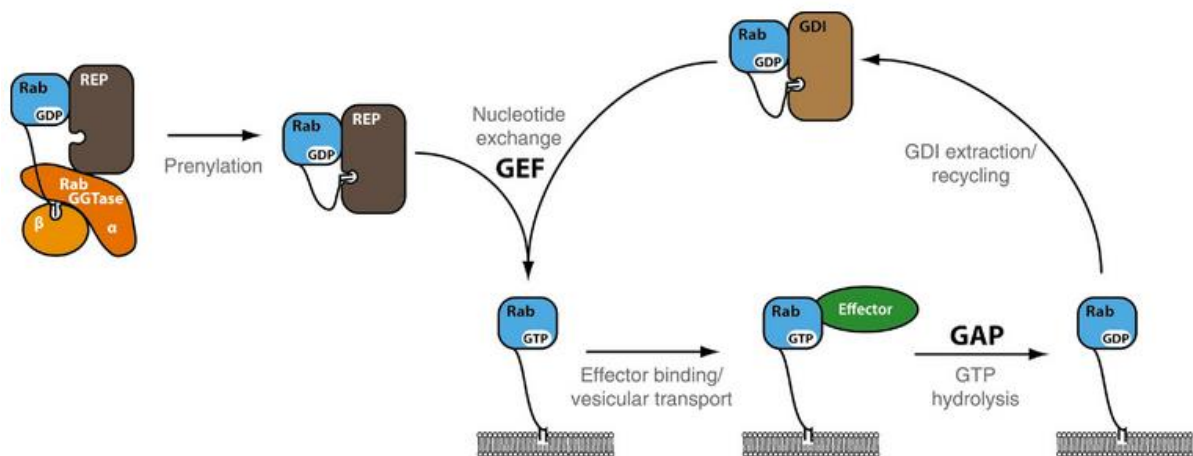


**Figure 24. The Rab proteins cycle.** The newly synthesized Rab-GDP associates with Rab escort protein (REP) and is presented to Rab geranylgeranyl transferase (RabGGTase) which consists of an alpha subunit and a catalytic beta subunit for prenylation. It is then delivered to the membrane where it is activated by a guanine nucleotide exchange factor (GEF) that exchanges GDP for GTP. The active Rab-GTP interacts with effector molecules to regulate different steps in vesicular trafficking. After that, Rab is deactivated by a GTPase activating protein (GAP) which catalyzes GTP hydrolysis to GDP. The inactive Rab-GDP can now be extracted from the membrane by GDP dissociation inhibitor (GDI), and is kept in a soluble complex with GDI in the cytosol where it can restart another round of vesicular transport. Figure from Goody et al., 2017.

## 4. SNAREs at the synapse

Synaptic membranes undergo constant rearrangements especially via endo- and exocytosis, which are fundamental biological events ensuring maintenance of synaptic function (Milovanovic & Jahn, 2015). The synaptic membrane-fusions mediating exocytosis is controlled by complex machinery that includes SNARE proteins (Südhof & Rizo, 2011). Indeed, SNAREs play a critical role in the synchronization of neurotransmitter release as well as receptor insertion at the post synapse. Modifications in synaptic exocytosis pathway, therefore, influence synaptic strength and plasticity.

### 4.1 SNARE proteins in synaptic vesicle exocytosis

The regulated exocytosis of synaptic vesicles at the presynaptic membrane is a well-orchestrated process during which membrane fusion leads to neurotransmitter release at the active zone mediating synaptic transmission. Each presynaptic nerve terminal contains hundreds of synaptic vesicles loaded with neurotransmitters. When the presynaptic membrane is depolarized by an action potential, voltage-gated calcium channels (VGCCs) are activated. The influx of calcium triggers the fusion of synaptic vesicles with the plasma membrane. Like most other cellular fusion events, the fusion of both the vesicular and plasma membrane is executed by SNARE proteins (Südhof & Rizo, 2011; Neher & Brose, 2018).

Early work through *in vitro* fusion assays has identified NSF and SNAPs as essential proteins for membrane traffic and fusion (Wilson et al., 1989). However, the first evidence of the functional importance of SNARE proteins for synaptic exocytosis came from discoveries in the early 1990s that these proteins are targets of clostridial neurotoxins that block membrane fusion and inhibit neurotransmitter release. VAMP/synaptobrevin was the first protein identified (later classified as a SNARE) as a target of tetanus and botulinum B neurotoxins (Schiavo et al., 1992; Link et al., 1992). Then, it was shown that SNAP-25 and syntaxin-1 are targets of specific botulinum neurotoxins (Blasi et al., 1993a,b). It was therefore proposed that these three proteins form the core of a fusion complex that requires NSF and SNAPs as cofactors (Blasi et al., 1993a). Additionally, homologies were observed between these proteins and proteins of membrane traffic in yeast supporting the notion of conserved fusion machinery (Novick et al., 1980). Shortly after, Rothman and colleagues discovered that synaptobrevin, SNAP-25 and syntaxin form a complex that is dissociated by NSF, and introduced the term ‘‘SNARE’’ for

“soluble NSF-attachment protein receptor” (Söllner et al. 1993). Now, the best-studied SNARE proteins are those that mediate synaptic vesicle fusion at the presynapse.

Synaptic vesicles are docked and primed at the active zone release sites. Docked vesicles are those in direct contact with the plasma membrane, whilst primed vesicles are a subset of docked vesicles whose SNARE fusion machinery is fully assembled (Gundersen, 2017). Recent evidence indicates that even at rest, these docked and primed vesicles are not static, but fluctuate between a loosely docked and primed state where SNARE complexes are only partially zippered, and a tightly docked and primed one as zippering progress further (Figure 25). Upon action potential arrival, vesicles fuse with the membrane with a certain probability ( $Pr$ ) in response to a rise in intracellular calcium concentrations (Neher and Brose, 2018). The influx of calcium through VGCC at the active zone is a crucial step for the exocytosis of synaptic vesicles and rapid neurotransmitter release. Nerve terminals  $Pr$  is considered the main parameter contributing to synaptic strength and the polarity of short-term potentiation (STP) (Fekete et al., 2019; Zucker & Regehr, 2002). The distance between VGCCs and synaptic vesicles could account for heterogeneity in release probability (Rebola et al., 2019). Strong synapses are composed of synaptic vesicles that are tightly coupled to the VGCC clusters (~10 nm), whilst weak synapses had a 5-fold longer coupling distance (~50 nm). However, the number of presynaptic calcium channels does not correlate with synaptic strength. There are surprisingly 3 times more VGCC in weak synapses compared to strong ones. (Rebola et al., 2019; Fekete et al., 2019; Rozov et al., 2001). Additionally, it has been shown that incompletely filled vesicles have a lower  $Pr$ ., pointing to the possible regulation of vesicle fusion by its degree of filling (Rost et al., 2015).

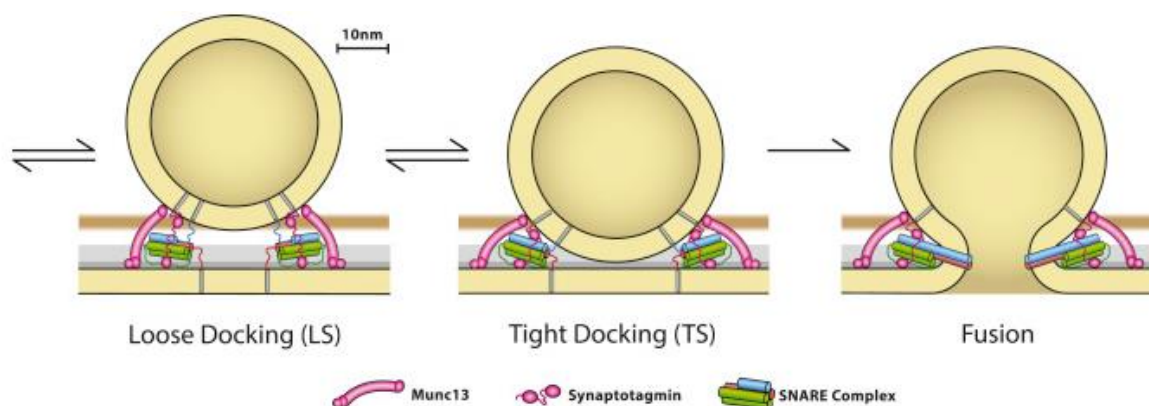


**Figure 25. Dynamicity of synaptic vesicles showing the loosely and tightly docked/primed states.** Image from Neher & Brose, 2018.

The rapid, synchronous release is mediated by the docked and primed vesicles which immediately fuse with the membrane upon stimulation and constitute the “readily releasable pool” (RRP). The interaction between  $\text{Ca}^{2+}$  channels and SNARE proteins contributes to the reduced distance between the vesicles and the presynaptic membrane, which ensures signal transmission within a millisecond temporal precision. The RRP is replenished by the rapid recycling of the fused vesicles or the recruitment of new vesicles from the “reserve pool”. With moderate physiological stimulation, after the RRP is depleted, the “recycling pool” is recruited which comprises 10-20% of all vesicles. All synaptic vesicles that take part in activity-induced moderate synaptic transmission are referred to as the total recycling pool, which is ~ 50% of the total synaptic vesicles. The remaining are the reserve or resting pool which are reluctant to release and are only recruited upon high-frequency stimulation. Therefore, synaptic vesicles despite having an identical ultrastructure appearance, are heterogeneous and organized into three functionally distinct “pools” (Figure 26) (Chanaday & Kavalali, 2018; Denker & Rizzoli, 2010).

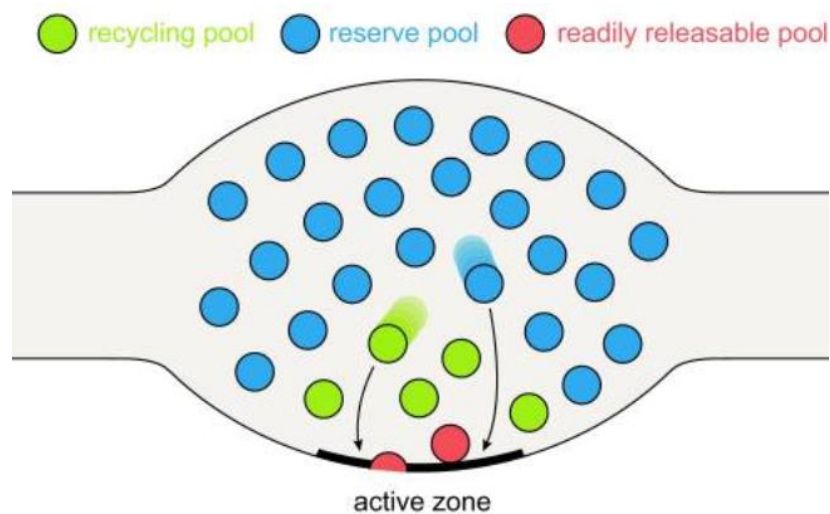


**Figure 26. A classical model for the localization of three distinct synaptic vesicle pools.** The RRP (in red) are vesicles that are docked and primed at the active zone. After RRP is depleted, the recycling pool (in green) is recruited to the active zone and released upon moderate stimulation. High-frequency stimulation causes the depletion of the recycling pool and the recruitment of the reserve pools (in blue) from areas that are further away from the active zone. Image from Denker & Rizzolio, 2010.

The fusion of synaptic vesicles is dependent on a well-characterized protein machinery which includes, the SNARE proteins, the  $\text{Ca}^{2+}$ -sensor synaptotagmin 1 (Syt1), the regulator complexin, the assembly factors Munc18 and 13, and the disassembly factors NSF and SNAP (Figure 27) (Brunger et al., 2019). The classical neuronal SNARE complex comprises syntaxin-1, VAMP2, and SNAP-25. VAMP2 is a predominant vSNARE that is essential for all forms of neurotransmission in the CNS, mainly synchronous rapid fusion (Schoch et al., 2001). VAMP4 has been identified to specifically drive asynchronous release (Raingo et al., 2012). Vesicles containing VAMP7, a prototypical longin (VAMP family), are less responsive to stimulation but can undergo stimulus-evoked and spontaneous release. They also constitute at least a fraction of vesicles within the resting pool (Hua et al., 2011) that can be mobilized by the glycoprotein reelin (Bal et al., 2013). Finally, Vti1a (Vps10p-tail-interactor-1a) appears to preferentially mediate spontaneous neurotransmission (Ramirez et al., 2012).

At least two SNARE complexes are required for synaptic vesicle fusion (Sinha et al., 2011). *In vitro* analysis shows that just one SNARE complex is sufficient to open the fusion pore, however, three or more are required to sustain the opening long enough for neurotransmitter release (Shi et al., 2012). SNARE themselves do not exhibit any  $\text{Ca}^{2+}$  sensitivity, thus  $\text{Ca}^{2+}$  binds to the calcium sensor Syt through the cytoplasmic C2 domains (C2A and C2B). Syt-1, Syt-2 and Syt-9 promote fast and synchronous transmitter release, whereas Syt-7 is required for asynchronous release (Xu et al., 2007; Bacaj et al., 2013; Brewer et al., 2015; Zhou et al., 2015, Pérez-Lara et al., 2016). Synaptotagmins require the cytoplasmic protein complexin as a cofactor (McMahon et al., 1995). In a pre-fusion state, a tripartite complex consisting of SNARE/complexin/synaptotagmin-1 is formed.  $\text{Ca}^{2+}$  binding to synaptotagmin leads to its dislodging from the tripartite interface allowing the trans-SNARE complex to fully zipper. This release-of-inhibition model of  $\text{Ca}^{2+}$  triggered fusion supports the fast sub millisecond fusion process that is required for action-potential evoked synchronous release (Brunger et al., 2018). Complexin has a dual facilitatory and inhibitory function. It binds to SNARE complex and enhances vesicle fusogenicity by lowering energy required for fusion. It stabilizes partially zippered SNARE complex and sensitizes them to synaptotagmin activation (Super-priming) (Xue et al., 2010). In contrast, it can also act as a clamp that blocks SNARE complex assembly progression by occupying synaptobrevin binding site in the SNARE complex to inhibit fusion. The clamp can then be released upon stimulation by action potential and  $\text{Ca}^{2+}$  entry (Kümmel et al., 2011).

The tripartite pre-fusion complex is important for synaptic vesicle priming, where synaptic vesicles are associated with presynaptic proteins and are ready for  $\text{Ca}^{2+}$  triggered fusion. Additionally, several other factors regulate the primed state including Munc 18 and Munc 13 (also known as SM proteins). Both proteins are required for proper SNARE complex assembly (Lai et al., 2017; Hammarlund et al., 2007). The deletion of Munc-18-1 in mice leads to a complete loss of neurotransmitter secretion (Verhage et al., 2000). Munc-18 interacts with free syntaxin-1A, blocking the accessibility to its partners and subsequent SNARE complex formation (Burkhardt et al., 2008; Misura et al., 2000). Munc-13 catalyzes the transition of syntaxin-Munc18 complex into the ternary SNARE complex and regulates the proper assembly of SNARE complex together with Munc-18. Therefore, Munc-13 and Munc-18 are viewed as assembly factors that ensure the proper functional sub configuration of the SNARE complex (Lai et al., 2017; Brunger et al., 2019).

The priming function of Munc-13 is regulated by RIM protein (Rab3A interacting molecule). RIM binds to Munc-13 as well as small GTP binding proteins Rab3 and Rab27 on the synaptic vesicles, hence mediating vesicle docking. The binding is mediated by the N-terminal domain which contains a Munc-13-binding zinc finger surrounded by the Rab3-binding  $\alpha$ -helices. Both Rim and RIM-interacting molecule (RIM-BP) bind  $\text{Ca}^{2+}$  channels and recruit them to the active zone, which is positioned less than 100 nm from docked vesicles. Thus, this protein complex functions to connect synaptic vesicles, priming factors, and  $\text{Ca}^{2+}$  channels at release sites, allowing fast coupling of an action potential to neurotransmitter release (Figure 27) (Südhof, 2013).

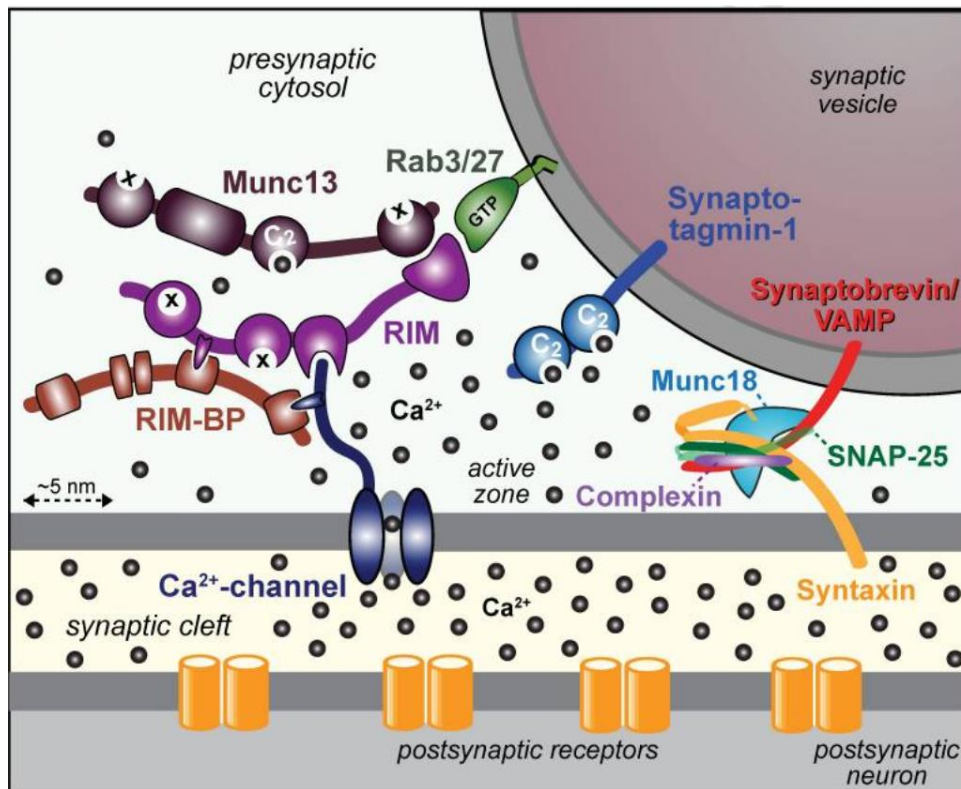


**Figure 27. Spatial organization of presynaptic release machinery.** The scheme shows a docked synaptic vesicle at the active zone. The core fusion machinery consists of the SNARE proteins; synaptobrevin/VAMP, syntaxin-1, SNAP-25 and the SM protein Munc18-1. Synaptotagmin-1 is a calcium sensor with two cytoplasmic C2 domains that bind calcium, and functions together with complexin protein. The active zone proteins are RIM, Munc13, RIM-BP, and Ca<sup>2+</sup> channel at the membrane. Figure from Südhof, 2013.

## 4.2 Post-synaptic SNARE fusion machinery

At the post-synapse, the regulated trafficking and exocytosis of neurotransmitter receptors and other cargo proteins to the synaptic membrane is a prerequisite for activity-dependent synaptic modifications in neuronal cells. Excitatory synaptic transmission is mediated by glutamate receptors, AMPA and NMDA. Post-synaptic infusion of the light chain of BoNT/B or TeNT inhibits LTP (Lledo et al. 1998; Lu et al. 2001) and evokes the run-down of synaptic currents (Lüscher et al. 1999), suggesting that AMPARs undergo constitutive and activity-dependent trafficking mediated by post-synaptic VAMP2. However, the SNARE machinery implicated in dendritic exocytosis at the post-synapse has not received much attention until recently, in contrast to the well-characterized presynaptic canonical SNAREs (Madrigal et al., 2019).

Postsynaptic compartments are thought to employ molecularly distinct SNARE complexes than that of the presynapse which could account for the functional differences in the nature of the two exocytic events (Jurado et al., 2013; Madrigal et al., 2019). For instance, presynaptic vesicles are docked at the plasma membrane and exocytosis occurs rapidly (<1 msec) in response to a rise in calcium levels. Contrarily, AMPAR-containing vesicles are not docked at the plasma membrane but are trafficked into dendritic spines via myosin motors. The speed of AMPAR exocytosis following LTP induction appears to be slower than presynaptic vesicle exocytosis and lasts tens of seconds or minutes (Petrini et al., 2009; Yang et al., 2008; Patterson et al., 2010; Yudowski et al., 2007; Makino and Malinow, 2009). The identification of the protein machinery mediating AMPAR trafficking is particularly important given its role in experience-dependent plasticity where any dysregulation can be linked to most neurological and neurodegenerative disorders (Jurado, 2018). Long term potentiation relies on the vesicular insertion of AMPARs upon the activation of calcium-permeable NMDARs. SNARE proteins enriched in vesicle membrane (VAMP or Syb) interact with target membrane SNAP and Stx proteins mediating exocytic insertion. Specific isoforms of these proteins are implicated in postsynaptic receptor trafficking and exocytosis (Madrigal et al., 2019).

The most abundant vSNARE throughout the brain is VAMP2 (Madrigal et al., 2019; Hoogstraaten et al., 2020). It is an integral molecule of synaptic vesicles but reaches dendrites during early development via transcytosis in which proteins are first delivered to somatodendritic compartments and then endocytosed and transported anterogradely for insertion into axon terminals (Ernst and Brunger, 2003; Brunger et al., 2009; Sampo et al., 2003). It is however suggested that VAMP2 does not exclusively reach the axon via transcytosis

(Sampo et al., 2003). Furthermore, VAMP2 is associated with GluA1-containing vesicles at the postsynapse and is suggested to be required for both AMPAR exocytosis during synaptic potentiation and spine growth (Murakoshi and Yasuda, 2012). Experiments from VAMP2 KO mice indicate that it regulates both constitutive and activity-dependent AMPAR trafficking (Jurado et al., 2013).

Stx-1 is predominantly localized at presynaptic membranes (Koh et al., 1993), and recently it has been shown to localize at the PSD (Hussain et al., 2016). The knockdown of both Stx-1a and Stx-1b did not affect glycine-induced LTP in culture or LTP in acute slices (Jurado et al., 2013). Stx-3 is widely distributed in both axons and dendrites. The interaction of Stx-3 with complexin has been proposed to control AMPAR exocytosis during LTP (Ahmad et al., 2012; Jurado et al., 2013). Stx-4 at the postsynapse has been shown to define a microdomain for the exocytosis of AMPAR-containing REs (Kennedy et al., 2010) and they also play a role in NMDAR constitutive trafficking (Gu and Huganir, 2016). A recent study showed that the KO of Stx-4 caused a decrease in basal synaptic transmission due to a reduction in both AMPA and NMDA receptors in cultured hippocampal neurons. Animals lacking Stx-4 had defective LTP and spatial learning and memory (Bin et al., 2018).

SNAP-25 has been extensively studied for its role in neurotransmitter release. However, several studies support a role of SNAP25 at the postsynapse as well. It has been shown to regulate dendritic spine morphogenesis. The knockdown of SNAP-25 reduced the number of mature spines in the hippocampal CA1 region (Tomasoni et al., 2013). Additionally, *in vivo* knockdown of SNAP-25 impaired LTP in hippocampal slices due to a reduction in synaptic NMDARs (Jurado et al., 2013). SNAP-25 has also been shown to regulate the constitutive trafficking of NMDARs (Gu and Huganir, 2016). SNAP-23, a ubiquitously expressed homolog of SNAP-25, has also been suggested to play a role in NMDA receptor trafficking. It has a somatodendritic expression and is particularly enriched at the PSD. The knockdown of SNAP-23 decreases NMDAR surface expression and current in hippocampal cultures (Suh et al., 2010). However, in another study, the *in vivo* knockdown of SNAP-23 failed to impair NMDAR-dependent LTP (Jurado et al., 2013). SNAP-47 can be found throughout the CNS in both axons and dendrites. It has a specific role in activity-dependent insertion of AMPARs during LTP with no effect on presynaptic properties or constitutive AMPA/NMDAR trafficking (Jurado et al., 2013). SNAP-29 has lower expression levels in the CNS compared to other SNAPs and its function in brain synaptic transmission and plasticity has not been yet studied (Madrigal et al., 2019).

In summary, accumulating evidence has expanded the important role of SNARE proteins in regulating postsynaptic dendritic membrane trafficking, synaptic transmission and plasticity. Different sets of SNAREs may be involved in different types of exocytosis i.e. constitutive versus regulated trafficking. AMPAR insertion during LTP is dependent on a complex formed by SNAP-47, VAMP2, and Stx-3 (Figure 28). Whereas, NMDARs constitutive trafficking may require SNAP-25, VAMP1 and Stx-4. However, it remains unknown which SNARE proteins control the constitutive delivery of AMPARs to the plasma membrane that is required for maintaining basal synaptic strength. It has been suggested that VAMP2 may also contribute to the constitutive trafficking of AMPARs (Jurado et al., 2013). Future efforts are needed to identify the possible involvement of other SNARE proteins in neurotransmitter receptor trafficking and elucidate the molecular mechanisms underlying such regulation.

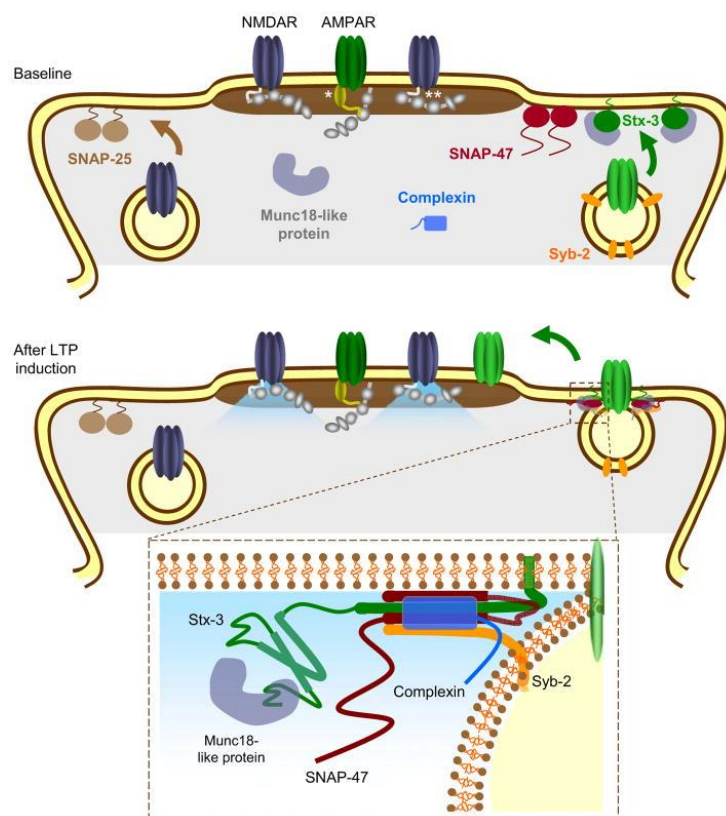


**Figure 28. Schematic of SNARE proteins mediating the regulated AMPAR exocytosis during LTP.** The top panel shows critical SNARE proteins including Stx-3, SNAP-47, and Syb-2 required for AMPAR trafficking. Anchored SNAP25 regulated NMDAR trafficking. The bottom Panel shows SNARE complex assembly upon NMDAR activation and calcium influx after LTP induction. Figure from Jurado et al., 2013.

## C. Membrane trafficking in synaptic plasticity

### 1. Endosomal recycling and LTP

Accurate and efficient endosomal recycling is a key process in synapse remodeling during experience-dependent plasticity. Neuronal cells internalize a variety of protein and lipid cargo which are usually transported to the EE where sorting occurs. Cargo can then deliver to late endosomes and lysosomes, to TGN, or recycle back to the plasma membrane. Sorting of these internalized molecules is particularly complex and requires a series of regulatory molecules that occur in various organelles within the endosomal system (Grant & Donaldson, 2009).

#### 1.1 TfR in constitutive recycling

Endosomal recycling balances the removal of membrane from the cell surface that occurs during endocytic uptake. The most well-understood endocytic process is receptor-mediated endocytosis by clathrin-coated pits (Maxfield & McGraw, 2004). The best characterized CME molecule in literature is the transferrin receptor (TfR) (Mettlen et al., 2018). This iron sensor undergoes rapid recycling from EEs to the plasma membrane which requires Rab4 and Rab35 and slow recycling which involves transport from EE to the RE, then to the plasma membrane. RE is a tubular compartment that extends from the EE and is defined molecularly by the presence of Rab11. Recycling of TfR back to the plasma membrane is a default pathway that does not require any cytoplasmic sorting signals. Therefore, TfR is considered an RE marker and a classic representative of the constitutive recycling pathway, which is important for maintaining a mobile pool of receptors at the plasma membrane (Grant & Donaldson, 2009; Petrini et al., 2009). In many cases, TfR is used as a surrogate marker of AMPAR trafficking pathways, however, this is not perpetually true.

For instance, recent evidence indicates that unlike TfR, the constitutive AMPAR internalization is clathrin-independent (Glebov et al., 2015). AMPARs primarily recycle in dynamin-independent endosomes containing the GTPase, Arf6, whereas, few recycle in TfR-positive REs (Zheng et al., 2015). In line with this, studies using *C. elegans* indicate the existence of genetically separable recycling pathways for cargoes in CME and CIE (Shi et al., 2007; Grant & Donaldson, 2009). It is therefore plausible that the constitutive recycling pathway of these two receptors in neuronal cells is similarly segregated. While REs might share common identity

molecules such as Rab11, further characterization of the molecular composition of such endosomes remains imperative for their functional distinction.

## **1.2 Activity-dependent recycling**

Under conditions of enhanced activity in response to LTP stimuli, there is a generalized increase in endocytic recycling to the neuronal plasma membrane. Notably, the regulated or activity-dependent trafficking of AMPARs is a prerequisite for the increase in synaptic strength and spine size during LTP (Kelly et al., 2010). AMPARs are recruited from the dendritic membrane surface to the synapse by lateral diffusion (Penn et al., 2017). They can also deliver from intracellular membranous compartments to the post-synaptic membrane. It has been reported that Rab11-dependent REs act as a local reservoir to supply AMPARs for LTP (Park et al., 2004). Rab11 can enter dendritic spines in a myosin (MyosinV) and kinesin (KIF1C)-dependent manner (Esteves da Silva et al., 2015). Rab11-endosomes translocate AMPARs from the dendritic shaft into spines, and the final insertion of REs is mediated by Rab8. Indeed, overexpression of both dominant negative mutants of Rab11 and Rab8 abolished synaptic potentiation (Brown et al., 2007).

Questions that remain under discussion are: to what extent are the AMPAR constitutive and regulated trafficking pathways interdependent? and is the enhanced local recycling of AMPARs sufficient to support LTP or there exist other intracellular trafficking sites?

Recent evidence indicates that AMPARs traffic through different endocytic pathways depending on neuronal activity. During activity-dependent recycling, AMPARs undergo CME and recycle back to the plasma membrane in TfR-labelled REs at strengthened synapses (Zheng et al., 2015). Moreover, it has been shown that FIP2 restricts AMPARs trafficking until the induction of LTP (Royo et al., 2019).

In this study, we focus on the role of 2 vesicular SNARE proteins: VAMP2 and VAMP4 in AMPAR trafficking at the post-synapse in basal and LTP conditions. We show that these two vSNAREs mediate distinct trafficking pathways and have differential effects on the constitutive and activity-dependent AMPAR recycling. We therefore propose a model of a bifurcated endosomal recycling system at the post-synapse.



# **MATERIALS AND METHODS**



## 1. Primary hippocampal Banker cultures

For imaging of protein trafficking, dissociated hippocampal cultures were prepared from embryonic (E18) Sprague-Dawley rats of either sex based on the protocol developed by Kaech and Banker (Kaech and Banker, 2006). Primary hippocampal neurons were cultured on glass coverslips facing a feeder layer of astrocytes in a petri dish. These astrocytes are necessary for the development and the viability of the neuronal cells. Hippocampi from E18 rats were dissected in HBSS (Hank Balanced Salt Solution) containing antibiotics penicillin-streptomycin (PS) and HEPES buffer.

Hippocampal cells were prepared by trypsinization for 15 minutes in a trypsin-EDTA solution at 37°C and by mechanical dissociation with Pasteur pipet pre-coated with horse serum. At the end of the dissociation, both population of neurons and glial cells are present. The number of cells can be determined by direct counting using a Malassez grid.

The cell suspensions were plated at a density of 300,000 cells per 60-mm dish on 1 mg/ml poly-L-lysine pre-coated 1.5H coverslips with paraffin dots (Marienfeld, cat. No. 117 580, 18 mm). After the cells achieved attachment, the coverslips were transferred to a culture dish containing a glial monolayer and were maintained in Neurobasal medium supplemented with 2 mM L-glutamine and 1X NeuroCult SM1 Neuronal supplement (STEMCELL technologies). Four days later (Days *in vitro* 4, DIV4), 5µM Cytosine arabinoside (Ara-C) (Sigma-Aldrich) was added to the culture medium to inhibit glial proliferation by blocking the DNA replication. This enables the selection of only the population of neurons.

Astrocyte feeder layers were prepared from embryos the same age at a density of 20,000 to 40,000 cells per 60-mm dish (per the Horse Serum batch used) pre-coated with 0.1 mg/ml of poly-L-lysine. The cells were cultured in MEM (Fisher Scientific, cat. No. 21090-022) containing 4.5g/l Glucose, 2 mM L-glutamine and 10% horse serum (Invitrogen) that favors the glial cell division.

Neurons were maintained at 37°C in a humidified incubator at 5% CO<sub>2</sub>. After 6 days, the media was progressively changed twice per week for Brainphys medium (StemCell Technologies, cat # 05791) supplemented with 1X NeuroCult SM1 Neuronal supplement. All neurons were between DIV 12-13 at the time of the experiment.

## 2. Organotypic hippocampal culture

All animal experiments complied with all relevant ethical regulations (study protocol approved by the Ethical Committee of Bordeaux CE50). Animals were raised in our animal facility; they were handled and euthanized according to European ethical rules. Hippocampi were dissected from wild type rats at postnatal age 7-8 in ice-cold low sodium dissection solution containing (in mM): 1 CaCl<sub>2</sub>, 10 D-glucose, 4 KCl, 5 MgCl<sub>2</sub>, 26 NaHCO<sub>3</sub>, 234 sucrose, 0.1% v/v phenol red solution 0.5% in DPBS. Transverse slices (350 μm) were cut with a tissue chopper (McIlwain) and positioned on small membrane segments (FHLC01300, Millipore) and culture inserts (PICM0RG50, Millipore) in 6-well plates containing 1 ml/well slice culture medium, which was minimum essential medium (MEM) supplemented with 15 % heat-inactivated horse serum, 0.25 mM ascorbic acid, 1 mM L-glutamine, 1 mM CaCl<sub>2</sub>, 2 mM MgSO<sub>4</sub>, 30 mM HEPES, 5.2 mM NaHCO<sub>3</sub>, 13 mM D-glucose and 1 mg/L insulin (pH7.3, osmolality adjusted to 320). Slices were maintained in an incubator at 35 °C with 5 % CO<sub>2</sub> and the culture medium was replaced every 2-3 days.

## 3. Expression of exogenous proteins and shRNA

### 3.1 Plasmid constructs

- **TfR-SEP** was kindly provided by C. Merrifield (Laboratory of Enzymology and Structural Biochemistry, Gif-sur-Yvette, France). It was used in previous studies from the laboratory involving live cell imaging in neurons (Jullié et al., 2014; Rosendale et al., 2017).
- **VAMP2-SEP** construct was kindly provided by Jürgen Klingauf (Institute of Medical Physics and Biophysics, Münster, Germany). It was used previously in the laboratory (Martineau et al., 2017)
- **TeNT WT** and **TeNT E234Q** constructs were kindly provided by Thierry Galli (Institute Jacques Monod, Paris, France).
- **VAMP4-SEP**: to generate VAMP4-SEP, we amplified VAMP4 from the VAMP4-GFP plasmid by PCR with the following primers: VAMP4 forward, GAATTCGC-CACCATGCCTCCCAAGTTTAAGCGCCACC.VAMP4 reverse GGATCCGAAG-TACGGTATTTTCATGAC. DNA amplification products were subcloned into TfR-SEP plasmid by insertion of BamHI/EcoRI restriction sites.

- To knockdown VAMP4, we generated 2 different versions of short hairpin RNA (shRNA). **shVAMP4-(1)** targets the 3'UTR and has the following sequences: shVAMP41 forward, ATCCCCTATCTTTATTTAACAACATTCAAGAG-ATGTTGTTAAATAAAGATAGTTTTTC; shVamp4-1 reverse, CGAGAAAA-ACTATCTTTATTTAACAACATCTCTTGAATGTTGTTAAATAAAGATAGGGG. **shVAMP4-(2)** is similar to the one published in (Gordeon et al., 2010) but is shifted by one nucleotide. It targets the translated VAMP4 mRNA. Forward: GATCCCCGGACCATCTGGACCAAGATTTCAAGAGAATCTTGGTCCAGATG GTCCTTTTTTC. Reverse: TCGAGAAAAAGGACCATCTGGACCAAGATTC-TCTTGAAATCTTGGTCCAGATGGTCCGGG.
- **Scramble shRNA** was provided by Oligoengine.
- **GluA1-SEP** was used in previous studies from the laboratory involving live cell imaging in neurons (Jullié et al., 2014; Rosendale et al., 2017)

### 3.2 Calcium phosphate transfection

Neurons from 6-7 days *in vitro* (DIV6-7) were transfected with different cDNA following calcium phosphate procedure. It is based on forming a calcium phosphate-DNA precipitate which binds to the cell surface and enters the cell by endocytosis.

HBSS (Hank's Balanced Salt Solution) without calcium and Brainphys solution are pre-warmed in the incubator for at least 30 min. 2 ml of Brainphys is added to each culture dish (containing 4 coverslips). The DNA (4-6 µg in total) is mixed with CaCl<sub>2</sub> solution (2.5M) and is then added dropwise to a BES buffer saline (BBS): 50 mM BES, 280 mM NaCl, 1.5 mM Na<sub>2</sub>HPO<sub>4</sub>·2H<sub>2</sub>O. The mixture is gently mixed by vortexing to ensure the formation of a fine precipitate which is necessary to efficiently enter the cell. It is then incubated for 15 min at room temperature in the dark. In the meantime, the coverslips are transferred to a 12-well plate in 450 µl of culture media from the initial petri dish. The DNA/CaCl<sub>2</sub>/BBS mixture (50 µl per well) is added, and the 12-well plate is placed in the incubator for 15-20 minutes. The precipitate on cells can be checked under the microscope. The coverslips are washed 2X with HBSS for 10-15 min and are returned back to their first dish.

### 3.3 Transduction with lentivirus

Lentiviral vector production was done by the service platform for lentiviral vector production ‘Vect’UB’ of the TMB-Core of the Bordeaux University. Lentiviral vectors (scramble-mScarlet, sh1VAMP4-mScarlet, and sh2VAMP4-mScarlet) were produced by transient transfection of 293T cells according to standard protocols (Sena-Esteves M, Tebbets JC, Steffens S, Crombleholme T, Flake AW. Optimized large-scale production of high titer lentivirus vector pseudotypes. *J Virol Methods*. 2004;122(2):131–139).

In brief, subconfluent 293T cells were cotransfected with lentiviral genome (psPAX2) (TOM DULL, ROMAIN ZUFFEREY, MICHAEL KELLY, R. J. MANDEL, MINH NGUYEN, DIDIER TRONO, AND LUIGI NALDINI. *JOURNAL OF VIROLOGY*, 1998, 8463–8471. A Third-Generation Lentivirus Vector with a Conditional Packaging System), with an envelope coding plasmid (pMD2G-VSVG) and with vector constructs by calcium phosphate precipitation. LVs were harvested 48 hours posttransfection and concentrated by ultracentrifugation. Concentrated virus was dissolved in a small volume of medium, aliquoted, and stored frozen at  $-80^{\circ}\text{C}$ .

A pulled glass pipette (4-5 Mohm) was loaded with virus and then lowered into the CA1 region of the organotypic hippocampal slice. A Picospritzer (Parker Hannifin, NJ, USA) was used to pulse the virus into the slice (Figure29).

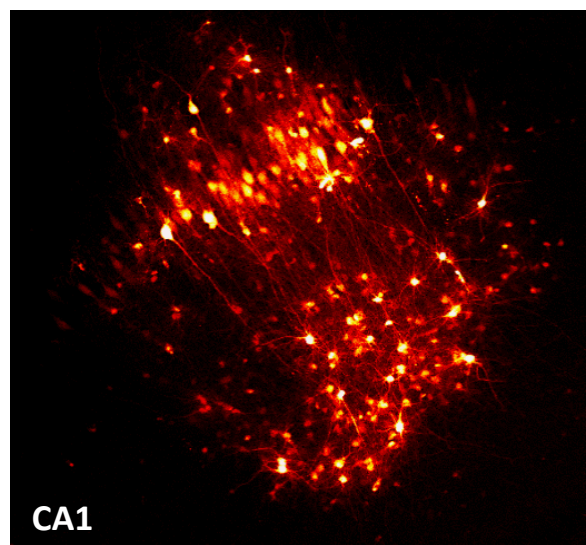


**Figure 29.** ScrambleRNA-mScarlet infected CA1 pyramidal neurons observed with confocal microscopy.

### 3.4 Single cell electroporation

After three to four days in culture, slices were individually transferred to the chamber of an upright microscope (Eclipse FN1, Nikon) where cells were transfected with TeNT by single-cell electroporation (SCE). The microscope chamber was cleaned with 70% ethanol before the beginning of the experiment. During SCE, the chamber contained sterile-filtered bicarbonate-containing Tyrode's solution maintained at ambient temperature and atmospheric conditions without perfusion. Bicarbonate-containing Tyrode's solution was composed of (in mM): 120 NaCl, 3.5 KCl, 2 CaCl<sub>2</sub>, 2 MgCl<sub>2</sub>, 10 HEPES, 10 D-Glucose, 2 NaHCO<sub>3</sub> and 1 Na-pyruvate (pH 7.3, 300 mOsm). Patch pipettes (~5 Mohm) pulled from 1 mm borosilicate capillaries (Harvard Apparatus) were filled with potassium-based solution (in mM): 135 K-methanesulfonate, 4 NaCl, 10 HEPES, 0.06 EGTA, 0.01 CaCl<sub>2</sub>, 2 MgCl<sub>2</sub>, 2 Na<sub>2</sub>-ATP and 0.3 Na-GTP (pH 7.3, 280 mOsm) supplemented with plasmid DNA (13 ng/μL). After obtaining loose-patch seals, electroporation was performed by applying 4 square pulses of negative voltage (-2.5 V, 25 ms duration) at 1 Hz, then the pipet was gently retracted. A total of 10–20 neurons (sometimes ~30 as in figure 30) were electroporated per slice. Each slice was kept no longer than 15 min in the chamber. Slices were then placed back in the incubator for 3-4 days before electrophysiology.

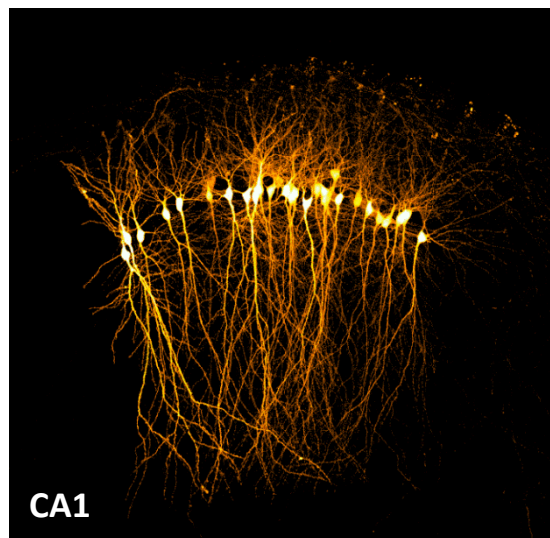


**Figure 30.** ScrambleRNA-mScarlet electroporated CA1 pyramidal neurons observed with confocal microscopy.

## **4. Live cell imaging**

### **4.1 Spinning disk confocal microscopy**

In conventional widefield microscopy, the whole sample is illuminated with excitation light of a specific wavelength. The fluorescence light emitted by the sample outside the focal plane of the objective yields a blurry image with high background because it interferes with the resolution of the in focus molecules. Due to such limitation, confocal microscopy was invented.

Confocal laser scanning microscopy is able to reject light coming from out-of-focus regions of the specimen by means of a pinhole. This system only probes a single point of the specimen and therefore, scanning must be used to obtain an image of the whole optical section. The light source is typically a laser and a photomultiplier tube is usually used as the photodetector. The laser scans the whole surface of the specimen and the image of each point is captured enabling the collection of serial (optical) sections from thick specimens. A three dimension (3D) image of the sample can then be reconstructed using proper softwares. This approach involves one confocal system, and the image is obtained serially by scanning of the spot in 3D with respect to the specimen.

To increase the speed of image acquisition, an optical layout is built which consists of many confocal systems lying side by side. This is achieved by using an aperture disk consisting of many pinholes. Each pinhole acts as both illumination and detection pinhole. Rotation of the disk allows many parts of the specimen to be imaged confocally at the same time, hence the name, spinning-disk confocal microscope. Image is usually captured by a CCD or an EM-CCD camera (Wilson, 2010) (Figure 31).

We have used an inverted Leica DMI6000B Microscope (Leica Microsystems, Wetzlar, Germany) equipped with a spinning-disk confocal system CSU22 Yokogawa Confocal Scanner Unit (Yokogawa Electric Corporation, Tokyo, Japan) in combination with the Leica HCX PL APO CS 63X or 40X oil immersion objective and QuantEM 512 SC EM-CCD camera (Photometrics, Tucson, USA). Cells were illuminated by diode laser of 473 nm wavelength. The system has a barrier filter and an emission Barrier Filters Wheel that rotates fast enough to allow a multicolour imaging in Timelapses with 1Hz frequency. The imaging system is controlled by MetaMorph software (Molecular Devices, Sunnyvale, USA). The microscope is contained inside of temperature control system (Life Imaging Services, Basel, Switzerland). The system controls precisely the temperature inside of its Box, keeping the sample at 37°C for live imaging and eliminating focus instabilities caused by temperature changes.

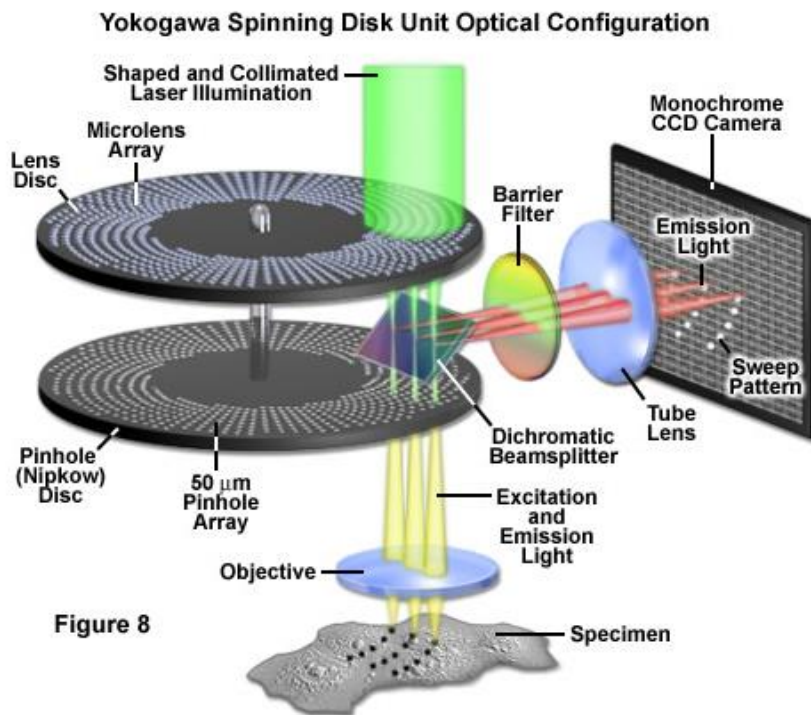


**Figure 31. A schematic of the optical configuration of a spinning disk confocal microscope.**

The sample is illuminated using a laser light which is projected onto a microlens disk with a collimating lens (green light). Light is focused through the dichromatic beamsplitter onto a 50 $\mu$ m pinhole array pattern arranged in a series of nested spirals. A single image is created with each 30-degree rotation of the disk, therefore a complete rotation of 360° can generate 12 frames, or 2000 images per second at the highest disk speeds. After the light exits the pinholes, individual beams of excitation light are projected as a reduced image in the specimen focal plane. Emitted fluorescence from the sample is captured by the objective and focused back onto the pinhole Nipkow disk passing to the dichromatic beamsplitter. The emission light passes through a barrier filter to remove any remaining stray light before it is focused on the CCD camera to create an image.

<http://zeiss-campus.magnet.fsu.edu/articles/spinningdisk/introduction.htm>

## 4.2 Visualization of single exocytic events

### a. SuperEcliptic pHLuorin (SEP)

SuperEcliptic pHLuorin (SEP) is a pH sensitive GFP variant. Fusing SEP to the extracellular domain of a membrane protein of interest allows the fluorophore to be positioned to the luminal side of the vesicle and the extracellular space of the cell. SEP is only fluorescent at a pH greater than 6, but is quenched at lower pH values. Thus, it fluoresces upon insertion in the plasma membrane (PM) but not in the acidic lumen of the vesicle allowing the visualization of exocytic events (Fox-Loe et al., 2017) (Figure 32). Additionally, exchanging extracellular solution with an acidic solution of pH 5.4 quenches surface fluorescence, allowing the visualization of newly formed endocytic vesicles.

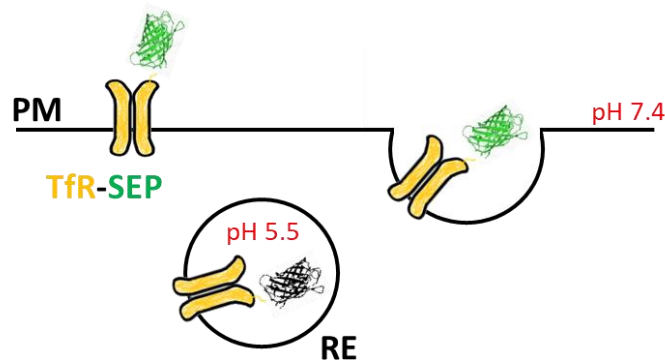


**Figure 32. Schematic of SEP fluorophore fused to transferrin receptor (TfR-SEP), a marker of recycling endosomes (RE).** SEP is quenched at the acidic pH of the RE, but is fluorescent upon vesicle fusion with the plasma membrane (PM) and exposure to the neutral pH of the extracellular space.

### b. Fusion events, imaging and analysis

To measure the rate of fusion events in somato-dendritic compartments, target protein was fused to SEP fluorophore. A single 1-color image was acquired every 1 second (1 Hz) for 2 min in baseline conditions to establish a basal rate of RE fusion, and then again during cLTP induction with glycine, and every 5 min for 20 min following cLTP stimulation to measure the activity-induced rate of RE fusion. cLTP stimulation solution is similar to the one described below.

For the analysis of exocytosis events, we used homemade MATLAB scripts (MathWorks, Natick, USA) developed by David Perrais as previously described in Jullié et al., 2014.

First, to detect the local increase in fluorescence corresponding to an exocytic event, a differential movie was created by subtracting each image from the one before and adding a constant number to avoid negative values ( $I_{diff} = image_{n+1} - image_n + C$ ). A manual threshold

was set to select candidate events (objects bigger than 2 pixels). If two consecutive events are less than 5 pixels apart, the second is excluded (usually a contracting tubule, increasing the individual pixel value after exocytosis). This threshold was calculated above the mean fluorescence of the cell mask. Additional criteria are established to exclude moving clusters and variations in intense clusters. For each detected event, a mini-movie (41x41 pixels, 10 images before and 30 images after exocytosis), and a series of 16 background-subtracted images (images minus average of 5 frames before the event) are generated. Detected events with an intensity less than 4X standard deviation of the average of the 5 initial frames were discarded. Additionally, individual events can be reviewed to discard false positive events. A graph of the cumulative frequency of events over time is generated, and the number of events is normalized to the surface of the cell defined by a mask to give a value in events/ $\mu\text{m}^2/\text{min}$ . For experiments with fast pH changes, events were detected directly on the full movie. Figure 33 shows an example of an automated detection of exocytic events in somatodendritic regions using Matlab.

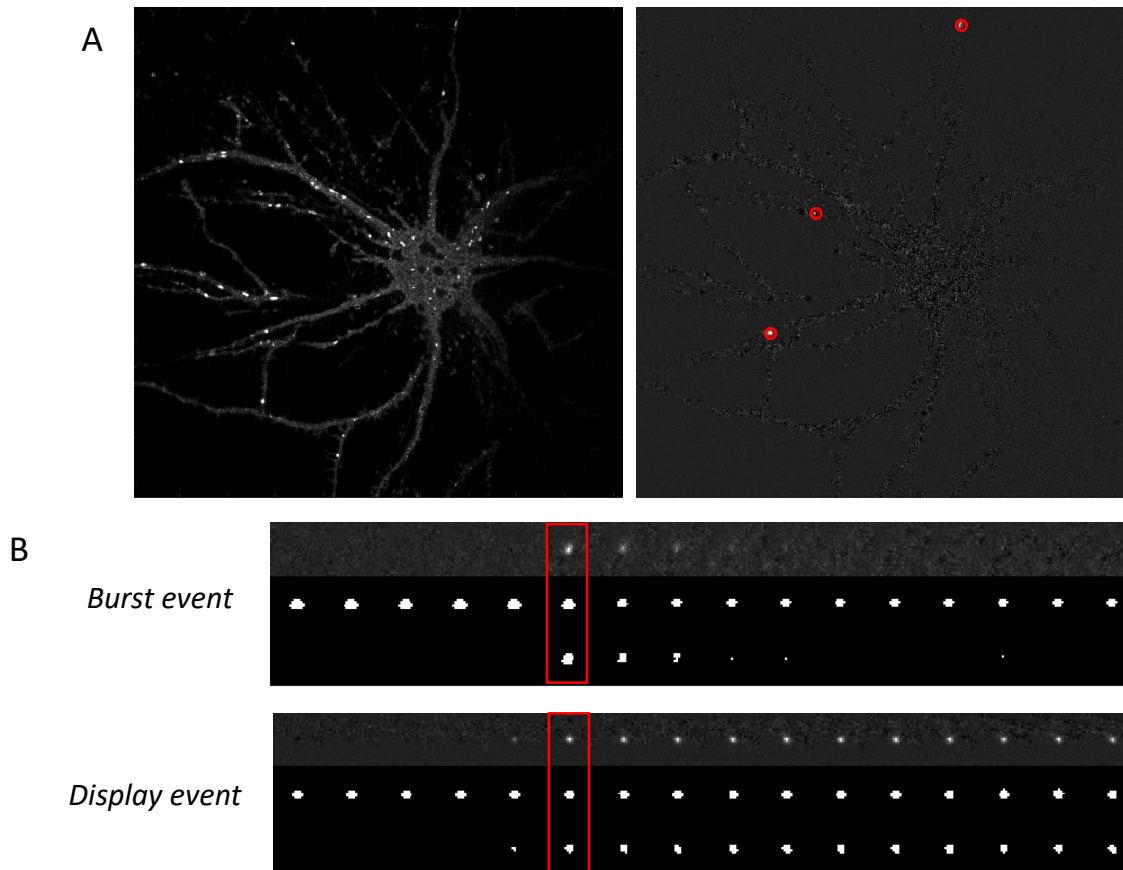


**Figure 33. Analysis of exocytic events in somatodendritic compartments using Matlab.** (A) Raw image of Tfr-SEP transfected neuron (*left*), and a differential image with detected exocytic events shown in red (*right*). (B) Processing of two types of exocytosis events labeled in red. First row, images minus the average of five images before exocytosis. Second row, binary image showing in white ROI pixels where exocytosis fluorescence before and after the event is quantified. Third row, white pixels with intensity value that remains above the threshold.

### 4.3 Glycine treatment on live cells after photobleaching

#### a. Chemical Long-term potentiation protocol

Chemical LTP (cLTP) can be induced in cultured hippocampal neurons using Glycine, an NMDA receptor co-agonist. This type of LTP, like the electrical one induced in hippocampal slices, is also dependent on  $\text{Ca}^{2+}$  influx through post-synaptic NMDA receptors, the activation of CAMKII and the increase in the insertion of AMPRs at the post-synaptic membrane. The exocytosis of AMPARs can be directly visualized by transfecting neurons with GluA1-SEP.

The cLTP stimulation solution used in this study was  $\text{Mg}^{2+}$ -free Tyrode's solution containing (in mM): 150 NaCl, 2  $\text{CaCl}_2$ , 5 KCl, 10 HEPES, 30 Glucose, supplemented with 0.5 Glycine,

0.001 TTX, 0.01 strychnine, and 0.03 picrotoxin (pH 7.4). For cLTP induction, neurons were preincubated in cLTP stimulation solution without glycine for 10 min, and then stimulated with glycine for 3-4 min before they were returned back to a Mg<sup>2+</sup> containing Tyrode solution (2mM MgCl<sub>2</sub>). cLTP is blocked by APV (100mM), an NMDA receptor antagonist which was added to all solutions in control conditions. Strychnine is a glycine receptor blocker which was added to avoid the potential activation of glycine receptors.

#### **b. Fluorescence Recovery after Photobleaching**

Live cells on coverslip (12-13 DIV) were mounted on the imaging chamber immersed in cLTP stimulation solution without glycine at 37°C. A Z stack image of the entire transfected neuron was acquired on a Yokogawa CSU-X1 spinning-disk confocal mounted on a Leica DMI6000B microscope, with a 63X 1.4 NA oil-immersion objective. The system was controlled with Metamorph software (Molecular Devices). Cells were photo bleached using high laser power and another Z stack image was taken to ensure that more than 90% reduction of fluorescence of GluA1-SEP was achieved. Glycine (500μM) was then perfused into the chamber for 4-5 min to induce cLTP followed by Mg<sup>2+</sup> containing tyrode's solution for the following 20 min. The recovery of fluorescence was captured at 5 min intervals for 20 min with a series of Z stack images, which reflects GluA1-SEP delivery to the plasma membrane.

Maximum intensity Z- projections were obtained from each time point using Metamorph software (Molecular Devices, Sunnyvale, USA). Fluorescence intensity was quantified using 50 μm dendritic segments. A mask of a dendritic segment was created using the first image (prebleach) of the time series and then applied on all images to extract total intensity under the same mask. Each intensity value was then normalized to the bleached image to calculate the GluA1-SEP recovery percentage.

#### **4.4 pH change for quantification of surface expression**

To estimate surface expression levels of TfR and GluA1 upon the downregulation of VAMP4, both proteins were fused with SEP fluorophore. Transfected neurons were mounted in imaging chamber perfused with HEPES buffered solution (HBS) with the following (in mM): 120 NaCl, 5 KCl, 2 MgCl<sub>2</sub>, 2 CaCl<sub>2</sub>, 25 HEPES, and 25 D-glucose, adjusted to pH 7.4. Imaging was done at 37°C with a 40X oil-immersion objective.

Cells were alternatively perfused with acidic ACSF pH5.5 to quench surface SEP (HEBES was replaced with 10 mM MES), followed by standard neutral imaging buffer pH7.4, then ACSF with ammonium chloride to reveal total SEP signal (50 mM NH<sub>4</sub>Cl substituted for 50 mM NaCl). Region of interests (ROIs) were selected on dendrites and spines (visible puncta during NH<sub>4</sub>Cl perfusion), and surface expression was calculated as percentage of total ((pH7.4 fluorescence-pH5.5 fluorescence)/NH<sub>4</sub>Cl fluorescence-pH5.5 fluorescence)x100.

## **5. Immunocytochemistry and Transferrin recycling assay**

For immunocytochemistry, cells were fixed for 10 min in warm 4% paraformaldehyde-4% sucrose in phosphate buffered saline solution. After rinse with PBS, cells were permeabilized with 0.1% Triton X-100 in PBS containing 1 % gelatin (to block nonspecific binding) for 20 min. VAMP4 was labeled with 1/500 rabbit anti VAMP4 (Synaptic Systems 136 002, dilution 1:500), followed by 1:1000 Alexa Fluor 568-conjugated goat anti-rabbit antibody (2 mg/ml, Invitrogen). Co-immunolabelling of TfR was performed with monoclonal mouse anti TfR (Thermofisher 13-6800) and anti EEA1 (BD Biosciences 610457, 1:1000), respectively, followed by 1:1000 Alexa Fluor 488-conjugated goat anti-mouse antibody. Coverslips were then mounted in fluoromount (Vector Laboratories). Single optical slices were imaged on the spinning disk confocal microscope (for localization Figure 2), or stacks of 10 planes, 0.2 µm apart for maximum intensity projections (for quantification of KD efficiency, Figure 3).

For pulse chase of transferrin, cells were starved for 5 min in HBS at 37°C 5% CO<sub>2</sub> before uptake of Alexa568-Tfn at 50 µg/ml for five minutes at 37°C 5% CO<sub>2</sub>. Chase was done with unlabeled holo-Tfn (Sigma) at 2 mg/ml for 5, 10, 15 and 20 min at 37°C 5% CO<sub>2</sub>. Cells were then fixed for 10 min in 4 % paraformaldehyde-4% sucrose in PBS. Cells were imaged in PBS on the spinning disk confocal microscope. A stack of 9 focal planes, 0.2 µm apart, was acquired in both GFP and A568-Tfn channel. We defined a mask of the cell in the GFP channel and used it for quantification of A568-Tfn labeling.

## 6. Electron Microscopy

Coverslips with attached neurons were placed in pre-warmed 4% paraformaldehyde (EMS 15710) in 0.15M Sorensen's phosphate buffer (PB, EMS 11682) at room temperature for 45 minutes. All subsequent steps were performed at room temperature. Neurons were rinsed 3 times in 0.15 M Sorensen's PB, once in 0.1M Millonig's PBS, and then blocked and permeabilized in a solution containing 0.1M Millonig's PBS with 2% BSA (Sigma 3359), 0.1% cold water fish skin gelatin (Aurion 900.033) and 0.1% Saponin for 60 minutes. Next, neurons were incubated for 90 minutes in primary antibody against TfR (Millipore) or VAMP4 (Synaptic System) diluted in the blocking/Saponin solution. Then, cover slips were rinsed twice in blocking/Saponin solution for 60 minutes before incubation with FluoroNanogold anti mouse Fab' Alexa Fluor 488 for TfR or anti rabbit Fab' Alexa Fluor 488 for VAMP4 (Nanoprobes 7202) diluted 1:100 in blocking/Saponin solution for 60 minutes, then rinsed once in Sorensen's PB, and placed in freshly prepared 2% paraformaldehyde in Sorensen's PB for 30 minutes to stabilize immunogold labeling. After, neurons were stored in Sorensen's PB until silver intensification. In some cases, the quality of FluoroNanogold labeling was confirmed by epifluorescence microscopy (Leica DM5000) before proceeding with electron microscopy.

FluoroNanogold was enhanced for 5-7 minutes using HQ Silver Reagent (Nanoprobes 2012) according to manufacturer's instructions and processed immediately for electron microscopy; all steps were carried out at room temperature. After several rinses in Sorensen's PB, neurons were incubated in 0.2% OsO<sub>4</sub> in Sorensen's PB for 30 minutes, and then rinsed 10 times in dH<sub>2</sub>O to remove all traces of PB before placing neurons in filtered 0.25% uranyl acetate dissolved in dH<sub>2</sub>O for 30 minutes. After several water rinses, neurons were dehydrated by 3 minute incubations in a graded series of ethanol: 50%, 70%, 95%, and twice in 100%. No propylene oxide was used to prevent loss of immunogold label. Samples were infiltrated during 1-2 hour steps in 70% Epon812/ ethanol mixture followed by 2 exchanges of 100% freshly prepared Epon812 (Taab, T004), and finally embedded in freshly prepared Epon812. To allow cutting of en face sections of neurons, cover slips were placed cell side facing up on a glass slide and gelatin capsules filled with Epon812 were inverted and placed on top of cover slip, and polymerized at 60°C for 48 hours. Cover slips were removed from polymerized samples by gentle heating over a flame while pulling slightly on the glass slide. Ultrathin sections (60 nm thickness) were cut using an Ultra 35° diamond knife (Diatome, USA) and a Leica Ultracut UCT M26 (Leica Microsystems, Germany) and picked up on 2mm slot grids with a 1% formvar support film. Sections were contrasted with 3% aqueous uranyl acetate for 5 minutes, and then

Reynolds's lead citrate for 5 minutes prior to imaging using a Hitachi H7650 transmission electron microscope operated at 80kV. Images were captured using an Orius CCD (Gatan Soc., USA).

## **7. In- vitro electrophysiology**

### **7.1 Whole-cell patch-clamp recordings**

Organotypic slices were transferred to the upright Leica DM5000 microscope (Leica Microsystems, Wetzlar, Germany) chamber perfused with carbogen-bubbled recording ACSF maintained at  $\sim 30^{\circ}\text{C}$  by an in-line solution heater (WPI). For whole-cell voltage clamp recordings of evoked EPSCs amplitudes, the recording ACSF contained (in mM): 125 NaCl, 26  $\text{NaHCO}_3$ , 10 D-glucose, 1.26  $\text{NaH}_2\text{PO}_4$ , 3 KCl, 2  $\text{CaCl}_2$ , 1  $\text{MgCl}_2$ , 0.025 picrotoxin (320 mOsm). Patch pipettes ( $\sim 4\text{-}6$  Mohm) for whole-cell voltage clamp recordings were filled with a caesium-based intracellular solution containing (in mM): 130 Cs-methanesulfonate, 4 NaCl, 10 HEPES, 5 QX-314 Cl, 1 EGTA, 2 Mg-ATP, 0.5 Na-GTP, 10 phosphocreatine (pH 7.3, 290 mOsm). To evoke the EPSCs response, the stimulating electrode was positioned in stratum radiatum of CA1 region. Schaffer collaterals were activated at 0.1 Hz using a Platinum-Iridium cluster bipolar stimulating electrode (25  $\mu\text{m}$ , FHC, USA). AMPAR-mediated currents were recorded at  $-70$  mV and NMDAR-mediated currents were recorded at  $+40$  mV and measured 100 ms after the stimulus.

Dual cell recordings of neighboring infected and uninfected pairs of pyramidal cells were recorded simultaneously in CA1 with Schaffer collateral stimulation (Figure 34). The AMPAR/NMDAR ratio was calculated as the peak averaged AMPAR EPSCs (30 consecutive events) at  $-70$  mV divided by the averaged NMDAR EPSCs (30 consecutive events) measured at  $+40$  mV with a delay of 100 ms after the start of the stimulus artefact.

Stimulation control, analogue signal filtering and digitization were performed with EPC-10 USB amplifier controlled by Patchmaster next software (HEKA Elektronik).

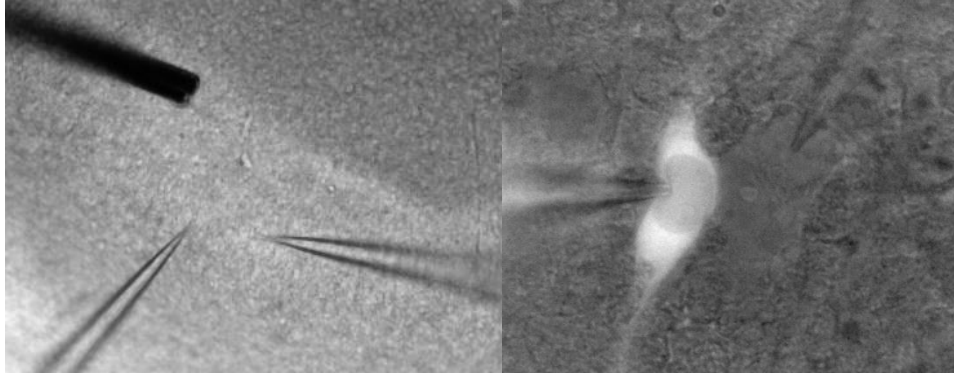


**Figure 34.** Dual whole-cell recording configuration of evoked EPSCs from neighbouring CA1 infected and uninfected pyramidal cell upon the stimulation of the schaffer collaterals.

## 7.2 Long term potentiation induction

For LTP recordings, the CA3 region was cut off, and slices were continuously perfused with warm (30°C), carbogen (95% O<sub>2</sub> / 5% CO<sub>2</sub>)-bubbled recording ACSF containing in (mM): 125 NaCl, 26 NaHCO<sub>3</sub>, 10 D-glucose, 1.26 NaH<sub>2</sub>PO<sub>4</sub>, 3 KCl, 4 CaCl<sub>2</sub>, 4 MgCl<sub>2</sub>, 0.025 picrotoxin. Calcium and magnesium concentrations were raised to 4mM to dampen excitability. Strictly 5 min after going whole-cell, LTP was induced by depolarization of the cells to 0 mV while stimulating the afferent Schaffer's collaterals at 3 Hz for 100 s. Pre-stimulation baseline was recorded for 3 min at 0.1 Hz. Short baseline recordings were necessary to prevent washout of LTP in slice culture whole-cell recordings.

## 8. Statistical tests

All data are presented as mean  $\pm$  SEM. Statistical significance was calculated on Graphpad Prism 8 software. We used two-tailed t-test between interleaved control cells and test cells or one-way ANOVA for multiple comparisons.



# RESULTS



## **VAMP4 controls constitutive recycling and sorting of post-synaptic receptors in neuronal dendrites**

**May Bakr<sup>1</sup>, Damien Jullié<sup>1,2</sup>, Julia Krapivkina<sup>1</sup>, Lou Bouit<sup>1</sup>, Jennifer Petersen<sup>1,3</sup>, Natacha Retailleau<sup>1</sup>, Christelle Breillat<sup>1</sup>, Daniel Choquet<sup>1,4</sup> & David Perrais<sup>1</sup>**

<sup>1</sup>Univ. Bordeaux, CNRS, Interdisciplinary Institute for Neuroscience, IINS, UMR 5297, F-33000 Bordeaux, France

<sup>2</sup>Present address: University of California, San Francisco, San Francisco, CA, USA.

<sup>3</sup>Present address: National Institute of Child Health and Human Development, National Institutes of Health, Bethesda, MD 20892

<sup>4</sup>Univ. Bordeaux, CNRS, INSERM, Bordeaux Imaging Center, BIC, UMS 3420, US 4, F-33000 Bordeaux, France

**Correspondence to:** David Perrais, [david.perrais@u-bordeaux.fr](mailto:david.perrais@u-bordeaux.fr)

**Number of figures:** 8

**Supplementary material:** 3+ movies

**Bullet points:**

- **VAMP4 mediates the exocytosis of somato-dendritic recycling endosomes (REs)**
- **VAMP4 controls the sorting of AMPARs to retromer dependent REs**
- **Knock-down of VAMP4 increases AMPAR recycling and post-synaptic currents**
- **Increased post-synaptic currents partially occlude LTP**

**Keywords:** synapse, synaptic plasticity, AMPA receptor, exocytosis, SNARE, recycling endosome.

## **ABSTRACT**

Post-synaptic  $\alpha$ -amino-3-hydroxy-5-methyl-4-isoxazolepropionate (AMPA) receptors exchange continuously between synaptic, extrasynaptic, and intracellular compartments through diffusion in dendrites, endocytosis, and recycling. Exocytosis, the last step of recycling, is directly involved in the expression of long-term potentiation (LTP), as tetanus toxin, which cleaves the SNARE (soluble NSF-attachment protein receptor) protein VAMP2, blocks LTP. However, a general description of the activity-dependent post-synaptic membrane trafficking remains elusive. Here we identify VAMP4 as the key vesicular SNARE protein that mediates most constitutive recycling in the somato-dendritic compartment while VAMP2 plays a minor part. Knock-down (KD) of VAMP4 reduces the recycling of transferrin receptor (TfR), a marker of recycling endosomes. In parallel, VAMP4 KD enhances AMPAR recycling. Consequently, it increases post-synaptic currents and partially impairs LTP in CA1 pyramidal neurons. Our data suggest a model where the depletion of VAMP4 leads to the missorting of AMPARs to the plasma membrane, which consequently impairs LTP via an occlusion mechanism. Additionally, the opposing changes in the levels of TfR and AMPAR on the cell surface upon VAMP4 KD reveal that these receptors are sorted and trafficked separately.

## INTRODUCTION

The endosomal system in neuronal dendrites is essential for the maintenance of neuronal polarity, synaptic transmission, and the expression of synaptic plasticity, as well as other forms of signaling (Bentley and Banker, 2016; Kennedy and Ehlers, 2011). In many forms of synaptic plasticity, such as long term potentiation (LTP) of excitatory synapses in CA1 hippocampal pyramidal neurons, the increase in synapse strength is mediated by the addition of post-synaptic glutamate AMPA-type receptors, which mediate excitatory post-synaptic currents (EPSCs) (Granger and Nicoll, 2014; Huganir and Nicoll, 2013). Consistent with a role for AMPAR exocytosis in LTP, specific block of vesicle fusion in the post-synaptic neuron by dialysis of botulinum toxin B (BoNT-B) or tetanus toxin (TeNT), which cleave the SNARE (soluble NSF-attachment protein receptor) proteins VAMP1-3, abolishes LTP in acute slices (Lledo et al., 1998) cultured organotypic slices (Penn et al., 2017) or dissociated cultures (Lu et al., 2001). Besides, dialysis of TeNT or BoNT-B induces a marked decrease of EPSC amplitude in 10-20 minutes (Lüscher et al., 1999; Penn et al., 2017; Wang et al., 2007). This suggests that exocytosis is not only required for synaptic plasticity but also for the maintenance of synaptic transmission at all times. By contrast, blocking receptor internalization acutely by blocking endocytosis mediated by dynamin leads to the increase of EPSC amplitude also within 10-20 min (Glebov et al., 2015; Lüscher et al., 1999; Wang et al., 2007). These results led to the model according to which AMPARs are constitutively internalized and recycled (Ehlers, 2000; Passafaro et al., 2001) and modulation of these processes mediate, at least in part, synaptic plasticity.

Effectively, recycling endosomes (REs), which contain internalized receptors, have been identified as the intracellular organelles necessary for the expression of LTP. Overexpression of a dominant negative mutant of Rab11a, a marker of REs and major regulator of RE function (Welz et al., 2014), blocks LTP (Brown et al., 2007; Park et al., 2004). Moreover, live-cell imaging of cultured neurons has shown that the transferrin receptor (TfR), a classical marker of REs, fused to GFP, is transported into dendritic spines after the chemical induction of LTP (cLTP) (Park et al., 2006) through calcium-dependent binding of myosin V (Correia et al., 2008; Wang et al., 2008). Finally, TfR exocytosis, detected with TfR fused to the pH sensitive variant of GFP surporecliptic pHluorin (SEP), is increased after cLTP induction (Hiester et al., 2017; Keith et al., 2012; Kennedy et al., 2010) and recycling of the internalized ligand transferrin (Tf)

is similarly increased (Park et al., 2004). Likewise, the exocytosis of AMPAR subunits GluA1-3 labeled with SEP is increased after the induction of LTP (Tanaka and Hirano, 2012; Yudowski et al., 2007). However, the rate of basal recycling and exocytosis differ between AMPARs and TfR by almost an order of magnitude (Jullié et al., 2014; Temkin et al., 2017) and the term 'recycling endosome' possibly regroups a large diversity of organelles in neuronal dendrites that have not been deciphered yet (Kennedy and Ehlers, 2006; van der Sluijs and Hoogenraad, 2011). This large diversity of REs could use different proteins and regulators to undergo transport and fusion. One way to address this issue is to identify the molecular determinants of RE function.

The fusion step required for exocytosis is mediated by cognate R and Q-SNAREs located on the vesicles and plasma membrane, respectively (Jahn and Scheller, 2006). Experiments using knock-down (KD) of individual SNARE proteins together with electrophysiology have identified SNAP47 and syntaxin-3 as the complementary Q-SNAREs which would form with the R-SNARE VAMP2 the SNARE complex mediating the exocytosis of compartments, most likely REs, necessary for the expression of LTP (Jurado et al., 2013). With the same strategy, complexin1 and 2 (Ahmad et al., 2012) as well as synaptotagmin1 and 7 (Wu et al., 2017), proteins involved in the calcium sensitivity of exocytosis (Brunger et al., 2019), were found to be necessary for the expression of LTP. Remarkably, KD of all these proteins (SNAP47, syntaxin3, complexin1 and 2, synaptotagmin1 and 7) selectively affect LTP without affecting basal AMPAR or NMDAR mediated synaptic transmission (Ahmad et al., 2012; Jurado et al., 2013; Wu et al., 2017). In contrast, the SNAREs and associated proteins mediating the constitutive recycling of AMPARs have remained elusive. Acute disruption of VAMP2 by clostridial toxins partially inhibits EPSCs (Lüscher et al., 1999; Penn et al., 2017; Wang et al., 2007). Moreover, surface localization of AMPARs is strongly reduced in cultured neurons from VAMP2 KO mice, consistent with impaired recycling (Jurado et al., 2013). This suggests that AMPAR recycling is mediated, at least in part, by VAMP2. However, whether or not VAMP2 is necessary for all RE exocytosis events is still unknown.

Given the importance of somato-dendritic recycling in neuronal physiology, our goal was to identify major players of dendritic RE exocytosis labelled with TfR-SEP. We found that VAMP2 plays only a minor role while VAMP4 is the major mediator of constitutive RE exocytosis. Knocking down VAMP4 reduced TfR recycling but increased AMPAR recycling, most likely by

missorting into a constitutive recycling pathway. Finally, we show that the increased surface localization of AMPARs is accompanied in organotypic hippocampal slices by an increased EPSC in CA1 pyramidal cells and partial occlusion of LTP.

## RESULTS

### **VAMP4 is a marker of recycling endosome exocytosis in neuronal dendrites**

The RE marker TfR-SEP reveals an intense constitutive exocytosis activity in neuronal dendrites (Jullié et al., 2014; Kennedy et al., 2010; Roman-Vendrell et al., 2014). We measured a frequency of  $0.037 \pm 0.004$  events. $\mu\text{m}^{-2}\cdot\text{min}^{-1}$  in cultured hippocampal neurons transfected with TfR-SEP and recorded at 13-15 DIV with time-lapse spinning disk confocal microscopy at 1 Hz (Figure 1C, Supplementary Movie 1). We reasoned that other transmembrane RE proteins fused to SEP should report their exocytosis as well. In particular, vesicular SNAREs, essential proteins for the fusion step, are interesting candidates. When expressed in neurons, VAMP2-SEP is highly polarized to the axon, as previously shown (Sampo et al., 2003; Sankaranarayanan and Ryan, 2000) (see Figure 3B). In soma and dendrites, with comparatively low fluorescence, we recorded exocytosis events (Figure 1B, Supplementary Movie 2). However, the frequency of these events was only  $0.0058 \pm 0.0015$  events. $\mu\text{m}^{-2}\cdot\text{min}^{-1}$ , much lower than the frequency of TfR-SEP events ( $p = 0.0012$ , Figure 1D). Therefore, VAMP2 cannot be the only vSNARE responsible for TfR-SEP exocytosis and we tested other candidate vesicular SNAREs which are expressed in neurons, VAMP4, and VAMP7. We could not detect exocytosis events in neurons transfected with VAMP7-SEP at 15 DIV even though exocytosis can be detected at earlier stages during neurite outgrowth (Burgo et al., 2012). In contrast, in neurons transfected with VAMP4-SEP, exocytosis events occur at high frequency ( $0.042 \pm 0.008$  events. $\mu\text{m}^{-2}\cdot\text{min}^{-1}$ ,  $n = 12$ , Figure 1C), very similar to the frequency observed with TfR-SEP (one-way ANOVA,  $p = 0.77$ , Figure 1D).

RE exocytosis events in neuronal dendrites can be categorized into burst events, for which the membrane marker quickly diffuses into the plasma membrane, and display events, for which the RE remains visible for many seconds after rapid closure of the fusion pore (Hiester et al., 2017; Jullié et al., 2014; Roman-Vendrell et al., 2014). For both VAMP2 and VAMP4, the two types of events could be observed. The proportion of display events was similar for TfR and VAMP2 and slightly higher for VAMP4 (one-way ANOVA  $p = 0.97$  and  $0.06$  for VAMP2 and

VAMP4 vs TfR, Figure 1D). Alternating between pH 7.4 and 5.5 revealed that, like for TfR (Jullié et al., 2014), some display events are still visible after the exchange with pH 5.5 solution (Figure 1F, G), hence report the transient opening of a fusion pore. Moreover, VAMP4-SEP exocytosis events occurred at TfR-mCherry clusters which label REs (Figure 1I, Supplementary Movie 3), which is also the case for VAMP2-SEP exocytosis events (Figure 1H). The TfR-mCherry signal is stable after display exocytosis while it decreases immediately after burst exocytosis (Figure 1H-K), consistent with display exocytosis reporting the transient opening of a fusion pore. This behavior is similar to the one observed with TfR-SEP and other RE markers such as internalized fluorescent transferrin and Rab11a-mCherry (Jullié et al., 2014). We conclude from this data that VAMP2-SEP and VAMP4-SEP both mark the sites of RE exocytosis with very similar properties. However, because VAMP4 reports about 10 times more events than VAMP2, we make the hypothesis that VAMP4 mediates most of the constitutive recycling in the neuronal somato-dendritic compartment.

We examined the location of VAMP4 in dendrites in more detail. In neurons transfected with TfR-mCherry and VAMP4-GFP, where GFP is located in the cytoplasmic side of VAMP4 hence visible in acidic intracellular compartments, the two markers are co-localized in the somato-dendritic compartment (Figure 2A) (Jain et al., 2014). Both markers are highly enriched in a perinuclear compartment which corresponds to the trans-Golgi network (TGN), as seen in other cell types (Peden et al., 2001; Tran et al., 2007). Also, clusters containing both proteins are visible along dendrites. Similarly, labelling of endogenous VAMP4 with immunocytochemistry revealed a clear co-localization with endogenous TfR at the TGN as well as dendritic labelling (Figure 2B). The dendritic labelling was not as clustered as for VAMP4-GFP but clear puncta were distributed along dendrites. Some of these puncta were colocalized or next to TfR puncta (Figure 2B). Moreover, co-labelling of the early endosome marker EEA1 showed some degree of colocalization as well (Figure 2C). To get a better insight into the localization of VAMP4 in dendrites, we performed silver intensified immunogold labeling in thin sections of neurons observed with transmission electron microscopy. Labelling of TfR showed a clear accumulation of staining in tubular organelles likely corresponding to REs (Figure 2D) (Cooney et al., 2002). Labelling of VAMP4 indicates that it is highly enriched in somatic perinuclear TGN and also found in dendritic tubular organelles, i.e. REs (Figure 2E).

Therefore, endogenous VAMP4 is present in dendritic REs and could participate in their exocytosis.

### **Downregulation of VAMP4 but not cleavage of VAMP2 reduces TfR exocytosis and recycling**

To determine the functional implication of VAMP2 and VAMP4 in RE exocytosis, we used molecular tools to suppress them or to block their action. VAMP2 and the closely related VAMP1 and VAMP3 are cleaved by TeNT (Binz et al., 2010), and expression of TeNT light chain (TeNT-LC) cleaves VAMP1-3 efficiently (Proux-Gillardeaux et al., 2005). VAMP3 is not expressed in hippocampal neurons (Schoch et al., 2001) while VAMP1 is expressed in the hippocampus specifically in interneurons late in development (Ferecskó et al., 2015; Vuong et al., 2018). Therefore, TeNT specifically targets VAMP2 in hippocampal pyramidal cells. However, expression of TeNT-LC in neurons for 7 days did not affect the frequency of TfR-SEP exocytosis events compared to the co-expression of the inactive mutant TeNT-LC E234Q (Figure 3A). TeNT-LC was active because no exocytosis events could be recorded in neurons co-expressing VAMP2-SEP while events could be recorded in neurons co-expressing the inactive mutant ( $0.0027 \pm 0.0009$  events. $\mu\text{m}^{-2}.\text{min}^{-1}$ ,  $n = 4$ ). Moreover, TeNT-LC disrupted the polarized targeting of VAMP2-SEP to the axon (Figure 3B) and affected synaptic plasticity (see below). This indicates that the vast majority of the detected TfR-SEP exocytosis does not rely on the targets of TeNT, i.e. VAMP2.

We have used a knock-down (KD) strategy with shRNAs to suppress the expression of VAMP4 as done before in neurons (Lin et al., 2020; Nicholson-Fish et al., 2015; Raingo et al., 2012). We selected two different shRNAs, KD1 which targets the 3' UTR of VAMP4 mRNA, and KD2 which targets the coding sequence (see Methods). As confirmed by immunofluorescence, the co-transfection of either or both shRNAs with GFP for 4-5 days led to a strong decrease of the endogenous VAMP4 levels compared to the cotransfection with a scramble shRNA (Figure 3C). In addition, their expression reduces TfR-SEP exocytosis frequency about 2-fold (Figure 3D). Co-expression of VAMP4-HA together with VAMP4 KD1 and TfR-SEP restored VAMP4 staining (Figure 3C) and the frequency of exocytosis events, while expression of VAMP4-HA alone did not affect event frequency (Figure 3D). This indicates that VAMP4 is involved in a fusion step necessary for the efficient recycling of TfR.

To test directly the involvement of VAMP4 in TfR recycling, we performed a pulse chase assay with Alexa568 labelled transferrin (A568-Tf). After 5 min pulse and 5 min chase with unlabeled holo-transferrin, the amount of internalized A568-Tf was similar for neurons expressing KD1 in a GFP vector ( $1860 \pm 180$  AFU,  $n = 74$  neurons in 4 independent experiments) as in neurons expressing a scrambled shRNA in the GFP vector ( $2130 \pm 161$  AFU,  $n = 74$  neurons in 4 independent experiments, unpaired t-test  $p = 0.27$ ) (Figure 3E). This suggests that TfR endocytosis is not impaired by VAMP4 KD. Moreover, in control conditions, TfR recycles rapidly to the cell surface such that most A568-Tf is lost in 15 minutes. On the other hand, in neurons knocked down for VAMP4, the A568-Tf labeling is significantly higher after 10 or 15 min chase compared to control (Figure 3E-F). This indicates that despite efficient endocytosis, recycling of TfR at the cell surface is strongly delayed in these cells.

If recycling of TfR is selectively impaired, it should affect its steady-state localization between the surface and intracellular pools. We measured the localization of TfR-SEP transfected in neurons with first an application of solution at pH 5.5 to reveal the proportion of surface receptors and then an application of ammonium solution at pH 7.4 which reveals the proportion of receptors in acidic intracellular compartments (Sankaranarayanan et al., 2000) (Figure 3G). As predicted, the surface fraction calculated from these measures was significantly smaller in neurons expressing KD1 ( $0.20 \pm 0.02$ ,  $n = 26$  neurons) than in neurons expressing scr ( $0.30 \pm 0.03$ ,  $n=27$  neurons) (Figure 3H).

#### **VAMP4 exocytosis increases after chemical induction of LTP**

To study the regulated fusion of TfR-labelled REs in somato-dendritic regions, we performed a chemical LTP (cLTP) induction protocol (glycine 500  $\mu$ M, 0  $Mg^{2+}$ , 30  $\mu$ M picrotoxin, and 10  $\mu$ M strychnine for 5 min) which has been shown previously to enhance Tf recycling (Park et al., 2004) and the frequency of TfR-SEP exocytosis events in primary hippocampal cultures (Hiester et al., 2017; Keith et al., 2012; Kennedy et al., 2010). Indeed, in neurons transfected with TfR-SEP and cultured in Brainphys medium for 12-15 DIV (see Methods), cLTP induces a robust and sustained increase in the frequency of exocytosis events (Figure 4 A-C) which was maximal 15 min after cLTP induction ( $180 \pm 21$  % of basal exocytosis frequency,  $n = 16$  neurons). This increase was blocked by the NMDA receptor antagonist APV (100  $\mu$ M) ( $91 \pm 8$  %,  $n = 12$  neurons), showing that this effect was due to the activation of NMDA receptors.

Also, cLTP induction increases dendrite fluorescence ( $1.24 \pm 0.04$ ,  $n = 16$  neurons), which reflects the number of receptors at the cell surface (Hiester et al., 2017; Park et al., 2006). This increase was also blocked by APV (Figure 4D) ( $0.99 \pm 0.06$ ,  $n = 12$  neurons).

We then tested the same cLTP protocol in neurons transfected with VAMP4-SEP. The frequency of exocytosis events ( $201 \pm 26$  %,  $n = 15$  neurons) and dendrite fluorescence ( $1.35 \pm 0.09$ ,  $n = 15$  neurons) were increased the same way after cLTP as TfR-SEP exocytosis event frequency (Figure 4E-G). Similarly, this increase was completely blocked by APV ( $95 \pm 21$  %,  $n = 10$  neurons;  $0.98 \pm 0.07$ ,  $n = 10$  neurons). Therefore, we conclude that VAMP4-SEP and TfR-SEP label the same population of REs, whose exocytosis can be modulated after cLTP induction.

### **VAMP4 KD does not impair the increase in RE exocytosis during cLTP induction**

We then investigated the effect of VAMP4 KD on the exocytosis frequency of REs upon cLTP induction in somato-dendritic regions. Neurons were co-transfected with TfR-SEP and either scr or VAMP4 KD1 to downregulate VAMP4. Neurons transfected with the VAMP4 KD plasmid and cultured in Brainphys medium had a reduced basal frequency of TfR-SEP exocytosis events ( $0.047 \pm 0.005$  events. $\mu\text{m}^{-2}\cdot\text{min}^{-1}$ ,  $n = 8$  neurons) compared to control neurons ( $0.146 \pm 0.028$  events. $\mu\text{m}^{-2}\cdot\text{min}^{-1}$ ,  $n = 10$  neurons), similar to neurons cultured in Neurobasal. Upon cLTP induction, VAMP4 KD neurons still had a significant increase in exocytosis frequency of TfR-SEP upon LTP induction ( $0.0653 \pm 0.005$  events. $\mu\text{m}^{-2}\cdot\text{min}^{-1}$ ,  $n = 8$  neurons) compared to control group ( $0.232 \pm 0.059$  events. $\mu\text{m}^{-2}\cdot\text{min}^{-1}$ ,  $n = 10$  neurons) (Figure 5 A). This was accompanied by a significant increase in fluorescence intensity in control ( $1.60 \pm 0.19$ ,  $n = 10$  neurons) and VAMP4-KD neurons ( $1.56 \pm 0.15$ ,  $n = 9$  neurons) (Figure 5 B,C).

TenT (or BoNT-B) has been shown to block the expression of LTP, i.e. the increase in EPSC amplitude following induction, in hippocampal neurons in acute slices (Lledo et al., 1998), organotypic slices (Penn et al., 2017), or in dissociated cultures (Lu et al., 2001). Surprisingly, the expression of TenT-LC did not impair the increase in exocytosis frequency of TfR-SEP upon LTP induction (basal:  $0.070 \pm 0.017$  events. $\mu\text{m}^{-2}\cdot\text{min}^{-1}$ ; cLTP:  $0.108 \pm 0.020$  events. $\mu\text{m}^{-2}\cdot\text{min}^{-1}$ ,  $n = 13$  neurons) compared to neurons expressing the inactive TenT-LC E234Q (basal:  $0.080 \pm 0.064$  events. $\mu\text{m}^{-2}\cdot\text{min}^{-1}$ ; cLTP:  $0.116 \pm 0.075$  events. $\mu\text{m}^{-2}\cdot\text{min}^{-1}$ ,  $n = 13$  neurons) (Figure 5 D). Instead, TenT-LC expression impaired the increase in surface fluorescence intensity of

TfR-SEP ( $0.96 \pm 0.05$ ,  $n=13$  neurons) observed in the TenT inactive control group ( $1.33 \pm 0.08$ ,  $n=13$  neurons) upon LTP induction (Figure 5 E, F). These results suggest that VAMP2 does not mediate the regulated exocytosis of most REs in somatodendritic compartments, but rather possibly functions in the stabilization of newly exocytosed receptors at the neuronal surface.

### **VAMP4 KD accelerates AMPAR recycling and impairs its modulation during LTP induction**

We then asked if VAMP4 KD would have an effect on the dendritic insertion of AMPARs upon cLTP induction. In neurons transfected with the AMPAR subunit GluA1 tagged with SEP (SEP-GluA1) and either scr or VAMP4 KD1, we performed whole-cell fluorescence recovery after photobleaching for 25 min to measure the rate of insertion of SEP-GluA1 from intracellular acidic organelles, in which SEP is not fluorescent and hence not bleached (Temkin et al., 2017; Wu et al., 2017). Neurons were initially imaged and then photobleached immediately before cLTP induction (Figure 6A). In the control group (scramble), the rate of SEP-GluA1 insertion was greatly increased after cLTP induction ( $16.2 \pm 1.0$  % recovery after 25 min,  $n= 42$ ) compared to block of cLTP induction with APV ( $5.9 \pm 0.4$  %,  $n = 39$ ,  $p < 0.0001$ ) (Figure 6B). However, in neurons expressing VAMP4 KD1, cLTP did not change the rate of SEP-GluA1 recovery (cLTP:  $6.8 \pm 0.5$  %,  $n = 45$  vs APV:  $8.4 \pm 0.6$  %,  $n = 41$ ) (Figure 6C). On the other hand, the basal SEP-GluA1 recovery rate of VAMP4 KD neurons was significantly higher than the one of control neurons (Figure 6D,  $p = 0.0007$ ). To further assess the effect of VAMP4 KD on the surface expression of SEP-GluA1, we measured the surface fraction of SEP-GluA1 by changing the pH of the perfusion buffer, similar to the experiment performed on TfR-SEP (Figure 3G). Indeed, SEP-GluA1 surface fraction is significantly higher in VAMP4 KD compared to control (Control:  $0.53 \pm 0.02$ ,  $n=15$  neurons; VAMP4 KD:  $0.62 \pm 0.03$ ,  $n=15$  neurons,  $p = 0.031$ ). This contrasts with the reduction of TfR-SEP recycling and surface expression (Figure 3G). This shows that the depletion of VAMP4 affects the basal levels of plasma membrane AMPAR and TfR in an opposing manner.

### **Effect of VAMP4 KD on synaptic transmission and plasticity**

If VAMP4 KD affects AMPAR expression at the plasma membrane, it might affect synaptic transmission. To test this hypothesis, we first assessed the effect of VAMP4 KD on EPSCs evoked by Schaffer collateral stimulation (eEPSCs) in CA1 pyramidal neurons of hippocampal organotypic slices. We used lentiviral vectors to deliver KD1 and KD2 shRNAs against VAMP4,

and scrambled shRNA as a control. The degree of VAMP4 reduction in neurons transduced with lentivirus was about 50 % in cultures and in slices, similar to the amount of knock-down obtained with plasmid transfection (Supplementary Figure XX). We made simultaneous patch-clamp recordings of eEPSCs from two neighboring CA1 pyramidal neurons, one transduced and the other not (Figure 7A, B). Expression of VAMP4 KD1 or KD2 enhanced AMPAR EPSCs by ~2 fold compared to neighboring, non-transduced neurons (Figure 7C, E) (KD1:  $218 \pm 36$  %,  $n = 14$  pairs, KD2:  $228 \pm 36$  %,  $n = 12$  pairs), while expression of scr had no effect ( $106 \pm 20$  %,  $n = 17$  pairs). Conversely, the NMDAR component of EPSCs recorded at +40 mV was unchanged in the scr, KD1 or KD2 conditions (Figure 7C, F). Consequently, the NMDA/AMPA ratio was reduced in KD cells compared to control (Figure 7G). The increase in AMPAR-EPSCs in VAMP4 KD cells is thus in line with the enhancement in GluA1 trafficking and surface expression detected in primary hippocampal cultures. We then tested the effect of TeNT-LC expression on synaptic transmission. We transfected individual CA1 pyramidal neurons by single-cell electroporation at 3-4 DIV and recorded neurons 3-4 days later. Cells expressing TeNT-LC showed a reduction in both AMPAR ( $62 \pm 10$  %,  $P = 0.0059$ ) and NMDAR ( $63 \pm 5$  %,  $p = 0.043$ ) EPSCs relative to control with no change in NMDA/AMPA ratio (Figure 7 D-G) ( $n = 8$  pairs).

Given the effect of VAMP4 KD on basal excitatory synaptic transmission, we wanted to test their effect on synaptic plasticity. NMDAR-dependent LTP was induced in hippocampal organotypic slices in the CA3-CA1 synapse using a standard pairing protocol of 100 stimulations at 1 Hz while holding the cell at 0 mV (Isaac et al., 1995). Cells transduced with scr shRNA lentivirus showed robust LTP ( $307 \pm 10$  % of basal EPSC amplitude 20-30 min after induction). On the other hand, LTP was significantly reduced in neurons expressing VAMP4 KD1 ( $176 \pm 9$  %) or KD2 ( $147 \pm 6$  %) (Figure 8A-C). Finally, cells expressing TeNT-LC showed no LTP, rather a depression ( $62 \pm 3$  %) compared to neighboring unelectroporated cells which displayed normal LTP ( $274 \pm 7$  %) (Figure 8D-F).

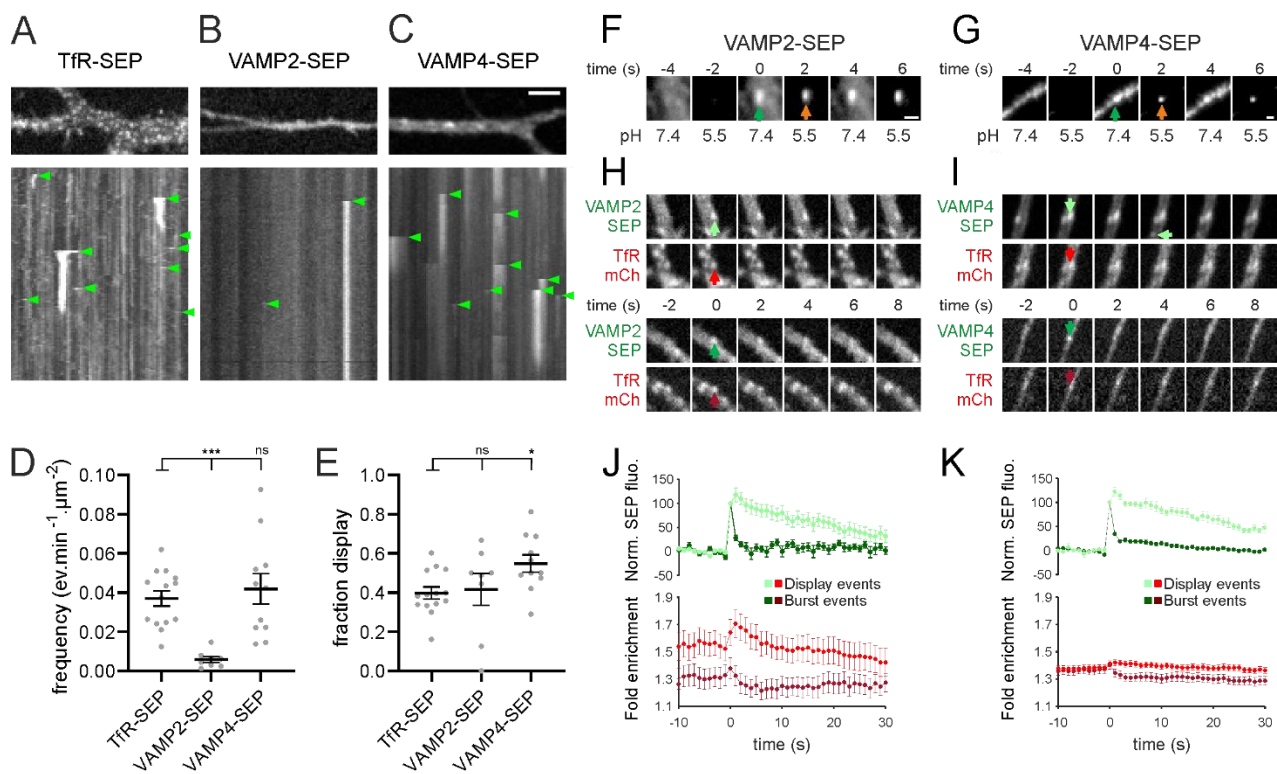


**Figure 1: VAMP4-SEP and VAMP2-SEP are markers of recycling endosome exocytosis in the soma and dendrites of hippocampal neurons.**

**A-C,** Images (top) and kymographs (bottom) of neurons (14 DIV) transfected with Tfr-SEP (A), VAMP2-SEP (B) or VAMP4-SEP (C). Exocytosis events (sudden appearance of a bright cluster) are marked with green arrowheads. In (A), dim stable spots represent clathrin coated endocytic zones. Scale bar 2  $\mu\text{m}$ . **D,** Average frequency of exocytosis for neurons expressing Tfr-SEP ( $n = 14$ ), VAMP2-SEP ( $n = 8$ ) or VAMP4-SEP ( $n = 11$ ). All neurons were 13-15DIV. Error bars represent s.e.m,  $***P = 0.0012$ . **E,** proportion of display events on the same sample as D. Error bars represent s.e.m,  $**P < 0.01$ . **F-G,** Examples of events recorded in neurons transfected with VAMP2-SEP (F) and VAMP4-SEP (G) with the ppH protocol. After exocytosis (green arrow), a cluster resistant to low pH solution is clearly visible (orange arrow), demonstrating closure of the fusion pore within 4s. Scale bars 1  $\mu\text{m}$ . **G-H,** Representative examples of exocytosis events recorded in 14DIV neurons expressing Tfr-mCherry and VAMP2-SEP (G) or VAMP4-SEP (H). Upper panels show display events, and lower panel show burst events. Green arrows indicate exocytosis sites, and red arrows the corresponding Tfr-mCherry clusters. Note that for display events, Tfr-mCherry clusters remain visible, whereas for burst events, they largely disappear. **I-J,** Average normalized fluorescence curves for VAMP2-SEP (I, 59 display and 60 burst events in 8 cells) and VAMP4-SEP (J, 276 display and 394 burst events in 11 cells), together with Tfr-mCherry fold enrichment (red curves). Light curves show display events and dark curves burst events.

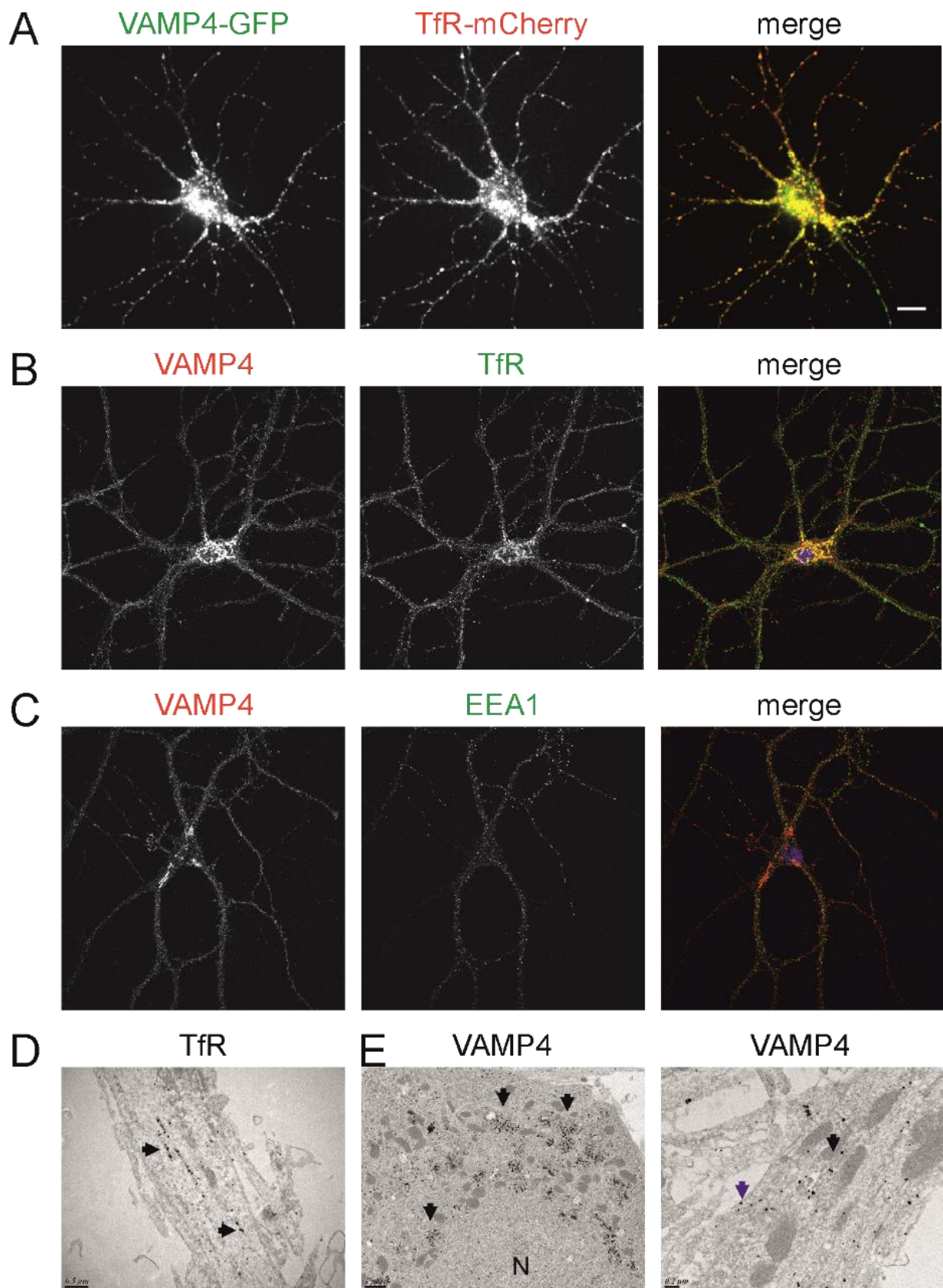


**Figure 2: Localization of VAMP4 in neuronal dendrites.** **A**, Images from a movie of a 15DIV neuron expressing VAMP4-GFP and TfR-mCherry. The somatic, peri-nuclear staining is saturated to enable the visualization of dendritic clusters. Many clusters of VAMP-GFP (green arrows) are co-localized with TfR-mCherry clusters (red arrows). **B**, Immunofluorescence of endogenous VAMP4 and the RE marker TfR. **C**, Immunofluorescence of endogenous VAMP4 and the RE marker EEA1. **D**, Electron micrograph showing TfR localization. **E**, Electron micrograph showing VAMP4 localization. **F**, Electron micrograph showing VAMP4 localization. Arrows indicate specific clusters. Scale bars are present in the bottom left of panels D, E, and F.

VAMP4 is enriched in the Golgi apparatus and shows a punctate localization in dendrites, as shown in enlarged regions of interest A and B. In the merge image, DAPI staining (blue) shows the neuronal nucleus. Scale bar C, Same as B for VAMP4 and the early endosome marker EEA1. D, Silver intensified immunogold labeling of endogenous Tfr shows enrichment in tubular endosomal structures (arrows). E, Silver intensified immunogold labeling of endogenous VAMP4. Labelling is enriched in the TGN (left, arrows) close to the nucleus (N). On a higher magnification view of a dendrite (right) VAMP4 is also found close to the membrane (blue arrow) and in endosomal compartments (black arrows) in dendrites.

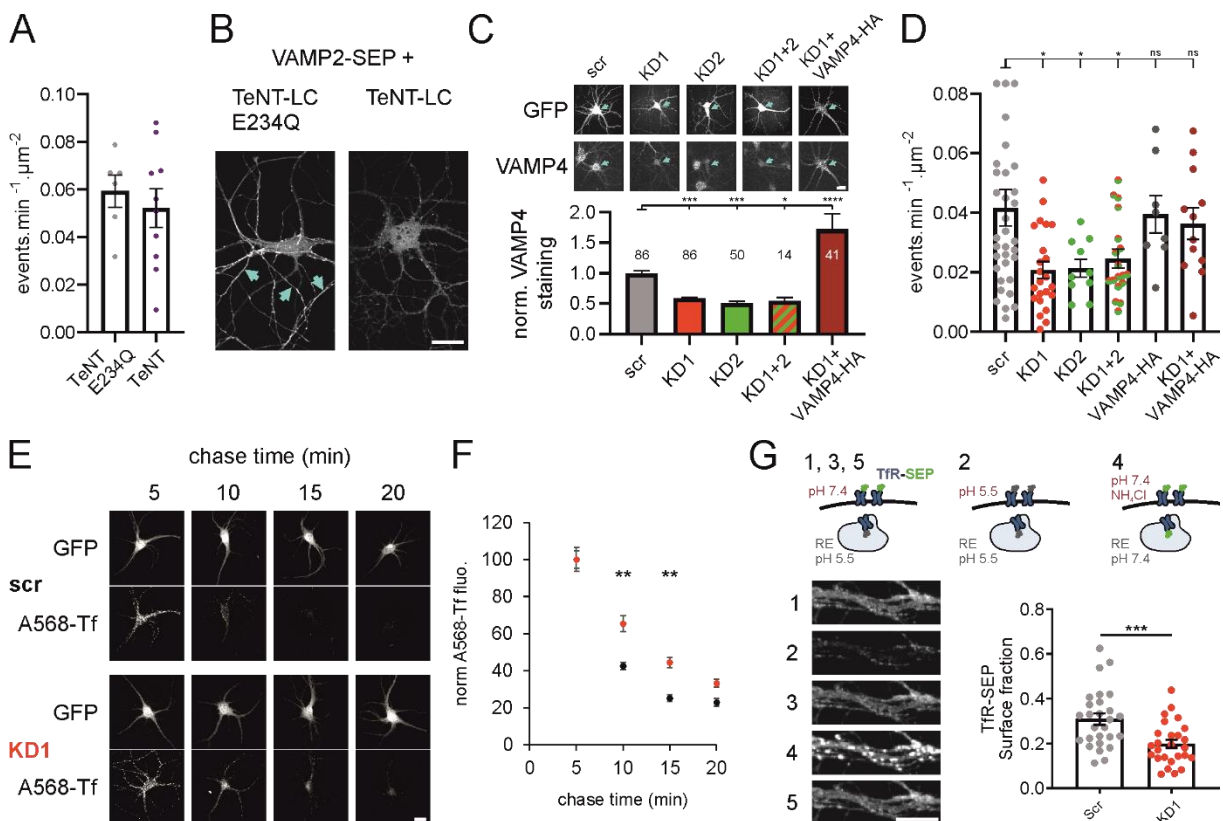


**Figure 3: Downregulation of VAMP4, but not VAMP2, impairs RE exocytosis and recycling to the plasma membrane.** **A**, Frequency of exocytosis events in neurons transfected with Tfr-SEP and TeNT-LC E234Q (n = 6) or TeNT-LC (n = 10). **B**, Images of neurons co-transfected with VAMP2-SEP and TeNT-LC E234Q or TeNT-LC. In the first case, VAMP2-SEP is enriched in the axon (cyan arrows) but not in the second case. Scale bar 10  $\mu\text{m}$ . **C**, Immunofluorescence images of endogenous VAMP4 in cells expressing GFP and a combination of shRNA targeted against VAMP4 for four days. In cells expressing GFP and the shRNA (cyan arrows), the labeling is strongly decreased compared to untransfected cells or cells expressing scramble shRNA. In cells co-expressing Tfr, VAMP4-HA and KD1 the VAMP4 staining is strong. Scale bar 10  $\mu\text{m}$ . Bottom, quantification of VAMP4 staining in the area delimited by the GFP mask (soma and dendrites). The staining is decreased by  $\sim 50\%$  in all KD conditions. Number of cells is indicated above the bars for all conditions. Comparison with scr with one-way ANOVA, \*  $P < 0.05$ ; \*\*\*  $P < 0.001$  **D**, Frequency of exocytosis events recorded in cells expressing Tfr-SEP and shRNAs targeted to VAMP4: scramble (33 cells; 3 cells have frequencies of  $0.132$ ,  $0.157$  and  $0.119$   $\text{events} \cdot \mu\text{m}^{-2} \cdot \text{min}^{-1}$  and

are represented above the axis limit), KD1 (23 cells), KD2 (10 cells), KD1+2 (18 cells), cells expressing VAMP4-HA (8 cells) and KD1+VAMP4-HA (12 cells) \* $P < 0.05$  one way ANOVA. **E**, Images of neurons expressing scr or KD1 shRNAs in GFP vectors, labeled with A568-Tf (50  $\mu\text{g}/\text{ml}$ ) for 5 minutes and chased with unlabeled transferrin (2 mg/ml) at 37°C for the indicated times. Scale bar, 10  $\mu\text{m}$ . **F**, Quantification of the Alexa568 fluorescence in the GFP mask from the pulse chase experiments described in (E). 70-88 cells per condition, from 4 independent experiments. Error bars represent s.e.m, \*\* $P < 0.01$ . **G**, Estimation of TfR-SEP surface fraction. Top, cartoons showing the fraction of fluorescent TfR-SEP. At pH 7.4, surface receptors are fluorescent but not at pH 5.5. Receptors in acidic intracellular organelles are not fluorescent, but become fluorescent with  $\text{NH}_4\text{Cl}$ . Bottom left, images of a dendrite bathed successively in solutions at pH 7.4 (images 1, 3, 5), pH 5.5 (image 2) and pH 7.4 containing  $\text{NH}_4\text{Cl}$  (image 4). For image 4, the contrast is 2x lower than in the other images. Bottom right, quantification of TfR-SEP surface fraction for neurons transfected with scr (n = 27) and KD1 (n = 26). See Methods for calculation. \*\*\* $P < 0.001$ .

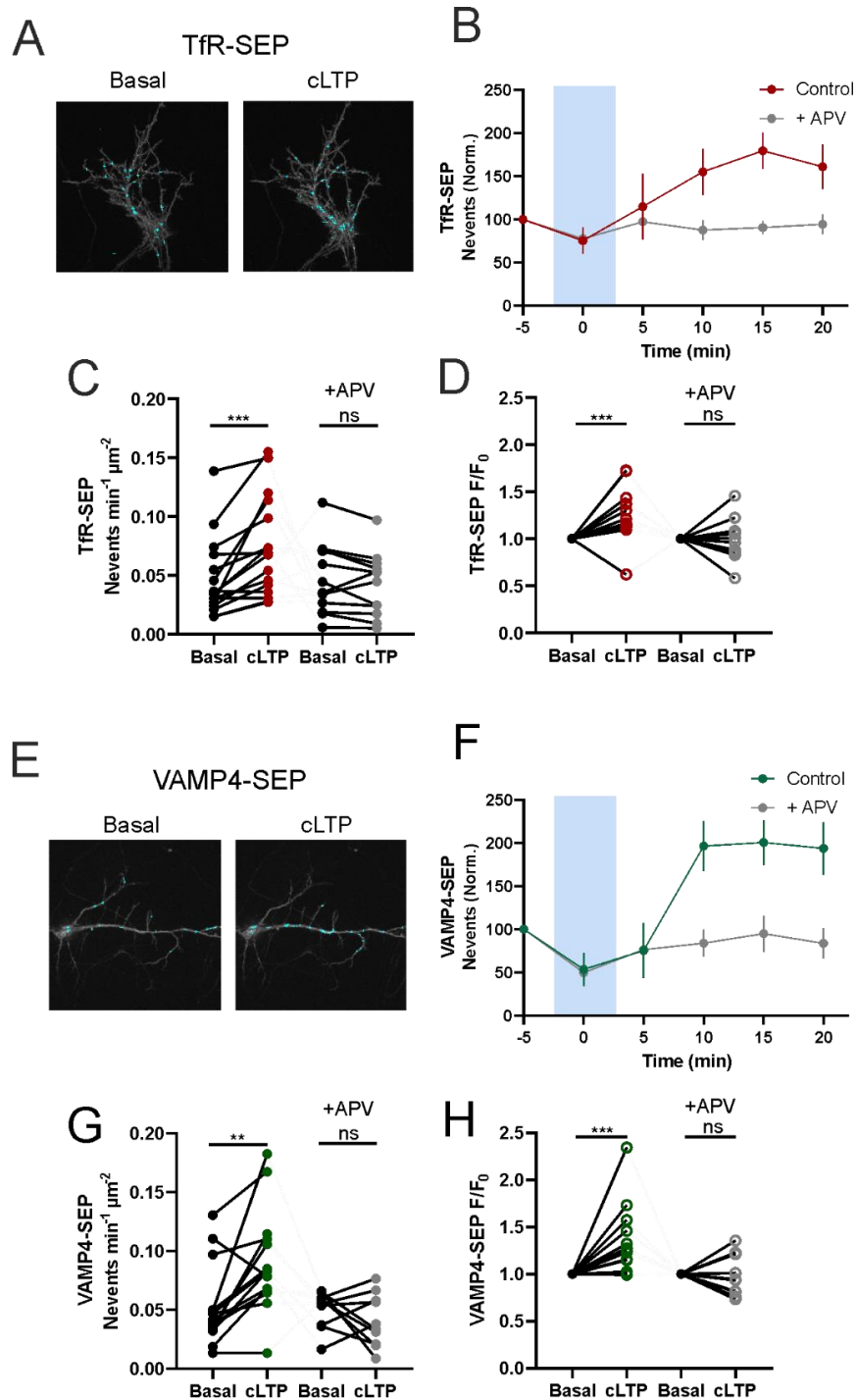


**Figure 4: Tfr-SEP and VAMP4-SEP exocytosis increase after chemical LTP.** **A**, Images of a neuron transfected with Tfr-SEP before and 15 minutes after induction of cLTP. Cyan crosses show the location of detected exocytosis events. Scale bar **B**, Normalized exocytosis frequency of neurons transfected with Tfr-SEP at times relative to cLTP induction (n = 16). The increase in frequency is significant 10 minutes or more after induction. In the presence of APV (100  $\mu\text{M}$ ) the frequency does not increase (n = 12). **C**, Frequencies before and 15 min after LTP induction. **D**, Normalized change in fluorescence intensity of Tfr-SEP before and after cLTP induction. **E-H**, Same as A-D for neurons transfected with VAMP4-SEP (n = 15), and with APV (n = 10). The increase in frequency is significant 10 minutes or more after induction.

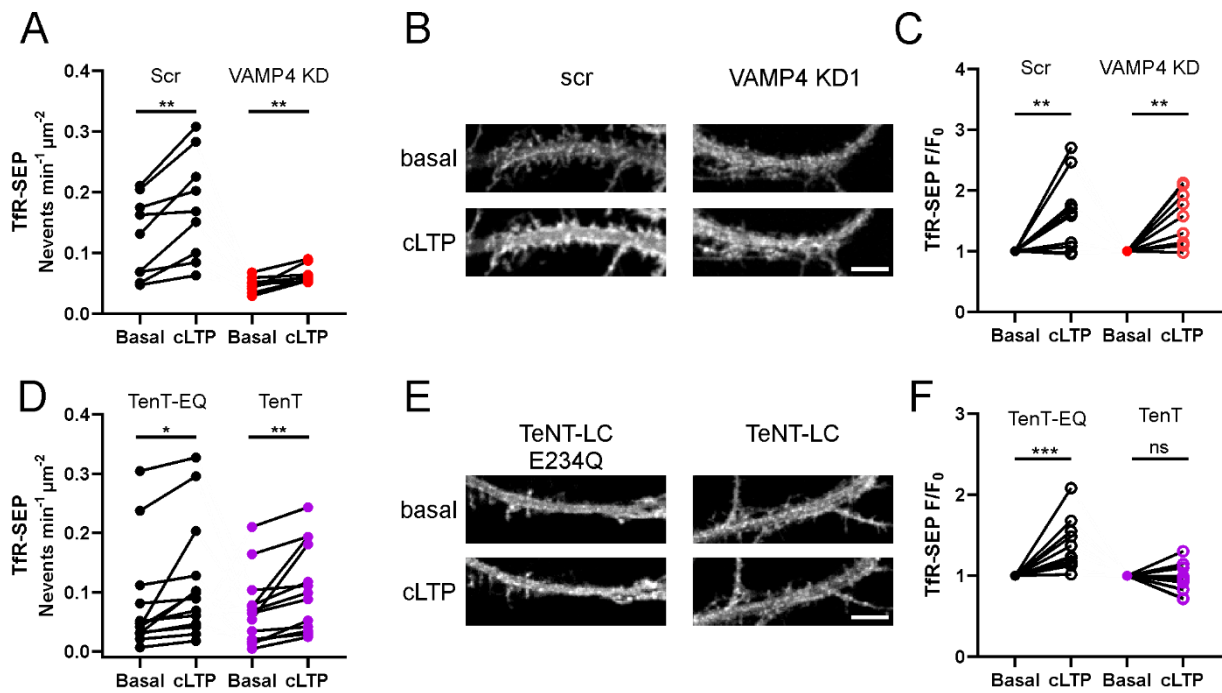


**Figure 5: Effect of VAMP4 KD and TeNT-LC on TfR-SEP exocytosis after cLTP.** **A**, Exocytosis frequencies before and after LTP induction in neurons expressing TfR-SEP and either scr ( $n = 10$ ) or VAMP4 KD1 ( $n = 8$ ) shRNA. In both conditions the increase in frequency is significant. **B**, Images of dendrites before and after induction of cLTP. Scale bar  $5 \mu\text{m}$ . **C**, TfR-SEP fluorescence in dendrites of neurons before and after cLTP induction. In both conditions, the increase is significant. **D-F**, Same as A-C for neurons expressing TfR-SEP and either TeNT-LC E234Q ( $n = 13$ ) or TeNT-LC ( $n = 13$ ). In neurons expressing inactive TeNT exocytosis frequency and surface fluorescence are increased significantly while in neurons expressing active TeNT the surface fluorescence does not increase.

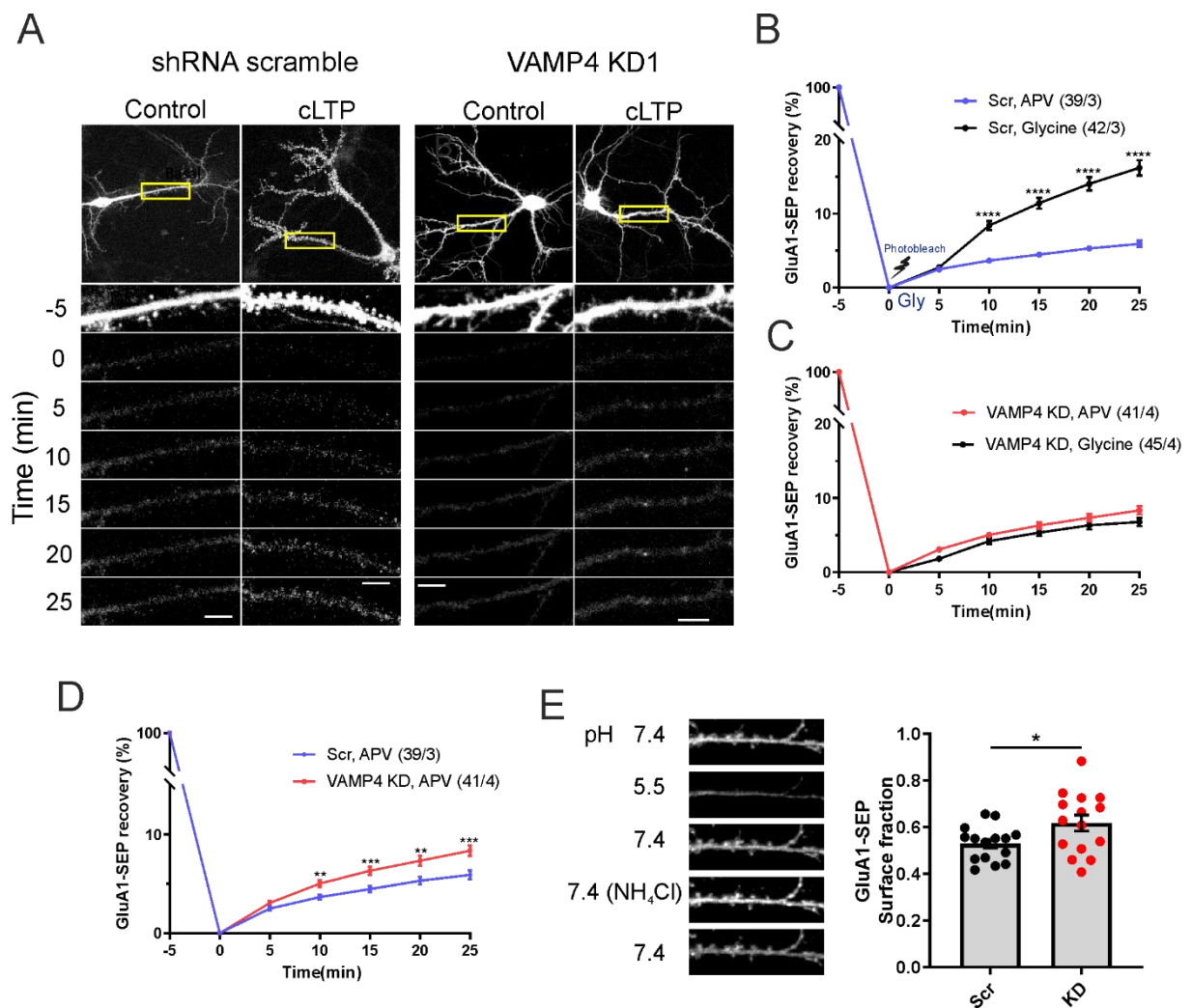


**Figure 6: VAMP4 regulates the recycling of AMPA receptors and its availability for cLTP.** **A**, Images of neurons expressing SEP-GluA1 and either scr or VAMP4 KD1 shRNA. Images are maximum projections of stacks of 9 planes. Below, images of the dendrite framed in yellow before and at the indicated time after photobleaching of the whole cell. Scale bars. Images before bleaching are displayed saturated to keep the same contrast as the ones after bleaching. **B-D**, Quantification of SEP-GluA1 fluorescence in dendritic segments, normalized to pre- and post-bleach values. Cells were kept if the total fluorescence was bleached by more than 90 %. In **B**, neurons expressing scr shRNA with glycine treatment for cLTP or APV. In **C**, neurons expressing VAMP4 KD1 shRNA with glycine treatment for cLTP or APV. In **D**, the two conditions of **B** and **C** in APV are replotted with a higher scale to highlight the difference between the two recovery rates. **E**, Images of a dendritic segment of a neuron transfected with SEP-GluA1 and scr shRNA, following the same protocol as described in Figure 3G. Right, quantification of SEP-GluA1 surface fraction in neurons expressing scr (n = 15) or VAMP4 KD1 shRNA (n = 15).

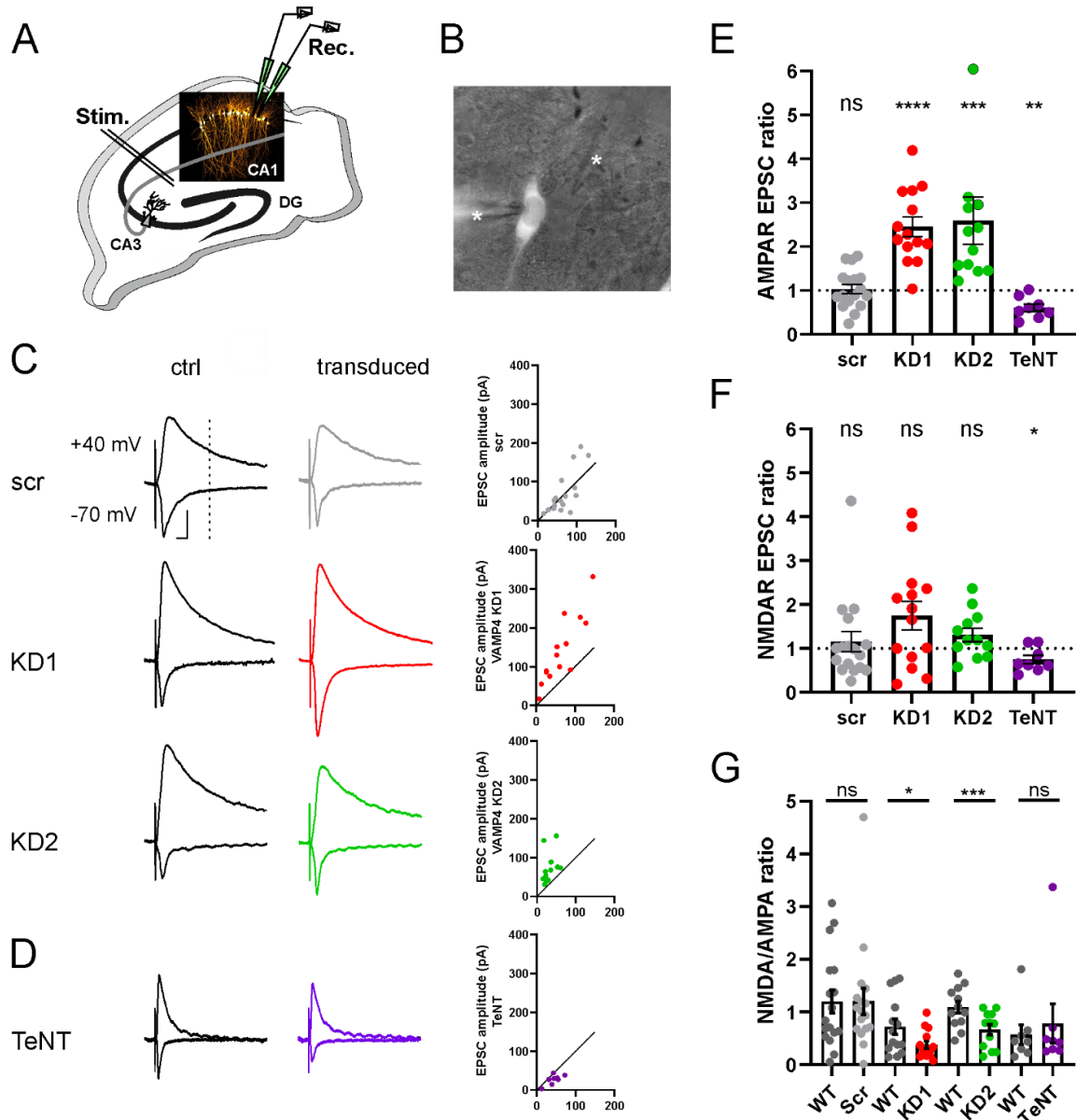


**Figure 7: Effect of post-synaptic VAMP4 KD and TeNT on glutamatergic synaptic transmission.** **A**, Confocal image of an organotypic hippocampal slice culture infected with scr-mScarlet lentivirus at 1 DIV and fixed at 9 DIV. Many pyramidal neurons in CA1 are brightly fluorescent. **B**, DIC image of two pyramidal neurons recorded simultaneously with patch pipettes (asterisks). Epifluorescent illumination shows that the neuron on the left is brightly fluorescent (infected) while the one on the right is not (uninfected control). **C**, Averages of 30 EPSCs evoked by the same stimulation in pairs of neurons, uninfected and infected with scr-mScarlet (top), shRNA KD1-mScarlet (middle) or shRNA KD2-mScarlet (bottom). Both neurons were held at -70 mV, then at +40 mV. Right, Plots of peak EPSC amplitude at -70 mV for each pair of neuron. In the scr condition, dots are spread around the diagonal while in the KD1 and KD2 conditions, the amplitudes are systematically higher for infected neurons. **D**, Same as C for neurons co-electroporated with TeNT-LC and GFP. In the neurons expressing TeNT-LC, the amplitude is systematically smaller than in control neurons. **E**, Peak EPSC amplitude recorded at -70 mV (AMPA component) normalized to the corresponding controls (uninfected, grey dots). **F**, EPSC amplitude 100 ms after stimulation at +40 mV (NMDAR component) normalized to the corresponding

controls (uninfected, grey dots). **G**, Ratio of NMDAR/AMPA EPSC amplitude for all conditions. In E-G, stars signal significant differences (paired t test, \*  $p < 0.05$ , \*\*  $p < 0.01$ , \*\*\*  $p < 0.001$ ).

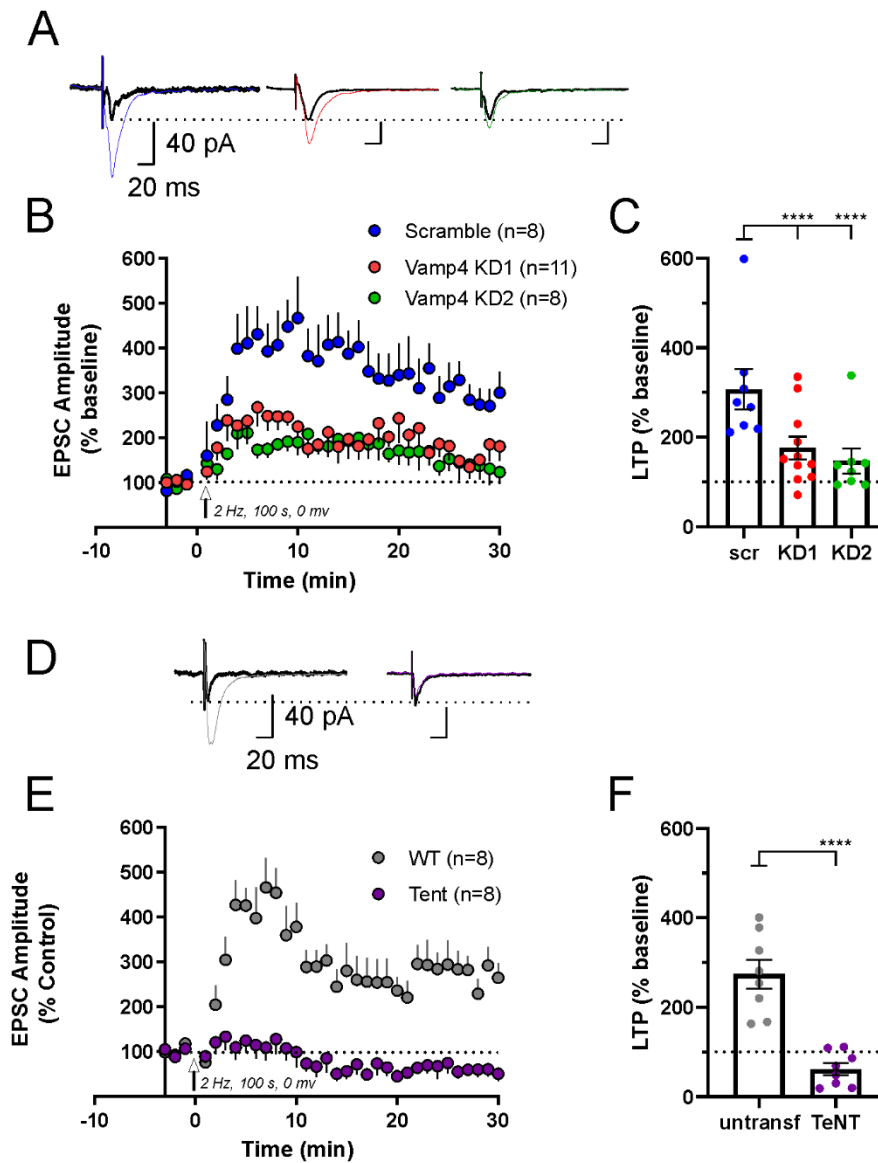


**Figure 8: Effect of post-synaptic VAMP4 KD and TeNT on LTP.** **A**, Average EPSC before (black traces) and 20-30 min after induction of LTP (color traces) in neurons infected with scr-mScarlet (blue), shRNA KD1-mScarlet (red) and shRNA KD2-mScarlet (green). Scale bars 40 pA and 20 ms. The dotted line shows the peak EPSC before LTP induction. **B**, Peak EPSC amplitude normalized to baseline for neurons infected with the corresponding viruses. **C**, Ratio of EPSC amplitude 20-30 min after LTP induction to baseline for neurons infected with the corresponding viruses. **D**, Average EPSCs evoked in two neurons, one untransfected (left) and on transfected with TeNT-LC and GFP (right), before (black traces) and 20-30 min after induction of LTP (gray or purple traces). **E**, Peak EPSC amplitude normalized to baseline for pairs of neurons transfected or not with TeNT-LC and GFP. **F**, Same as A-C for untransfected neurons and neurons transfected with TeNT-LC and GFP.

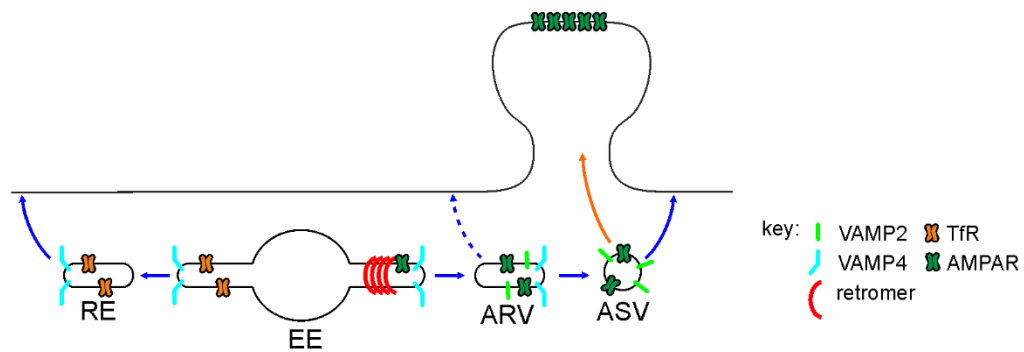


**Figure 9. Model of dendritic receptor trafficking.**

**Supplementary Movie 1:** neuron transfected with TfR-SEP and recorded with time lapse spinning disk confocal microscopy at 1 Hz.

**Supplementary Movie 2:** neuron transfected with VAMP2-SEP and recorded with time lapse spinning disk confocal microscopy at 1 Hz.

**Supplementary Movie 3:** neuron transfected with VAMP4-SEP and recorded with time lapse spinning disk confocal microscopy at 1 Hz.

## DISCUSSION

In the present study, we have investigated the role of 2 vSNARE proteins, VAMP2 and VAMP4, in both the constitutive and regulated endosomal trafficking at the post-synapse. Using a combination of live-cell imaging and electrophysiology techniques, we demonstrate that the exocytosis of TfR-labelled REs is mainly mediated by the TeNT insensitive VAMP4. This vSNARE, classically involved in EE homotypic fusion and retrograde trafficking to the TGN (Brandhorst et al. 2006; Laufman et al., 2011; Mallard et al., 2002), is also involved in the endosomal sorting of AMPARs, whereas VAMP2 preferentially mediates AMPAR trafficking to the plasma membrane. These results support a model of a segregated endosomal recycling system at the post-synapse.

### Involvement of VAMP4 in dendritic exocytosis

We have shown here that VAMP4 is the main vesicular SNARE involved in RE exocytosis in neuronal soma and dendrites. VAMP4-SEP co-localizes with TfR-mCherry, a classical RE marker, and reports the same frequency of exocytosis events as TfR-SEP, in control or increased after cLTP induction. Moreover, VAMP4 KD decreases the frequency of TfR-SEP exocytosis events, the rate of TfR recycling, and the fraction of TfR at the plasma membrane. In contrast, cleavage of VAMP2 by TeNT-LC does not affect the frequency of exocytosis events in neuronal dendrites. TeNT-LC also cleaves VAMP3/cellubrevin, which participates in TfR recycling in other, non-neuronal cell types (Galli et al.,

1994; Proux-Gillardeaux et al., 2005). However, VAMP3 appears not to be expressed in neurons (Schoch et al., 2001).

VAMP4 has been implicated in other exocytosis processes in neurons. In presynaptic terminals, in addition to VAMP2, the main SNARE mediating calcium-dependent synaptic vesicle exocytosis (Schoch et al., 2001), VAMP4 is responsible for the exocytosis of vesicles that mediate so-called asynchronous exocytosis. It forms a complex with syntaxin-1 and SNAP-25 (Raingo et al., 2012), the other SNAREs classically involved in synaptic vesicle exocytosis together with VAMP2 (Jahn and Scheller, 2006). Interestingly, the SNARE complex formed by VAMP4, syntaxin-1, and SNAP-25 does not bind complexins or synaptotagmin-1 (Raingo et al., 2012), proteins involved in the calcium-dependent synchronous exocytosis of synaptic vesicles (Brunger et al., 2019). Moreover, VAMP4 is involved in an endocytic process, activity-dependent bulk endocytosis (Nicholson-Fish et al., 2015) which participate in the recycling of synaptic vesicles. Lastly, VAMP4 has been implicated in the exocytosis of organelles called enlargeosomes, responsible for fast neurite outgrowth in the neuroendocrine cell line PC12-27 as well as in primary neurons (Borgonovo et al., 2002; Cocucci et al., 2008). Until now, even though VAMP4 is primarily located in the somato-dendritic compartment of hippocampal neurons (Jain et al., 2014), no specific role was assigned to VAMP4 in dendritic membrane trafficking. To our knowledge, VAMP4 is the first vesicular membrane protein to have a major role in RE exocytosis in neuronal soma and dendrites. Nevertheless, VAMP2 is also involved in dendritic exocytosis of a subset of REs labelled with TfR-mCherry. Because the frequency of VAMP2-SEP exocytosis events represents only about 13 % of the frequency of VAMP4-SEP exocytosis events, the quantitative role of VAMP2 in recycling is minor, which explains why TeNT-LC does not detectably affect the frequency of TfR-SEP exocytosis events. However, specific cargo may travel through VAMP2 dependent vesicles. In particular, the exocytosis of the AMPAR subunits SEP-GluA1 and SEP-GluA2 or the GABAAR  $\gamma 2$  are sensitive to TeNT-LC (Lin et al., 2009) or VAMP2 KD (Gu et al., 2016). Consistent with this, we show that chronic expression of TeNT-LC completely blocks LTP, as does acute block during recording (Lledo et al., 1998; Lu et al., 2001; Penn et al., 2017).

### **VAMP4 is necessary for endosomal sorting of AMPAR**

In addition to largely inhibit RE exocytosis, knock-down of VAMP4 also increases GluA1 recycling and the fraction of surface receptors. Consistent with this effect, the amplitude of EPSCs mediated by AMPAR is increased in VAMP4 KD neurons. This effect is opposite to the one on TfR trafficking and points to a second function of VAMP4 distinct from RE exocytosis. Effectively, the most documented role of VAMP4 in cells is in the so-called retrograde transport from early endosomes to the TGN (Laufman et al., 2011; Mallard et al., 2002) which corresponds to its main localization in TGN of neurons

(this study) and other cell types (Peden et al., 2001; Tran et al., 2007). The retrograde trafficking is mediated by the formation of tubulo-vesicular carriers in early endosomes by the retromer complex composed of the core subunits Vps26a,b/29/35 (Burd and Cullen, 2014). In neurons, this complex also mediates direct recycling of cargo, such as  $\beta$ 2 adrenergic receptors or AMPARs, to the plasma membrane through the retromer associated protein SNX27 (Hussain et al., 2014; Lauffer et al., 2010). Subunits of the retromer complex are present throughout dendrites next to early endosomal markers such as EEA1 (Choy et al., 2014). The knock-down of the retromer core subunit Vps35 inhibits AMPAR recycling in neurons in culture and LTP in CA1 pyramidal neurons in slices (Temkin et al., 2017). Interestingly, in differentiated 3T3-L1 adipocytes, the formation and stability of storage vesicles containing the glucose transporter GLUT4 (GSVs) (Leto and Saltiel, 2012) depend on the retromer complex (Pan et al., 2017). Moreover, GSV exocytosis, which is elicited by stimulation with insulin, specifically depends on VAMP2 while VAMP4 controls the targeting of GLUT4 to GSVs: after VAMP4 KD GLUT4 exocytosis largely occurs without stimulation (Williams and Pessin, 2008). Control of AMPARs exocytosis in neurons or GLUT4 exocytosis in adipocytes could share common pathways.

Based on these results, we can draw a model of dendritic recycling in neuronal dendrites (Figure 9). After internalization into the early endosome, receptor cargo is sorted in at least two endosomal compartments. The majority of compartments are composed of REs which are formed independently of retromer and contain TfRs; their exocytosis is mediated by VAMP4. A second type of compartment, which we call ARV (AMPAR recycling vesicle), depends on the retromer complex for its formation. We suggest that ARVs are subject to more regulation than conventional REs, which seem to recycle back to the plasma membrane by default. Particularly, ARVs use VAMP4 to mature into a storage compartment containing AMPARs, AMPAR storage vesicle (ASV), which uses VAMP2 for exocytosis. In the absence of VAMP4, the ARV does not mature into an ASV and is recycled to the plasma membrane, enhancing the speed of AMPAR recycling but decreasing the cell's capacity to potentiate after LTP inductions (Figure 9). This provides a mechanistic explanation as to why, in the absence of VAMP4, AMPAR exocytosis is not enhanced during cLTP in cultured neurons and synaptic LTP is partially occluded by already potentiated synapses. ASVs could contain FIP2, initially characterized as an effector of Rab11 and a potential mediator of RE movement through interaction with myosin V (Wang et al., 2008), but recently re-characterized as mediating the intracellular retention of AMPARs through direct binding (Royo et al., 2019). Interestingly, FIP2 KD decreases the fraction of TfR at the neuronal surface and increases the surface fraction of GluA1, a phenotype similar to the one we describe here with VAMP4 KD. Moreover, upon LTP induction, FIP2 is dephosphorylated and dissociates from AMPARs, freeing the cargo to translocate to the plasma membrane and undergo exocytosis (Royo et

al., 2019). More work would be required to characterize the ASV and its behavior after the induction of LTP.

### **A sequence of fusion events for the expression of LTP**

LTP-inducing stimuli enhance the overall endocytic recycling to the plasma membrane in hippocampal neurons (Park et al., 2004). The induction of cLTP in primary cultures causes an increase in TfR-SEP exocytosis frequency and surface fluorescence intensity as previously reported (Hiester et al., 2017; Keith et al., 2012; Kennedy et al., 2010). Our results show that VAMP4-SEP exhibits similar behavior to that of TfR-SEP upon cLTP induction. However, even though VAMP4 KD reduced basal TfR recycling, cLTP induction similarly increased in proportion TfR-SEP exocytosis frequency and surface fluorescence intensity. The residual regulated fusions might be due to the partial KD of VAMP4 or the existence of other TfR-positive REs that are mediated by a different vSNARE, e.g. VAMP2. Nevertheless, these data suggest that VAMP4 mediates the majority of TfR-labelled REs basal and regulated exocytosis during LTP expression.

In contrast, the expression of TeNT-LC did not affect the basal exocytosis frequency of TfR-SEP. Moreover, it did not prevent the increase in frequency after cLTP induction, excluding a major contribution of VAMP2 in mediating RE fusion events. However, VAMP2 cleavage by TeNT-LC abolished the accompanied increase in TfR-SEP fluorescence intensity, also observed in other studies (Hiester et al., 2018). These results strongly suggest that TeNT-LC effect on surface TfR-SEP is not caused by a block in activity-triggered RE fusion, but rather due to a failure to stabilize newly exocytosed receptors at the plasma membrane. One possibility is that VAMP2 mediates the exocytosis of a yet unidentified molecule that is necessary for the stabilization of surface receptors for LTP expression. This goes in line with a study showing that TeNT-LC prevented the stabilization of AMPARs initially recruited with activity to spines by lateral diffusion (Hiester et al., 2018). Factors released during cLTP induction which are sensitive to TeNT-LC could include brain-derived neurotrophic factor (BDNF) (Harward et al., 2016) or other factors not yet identified. Altogether, this observation reinstates the importance of membrane exocytosis for the maintenance of surface receptors after LTP inducing stimuli, seemingly regardless of their trafficking site (Choquet, 2018).

In conclusion, our study identifies VAMP4 as a new player in the post-synaptic SNARE fusion machinery which mediates the majority of TfR-labelled RE fusions. Also, VAMP4 controls the sorting of AMPARs into ASVs, which can be mobilized upon LTP induction. This represents an additional trafficking route of AMPARs for LTP expression. Yet, the precise sequence of various trafficking events and the specific organelles involved during the expression of LTP await further investigation.

## REFERENCES

- Ahmad, M., Polepalli, J.S., Goswami, D., Yang, X., Kaeser-Woo, Y.J., Südhof, T.C., and Malenka, R.C. (2012). Postsynaptic Complexin Controls AMPA Receptor Exocytosis during LTP. *Neuron* 73, 260–267.
- Bardy, C., Van Den Hurk, M., Eames, T., Marchand, C., Hernandez, R.V., Kellogg, M., Gorris, M., Galet, B., Palomares, V., Brown, J., et al. (2015). Neuronal medium that supports basic synaptic functions and activity of human neurons in vitro. *Proceedings of the National Academy of Sciences* 112, E2725–E2734.
- Bentley, M., and Banker, G. (2016). The cellular mechanisms that maintain neuronal polarity. *Nature Reviews Neuroscience*.
- Bindels, D.S., Haarbosch, L., van Weeren, L., Postma, M., Wiese, K.E., Mastop, M., Aumonier, S., Gotthard, G., Royant, A., Hink, M.A., et al. (2017). mScarlet: a bright monomeric red fluorescent protein for cellular imaging. *Nat Meth* 14, 53–56.
- Binz, T., Sikorra, S., and Mahrhold, S. (2010). Clostridial Neurotoxins: Mechanism of SNARE Cleavage and Outlook on Potential Substrate Specificity Reengineering. *Toxins* 2, 665–682.
- Borgonovo, B., Cocucci, E., Racchetti, G., Podini, P., Bachi, A., and Meldolesi, J. (2002). Regulated exocytosis: a novel, widely expressed system. *Nature Cell Biology* 4, 955–963.
- Brown, T.C., Correia, S.S., Petrok, C.N., and Esteban, J.A. (2007). Functional Compartmentalization of Endosomal Trafficking for the Synaptic Delivery of AMPA Receptors during Long-Term Potentiation. *Journal of Neuroscience* 27, 13311–13315.
- Brunger, A.T., Choi, U.B., Lai, Y., Leitz, J., White, K.I., and Zhou, Q. (2019). The pre-synaptic fusion machinery. *Current Opinion in Structural Biology* 54, 179–188.
- Burd, C., and Cullen, P.J. (2014). Retromer: A Master Conductor of Endosome Sorting. *Cold Spring Harb Perspect Biol* 6, a016774.
- Burgo, A., Proux-Gillardeaux, V., Sotirakis, E., Bun, P., Casano, A., Verraes, A., Liem, R.K.H., Formstecher, E., Coppey-Moisan, M., and Galli, T. (2012). A Molecular Network for the Transport of the TI-VAMP/VAMP7 Vesicles from Cell Center to Periphery. *Developmental Cell* 23, 166–180.
- Choquet, D. (2018). Linking Nanoscale Dynamics of AMPA Receptor Organization to Plasticity of Excitatory Synapses and Learning. *J. Neurosci.* 38, 9318–9329.
- Choy, R.W.-Y., Park, M., Temkin, P., Herring, B.E., Marley, A., Nicoll, R.A., and von Zastrow, M. (2014). Retromer Mediates a Discrete Route of Local Membrane Delivery to Dendrites. *Neuron* 82, 55–62.
- Cocucci, E., Racchetti, G., Rupnik, M., and Meldolesi, J. (2008). The regulated exocytosis of enlargeosomes is mediated by a SNARE machinery that includes VAMP4. *Journal of Cell Science* 121, 2983–2991.
- Cooney, J.R., Hurlburt, J.L., Selig, D.K., Harris, K.M., and Fiala, J.C. (2002). Endosomal compartments serve multiple hippocampal dendritic spines from a widespread rather than a local store of recycling membrane. *The Journal of Neuroscience* 22, 2215–2224.
- Correia, S.S., Bassani, S., Brown, T.C., Lisé, M.-F., Backos, D.S., El-Husseini, A., Passafaro, M., and Esteban, J.A. (2008). Motor protein-dependent transport of AMPA receptors into spines during long-term potentiation. *Nat Neurosci* 11, 457–466.

- Ehlers, M.D. (2000). Reinsertion or degradation of AMPA receptors determined by activity-dependent endocytic sorting. *Neuron* 28, 511–525.
- Ferecskó, A.S., Jiruska, P., Foss, L., Powell, A.D., Chang, W.-C., Sik, A., and Jefferys, J.G.R. (2015). Structural and functional substrates of tetanus toxin in an animal model of temporal lobe epilepsy. *Brain Struct Funct* 220, 1013–1029.
- Glebov, O.O., Tigaret, C.M., Mellor, J.R., and Henley, J.M. (2015). Clathrin-Independent Trafficking of AMPA Receptors. *Journal of Neuroscience* 35, 4830–4836.
- Gordon, D.E., Bond, L.M., Sahlender, D.A., and Peden, A.A. (2010). A Targeted siRNA Screen to Identify SNAREs Required for Constitutive Secretion in Mammalian Cells. *Traffic* 11, 1191–1204.
- Granger, A.J., and Nicoll, R.A. (2014). Expression mechanisms underlying long-term potentiation: a postsynaptic view, 10 years on. *Philosophical Transactions of the Royal Society B: Biological Sciences* 369, 20130136.
- Gu, Y., Chiu, S.-L., Liu, B., Wu, P.-H., Delannoy, M., Lin, D.-T., Wirtz, D., and Huganir, R.L. (2016). Differential vesicular sorting of AMPA and GABA A receptors. *Proceedings of the National Academy of Sciences* 113, E922–E931.
- Harward, S.C., Hedrick, N.G., Hall, C.E., Parra-Bueno, P., Milner, T.A., Pan, E., Laviv, T., Hempstead, B.L., Yasuda, R., and McNamara, J.O. (2016). Autocrine BDNF–TrkB signalling within a single dendritic spine. *Nature* 538, 99–103.
- Hiester, B.G., Bourke, A.M., Sinnen, B.L., Cook, S.G., Gibson, E.S., Smith, K.R., and Kennedy, M.J. (2017). L-Type Voltage-Gated Ca<sup>2+</sup> Channels Regulate Synaptic Activity-Triggered Recycling Endosome Fusion in Neuronal Dendrites. *Cell Reports* 21, 2134–2146.
- Hiester, B.G., Becker, M.I., Bowen, A.B., Schwartz, S.L., and Kennedy, M.J. (2018). Mechanisms and Role of Dendritic Membrane Trafficking for Long-Term Potentiation. *Front. Cell. Neurosci.* 12.
- Huganir, R.L., and Nicoll, R.A. (2013). AMPARs and Synaptic Plasticity: The Last 25 Years. *Neuron* 80, 704–717.
- Hussain, N.K., Diering, G.H., Sole, J., Anggono, V., and Huganir, R.L. (2014). Sorting Nexin 27 regulates basal and activity-dependent trafficking of AMPARs. *PNAS* 111, 11840–11845.
- Isaac, J.T.R., Nicoll, R.A., and Malenka, R.C. (1995). Evidence for silent synapses: Implications for the expression of LTP. *Neuron* 15, 427–434.
- Jahn, R., and Scheller, R.H. (2006). SNAREs — engines for membrane fusion. *Nature Reviews Molecular Cell Biology* 7, 631–643.
- Jain, S., Farías, G.G., and Bonifacino, J.S. (2014). Polarized sorting of the copper transporter ATP7B in neurons mediated by recognition of a dileucine signal by AP-1. *MBoC* 26, 218–228.
- Jullié, D., Choquet, D., and Perraïs, D. (2014). Recycling Endosomes Undergo Rapid Closure of a Fusion Pore on Exocytosis in Neuronal Dendrites. *Journal of Neuroscience* 34, 11106–11118.
- Jurado, S., Goswami, D., Zhang, Y., Molina, A.J.M., Südhof, T.C., and Malenka, R.C. (2013). LTP Requires a Unique Postsynaptic SNARE Fusion Machinery. *Neuron* 77, 542–558.
- Kaech, S., and Banker, G. (2006). Culturing hippocampal neurons. *Nature Protocols* 1, 2406–2415.

- Keith, D.J., Sanderson, J.L., Gibson, E.S., Woolfrey, K.M., Robertson, H.R., Olszewski, K., Kang, R., El-Husseini, A., and Dell'acqua, M.L. (2012). Palmitoylation of A-kinase anchoring protein 79/150 regulates dendritic endosomal targeting and synaptic plasticity mechanisms. *J. Neurosci.* 32, 7119–7136.
- Kennedy, M.J., and Ehlers, M.D. (2006). Organelles and trafficking machinery for postsynaptic plasticity. *Annual Review of Neuroscience* 29, 325.
- Kennedy, M.J., and Ehlers, M.D. (2011). Mechanisms and Function of Dendritic Exocytosis. *Neuron* 69, 856–875.
- Kennedy, M.J., Davison, I.G., Robinson, C.G., and Ehlers, M.D. (2010). Syntaxin-4 defines a domain for activity-dependent exocytosis in dendritic spines. *Cell* 141, 524–535.
- Lauffer, B.E.L., Melero, C., Temkin, P., Lei, C., Hong, W., Kortemme, T., and von Zastrow, M. (2010). SNX27 mediates PDZ-directed sorting from endosomes to the plasma membrane. *The Journal of Cell Biology* 190, 565–574.
- Laufman, O., Hong, W., and Lev, S. (2011). The COG complex interacts directly with Syntaxin 6 and positively regulates endosome-to-TGN retrograde transport. *J Cell Biol* 194, 459–472.
- Leto, D., and Saltiel, A.R. (2012). Regulation of glucose transport by insulin: traffic control of GLUT4. *Nat Rev Mol Cell Biol* 13, 383–396.
- Lin, D.-T., Makino, Y., Sharma, K., Hayashi, T., Neve, R., Takamiya, K., and Huganir, R.L. (2009). Regulation of AMPA receptor extrasynaptic insertion by 4.1N, phosphorylation and palmitoylation. *Nature Neuroscience* 12, 879–887.
- Lin, P.-Y., Chanaday, N.L., Horvath, P.M., Ramirez, D.M.O., Monteggia, L.M., and Kavalali, E.T. (2020). VAMP4 maintains a Ca<sup>2+</sup>-sensitive pool of spontaneously recycling synaptic vesicles. *J. Neurosci.*
- Lledo, P.M., Zhang, X., Südhof, T.C., Malenka, R.C., and Nicoll, R.A. (1998). Postsynaptic membrane fusion and long-term potentiation. *Science* 279, 399–403.
- Lu, W., Man, H., Ju, W., Trimble, W.S., MacDonald, J.F., and Wang, Y.T. (2001). Activation of synaptic NMDA receptors induces membrane insertion of new AMPA receptors and LTP in cultured hippocampal neurons. *Neuron* 29, 243–254.
- Lüscher, C., Xia, H., Beattie, E.C., Carroll, R.C., von Zastrow, M., Malenka, R.C., and Nicoll, R.A. (1999). Role of AMPA receptor cycling in synaptic transmission and plasticity. *Neuron* 24, 649–658.
- Mallard, F., Tang, B.L., Galli, T., Tenza, D., Saint-Pol, A., Yue, X., Antony, C., Hong, W., Goud, B., and Johannes, L. (2002). Early/recycling endosomes-to-TGN transport involves two SNARE complexes and a Rab6 isoform. *The Journal of Cell Biology* 156, 653–664.
- Martineau, M., Somasundaram, A., Grimm, J.B., Gruber, T.D., Choquet, D., Taraska, J.W., Lavis, L.D., and Perrais, D. (2017). Semisynthetic fluorescent pH sensors for imaging exocytosis and endocytosis. *Nature Communications* 8, 1412.
- Nicholson-Fish, J.C., Kokotos, A.C., Gillingwater, T.H., Smillie, K.J., and Cousin, M.A. (2015). VAMP4 Is an Essential Cargo Molecule for Activity-Dependent Bulk Endocytosis. *Neuron* 1–12.
- Pan, X., Zaarur, N., Singh, M., Morin, P., and Kandrór, K.V. (2017). Sortilin and retromer mediate retrograde transport of Glut4 in 3T3-L1 adipocytes. *MBoC* 28, 1667–1675.

- Park, M., Penick, E.C., Edwards, J.G., Kauer, J.A., and Ehlers, M.D. (2004). Recycling endosomes supply AMPA receptors for LTP. *Science* 305, 1972–1975.
- Park, M., Salgado, J.M., Ostroff, L., Helton, T.D., Robinson, C.G., Harris, K.M., and Ehlers, M.D. (2006). Plasticity-induced growth of dendritic spines by exocytic trafficking from recycling endosomes. *Neuron* 52, 817–830.
- Passafaro, M., Piëch, V., and Sheng, M. (2001). Subunit-specific temporal and spatial patterns of AMPA receptor exocytosis in hippocampal neurons. *Nature Neuroscience* 4, 917–926.
- Peden, A.A., Park, G.Y., and Scheller, R.H. (2001). The Di-leucine Motif of Vesicle-associated Membrane Protein 4 Is Required for Its Localization and AP-1 Binding. *Journal of Biological Chemistry* 276, 49183–49187.
- Penn, A.C., Zhang, C.L., Georges, F., Royer, L., Breillat, C., Hosy, E., Petersen, J.D., Humeau, Y., and Choquet, D. (2017). Hippocampal LTP and contextual learning require surface diffusion of AMPA receptors. *Nature* 549, 384–388.
- Proux-Gillardeaux, V., Gavard, J., Irinopoulou, T., Mège, R.-M., and Galli, T. (2005). Tetanus neurotoxin-mediated cleavage of cellubrevin impairs epithelial cell migration and integrin-dependent cell adhesion. *PNAS* 102, 6362–6367.
- Raingo, J., Khvotchev, M., Liu, P., Darios, F., Li, Y.C., Ramirez, D.M.O., Adachi, M., Lemieux, P., Toth, K., Davletov, B., et al. (2012). VAMP4 directs synaptic vesicles to a pool that selectively maintains asynchronous neurotransmission. *Nat. Neurosci.* 15, 738–745.
- Rimbault, C., Maruthi, K., Breillat, C., Genuer, C., Crespillo, S., Puente-Muñoz, V., Chamma, I., Gauthereau, I., Antoine, S., Thibaut, C., et al. (2019). Engineering selective competitors for the discrimination of highly conserved protein-protein interaction modules. *Nature Communications* 10, 4521.
- Roman-Vendrell, C., Chevalier, M., Acevedo-Canabal, A.M., Delgado-Peraza, F., Flores-Otero, J., and Yudowski, G.A. (2014). Imaging of kiss-and-run exocytosis of surface receptors in neuronal cultures. *Frontiers in Cellular Neuroscience* 8.
- Rosendale, M., Jullié, D., Choquet, D., and Perrais, D. (2017). Spatial and Temporal Regulation of Receptor Endocytosis in Neuronal Dendrites Revealed by Imaging of Single Vesicle Formation. *Cell Reports* 18, 1840–1847.
- Royo, M., Gutiérrez, Y., Fernández-Monreal, M., Gutiérrez-Eisman, S., Jiménez, R., Jurado, S., and Esteban, J.A. (2019). A retention–release mechanism based on RAB11FIP2 for AMPA receptor synaptic delivery during long-term potentiation. *J Cell Sci* 132.
- Sampo, B., Kaech, S., Kunz, S., and Banker, G. (2003). Two distinct mechanisms target membrane proteins to the axonal surface. *Neuron* 37, 611–624.
- Sankaranarayanan, S., and Ryan, T.A. (2000). Real-time measurements of vesicle-SNARE recycling in synapses of the central nervous system. *Nature Cell Biology* 2, 197–204.
- Sankaranarayanan, S., De Angelis, D., Rothman, J.E., and Ryan, T.A. (2000). The use of pHluorins for optical measurements of presynaptic activity. *Biophysical Journal* 79, 2199–2208.
- Schoch, S., Deák, F., Königstorfer, A., Mozhayeva, M., Sara, Y., Südhof, T.C., and Kavalali, E.T. (2001). SNARE function analyzed in synaptobrevin/VAMP knockout mice. *Science* 294, 1117–1122.

- van der Sluijs, P., and Hoogenraad, C.C. (2011). New insights in endosomal dynamics and AMPA receptor trafficking. *Seminars in Cell & Developmental Biology* 22, 499–505.
- Tanaka, H., and Hirano, T. (2012). Visualization of Subunit-Specific Delivery of Glutamate Receptors to Postsynaptic Membrane during Hippocampal Long-Term Potentiation. *Cell Reports* 1, 291–298.
- Temkin, P., Morishita, W., Goswami, D., Arendt, K., Chen, L., and Malenka, R. (2017). The Retromer Supports AMPA Receptor Trafficking During LTP. *Neuron* 94, 74-82.e5.
- Tran, T.H.T., Zeng, Q., and Hong, W. (2007). VAMP4 cycles from the cell surface to the trans-Golgi network via sorting and recycling endosomes. *Journal of Cell Science* 120, 1028–1041.
- Vuong, C.K., Wei, W., Lee, J.-A., Lin, C.-H., Damianov, A., Torre-Ubieta, L. de la, Halabi, R., Otis, K.O., Martin, K.C., O’Dell, T.J., et al. (2018). Rbfox1 Regulates Synaptic Transmission through the Inhibitory Neuron-Specific vSNARE Vamp1. *Neuron* 98, 127-141.e7.
- Wang, X., Yang, Y., and Zhou, Q. (2007). Independent Expression of Synaptic and Morphological Plasticity Associated with Long-Term Depression. *J. Neurosci.* 27, 12419–12429.
- Wang, Z., Edwards, J.G., Riley, N., Provance, D.W., Karcher, R., Li, X.-D., Davison, I.G., Ikebe, M., Mercer, J.A., Kauer, J.A., et al. (2008). Myosin Vb mobilizes recycling endosomes and AMPA receptors for postsynaptic plasticity. *Cell* 135, 535–548.
- Welz, T., Wellbourne-Wood, J., and Kerkhoff, E. (2014). Orchestration of cell surface proteins by Rab11. *Trends in Cell Biology* 24, 407–415.
- Williams, D., and Pessin, J.E. (2008). Mapping of R-SNARE function at distinct intracellular GLUT4 trafficking steps in adipocytes. *J Cell Biol* 180, 375–387.
- Wu, D., Bacaj, T., Morishita, W., Goswami, D., Arendt, K.L., Xu, W., Chen, L., Malenka, R.C., and Südhof, T.C. (2017). Postsynaptic synaptotagmins mediate AMPA receptor exocytosis during LTP. *Nature*.
- Yudowski, G.A., Puthenveedu, M.A., Leonoudakis, D., Panicker, S., Thorn, K.S., Beattie, E.C., and von Zastrow, M. (2007). Real-Time Imaging of Discrete Exocytic Events Mediating Surface Delivery of AMPA Receptors. *Journal of Neuroscience* 27, 11112–11121.



# **General Discussion and Perspectives**



### **Further comments on the diversity of the endosomal system in dendrites**

The endosomal recycling system modulates synaptic transmission and strength by providing a spatiotemporal control on the supply of AMPARs and other cargo molecules via rounds of endo- and exocytosis. Therefore, the molecular characterization of different endosomes along this pathway is key in understanding how such a system functions in health and disease. Here we focus on the role of vSNAREs, which are part of the exocytic fusion machinery, in mediating post-synaptic membrane trafficking. Our findings imply that VAMP4 and VAMP2 decipher two distinct recycling routes to the plasma membrane with different transport kinetics, supporting the functional diversity of REs.

First, this study reinstates that endosomal recycling in neurons is not limited to TfR-labelled REs. We show that the majority of RE fusion events labelled with TfR are mediated by VAMP4. The exocytosis of these REs is fairly fast and appears to be TeNT insensitive, excluding a major contribution of VAMP2 in this pathway. VAMP2 fuses at a much slower rate and seems to preferentially mediate AMPAR exocytosis. Accordingly, considering TfR to be a marker of AMPAR constitutive recycling pathway is a simplistic model that probably does not faithfully reflect the complex nature of the endosomal system. It is important to note that in general, sorting receptors to recycling compartments is a way to maintain them since their prolonged residence in the EEs after internalization would eventually lead to their degradation by lysosomes. Therefore, receptor recycling saves energy of de-novo protein synthesis and is probably a favorable pathway to the cell. For instance, TfR is known to be a long-lived receptor which recycles back to the cell surface by default with very high efficiency (99%) and without any specific cytoplasmic sorting signals (Baratti-Elbaz et al., 1999; Grant & Donaldson, 2009). Nevertheless, the pathway taken by a recycling molecule can be complex and can involve a series of sorting events that are only partially understood.

Given that AMPARs and TfRs recycle at different rates and can be differentially modulated by vSNAREs, it is unlikely that the two receptors reside in the same classical TfR-labelled REs, especially under basal synaptic conditions. To resolve such dispute, we propose that two distinct recycling pathways exist from the EE: one that constitutively recycles TfR back to the plasma membrane, and is mediated by VAMP4, and a second slower AMPAR recycling endosome which we call ARV and uses VAMP2 for exocytosis. While both REs might share common cargo molecules, AMPAR-containing compartments are subject to more sorting and regulatory signals. These signals tightly control AMPAR exocytosis and synaptic insertion, thereby tuning basal synaptic transmission. In particular, AMPARs can be sorted to the retrograde trafficking

pathway that is mediated by VAMP4. In this context, they transport away from the plasma membrane, either to the TGN, or to an ASV which we propose matures from the ARV. Accordingly, the depletion of VAMP4 would block AMPARs trafficking to the ASV and lead to their basal state missorting to the constitutive recycling pathway.

The reason as to why VAMP4 is not similarly mediating the retrograde transport of TfR can be explained by the fact that this receptor seems to recycle by default. Recent evidence indicates that in HeLa cells, Stx 13 and Stx 6, the cognate SNARE partners of VAMP4, are responsible for targeting the endosome for recycling. They then show that almost all endogenous TfRs are colocalized with both Stxs, and are therefore recycled back to the plasma membrane (Koike & Jahn, 2019). In contrary, endosomes that contain only stx 6 are targeted for the retrograde pathway, which we believe are perhaps the site for AMPAR sorting to the TGN and ASV formation.

Indeed, the regulated exocytosis of non-secretory vesicles has been recognized for a long time in non-neuronal cells. The best-described example is the GLUT-4-rich storage vesicles (GSVs) in adipocytes that are competent for exocytosis in response to insulin (Li et al., 2019; Leto & Saltiel, 2012). It has been shown that the depletion of VAMP4 in these cells leads to high levels of GLUT4 at the plasma membrane in the basal state, but the insulin-stimulated translocation of GSVs to the plasma membrane is mediated by VAMP2 (Williams & Pessin, 2008). This phenotype is reminiscent of what we observe in hippocampal neurons. The molecular characterization of GSVs and their regulation is very advanced and could provide useful guidance for the study of ASVs in neurons. For example, Stx 6 has been shown to regulate the retrograde trafficking of GLUT4 from endosomes back into GSVs in 3T3-L1 adipocytes (Perera et al., 2003).

The presence of an ASV in neuronal cells would enable neurons to prevent the routing of internalized AMPARs to degradative lysosomes, control their basal state recycling and provide a reservoir of AMPARs that can be readily mobilized upon LTP induction. Certainly, it has been established that the exocytosis of Rab11 REs supply AMPARs during LTP expression. After mobilization, ASV could reach the plasma membrane using Rab11 and effectors (Wang et al., 2008; Royo et al., 2019). AMPARs can also reach the synapse by lateral diffusion from extrasynaptic sites where they are trapped at synapses for short-term potentiation. However, the fact that AMPAR endocytosis is similarly enhanced upon LTP induction argues against the sufficiency of enhanced local recycling to provide a net increase in surface receptors for LTP expression (Zheng et al., 2015). A high cycling rate per se would not alter the steady-state

surface expression of AMPARs, but would render the synapse more sensitive to stimuli that govern AMPAR trafficking (Lin et al., 2000). This suggests that AMPARs can be trafficked from other sources outside the potentiated spine during LTP expression.

Interestingly, it has been recently reported that GluA1 associates with FIP2, an effector of Rab11, at extrasynaptic compartments under basal conditions in hippocampal neurons. This association occurs in immobile compartments that are separate from Rab11 REs and function to prevent GluA1 containing AMPARs from reaching the synaptic membrane without neuronal stimulation. Upon LTP induction, FIP2 dissociates from GluA1 allowing the receptor to deliver to the membrane via Rab11-dependent trafficking (Royo et al., 2019). This can perhaps allow the synaptic insertion of high-conductance AMPAR GluA1 homomers for LTP expression (Benke and Traynelis, 2018).

In summary, it is now becoming more evident that recycling endosomes represent a heterogeneous pool of organelles that are molecularly and functionally distinct. This emerging diversity of the endosomal system calls for new discoveries of key players that serve to define membrane identity. In our study, we identify VAMP4 as the major vSNARE protein mediating TfR-labelled fusion events at the post-synapse. However, it remains unclear whether the residual TfR exocytic events upon VAMP4 depletion is due to the partial KD of VAMP4 or there exist other TfR-positive vesicles that fuse independently of VAMP4. It would therefore be interesting to study TfR trafficking in the currently existing VAMP4 KO mouse model (FENS meeting abstract). However, such data should be explained with caution, given that some SNARE proteins can functionally substitute for each other.

The next challenge is to employ super-resolution imaging techniques to provide direct proof of segregated recycling pathways taken by both TfRs and AMPARs upon internalization. Additionally, further research is necessary to conclude how the recycling pathway is modulated during synaptic plasticity and to what extent it contributes to LTP expression. Indeed, evidence on the regulated trafficking of immobile AMPAR compartments or “ASVs” needs to be disclosed. We can later envision that memories reside in membrane-bound vesicles.

## **Implications for neuropathology**

Finally, this research might have implications for understanding the pathophysiology of common disorders tied to memory such as AD. One in three people now develops AD by the age of 85 (Perdigão et al., 2020). The late-onset or sporadic form of AD accounts for over 95% of all cases. Among the genes that have been strongly linked to late-onset AD are the “endosomal trafficking” class of genes. The genes that best represent this class are SORL1 (Sortilin related receptor 1), BIN1 (Bridging Integrator 1), PICALM (Phosphatidylinositol Binding Clathrin Assembly Protein), and CD2AP (CD2 Associated Protein). The disease-associated variants of these genes directly cause endosomal enlargements indicatively of endosomal traffic jams. Enlarged endosomes have now emerged as a cytopathological hallmark of the disease (Kwart et al., 2019; Botté et al., 2019). This class of genes can also have secondary consequences of increasing intracellular APP (Amyloid precursor protein), which can be misprocessed and accumulate, thereby exacerbating traffic jams. Indeed, A $\beta$  peptides can accumulate interneuronally within the early endosomes (Gouras et al., 2010), but how exactly they exert their toxicity remains vague.

An appealing model has been proposed which suggests that jamming from early endosomes can represent a pathogenic hub onto which nearly all AD genes can converge (Small et al., 2017). The model therefore supports the existence of a vicious feedback loop between traffic jams and intracellular amyloid which is critical in the pathology of the disease. Jamming the outflow from early endosomes is suggested to act as upstream drivers of AD pathogenesis, which can lead to a reduction in glutamate receptor recycling to the cell surface mediating synaptic toxicity, sometimes even independent of A $\beta$  peptides (Choy et al., 2014).

Given such a model, it would be interesting to study how prompting traffick jams, in our case by manipulating vSNARE proteins, might affect APP synaptic levels and A $\beta$  secretion.

An AD pathology paradigm centralized on traffick jams as an alternative to the mainstream “amyloid hypothesis” would explain why drugs that simply reduce intracellular amyloid production fail to show efficacy in clinical trials. Discerning the root cause of synaptic failure in AD pathology would help create patient-specific drug formulations ensuring the most optimal treatment for every AD patient.





## References

- Ackermann, M., & Matus, A. (2003). Activity-induced targeting of profilin and stabilization of dendritic spine morphology. *Nature Neuroscience*, 6(11), 1194–1200.
- Ahmad, M., Polepalli, J. S., Goswami, D., Yang, X., Kaeser-Woo, Y. J., Südhof, T. C., & Malenka, R. C. (2012). Postsynaptic complexin controls AMPA receptor exocytosis during LTP. *Neuron*, 73(2), 260–267.
- Alcamí, P., & Pereda, A. E. (2019). Beyond plasticity: the dynamic impact of electrical synapses on neural circuits. *Nature Reviews Neuroscience*.
- Alexandrov, K., Horiuchi, H., Steele-Mortimer, O., Seabra, M. C., & Zerial, M. (1994). Rab escort protein-1 is a multifunctional protein that accompanies newly prenylated rab proteins to their target membranes. *The EMBO journal*, 13(22), 5262–5273.
- Anand, K. S., & Dhikav, V. (2012). Hippocampus in health and disease: An overview. *Annals of Indian Academy of Neurology*, 15(4), 239–246.
- Andres, D. A., Seabra, M. C., Brown, M. S., Armstrong, S. A., Smeland, T. E., Cremers, F. P. M., & Goldstein, J. L. (1993). cDNA cloning of component A of Rab geranylgeranyl transferase and demonstration of its role as a Rab escort protein. *Cell*, 73(6), 1091–1099.
- Araki, Y., Lin, D. T., & Huganir, R. L. (2010). Plasma membrane insertion of the AMPA receptor GluA2 subunit is regulated by NSF binding and Q/R editing of the ion pore. *Proceedings of the National Academy of Sciences of the United States of America*, 107(24), 11080–11085.
- Arnon, S. S., Schechter, R., Inglesby, T. V., Henderson, D. A., Bartlett, J. G., Ascher, M. S., ... for the Working Group on Civilian Biodefense. (2001). Botulinum Toxin as a Biological Weapon. *JAMA*, 285(8), 1059.
- Bal, M., Leitz, J., Reese, A. L., Ramirez, D. M., Durakoglugil, M., Herz, J., Monteggia, L. M., & Kavalali, E. T. (2013). Reelin mobilizes a VAMP7-dependent synaptic vesicle pool and selectively augments spontaneous neurotransmission. *Neuron*, 80(4), 934–946.
- Barbero, P., Bittova, L., & Pfeffer, S. R. (2002). Visualization of Rab9-mediated vesicle transport from endosomes to the trans-Golgi in living cells. *The Journal of cell biology*, 156(3), 511–518.

- Bennett, M. K. (1992). Synaptic vesicle membrane proteins interact to form a multimeric complex. *The Journal of Cell Biology*, 116(3), 761–775.
- Bernardinelli, Y., Nikonenko, I., & Muller, D. (2014). Structural plasticity: mechanisms and contribution to developmental psychiatric disorders. *Frontiers in neuroanatomy*, 8, 123.
- Bethani, I., Lang, T., Geumann, U., Sieber, J. J., Jahn, R., & Rizzoli, S. O. (2007). The specificity of SNARE pairing in biological membranes is mediated by both proof-reading and spatial segregation. *The EMBO journal*, 26(17), 3981–3992.
- Bhattacharya, S., Stewart, B. A., Niemeyer, B. A., Burgess, R. W., McCabe, B. D., Lin, P., ... Schwarz, T. L. (2002). Members of the synaptobrevin/vesicle-associated membrane protein (VAMP) family in *Drosophila* are functionally interchangeable in vivo for neurotransmitter release and cell viability. *Proceedings of the National Academy of Sciences*, 99(21), 13867–13872.
- Bhuin, T., & Roy, J. K. (2014). Rab proteins: The key regulators of intracellular vesicle transport. *Experimental Cell Research*, 328(1), 1–19.
- Bigalke, H., & Rummel, A. (2005). Medical aspects of toxin weapons. *Toxicology*, 214(3), 210–220.
- Bin, N.-R., Ma, K., Harada, H., Tien, C.-W., Bergin, F., Sugita, K., ... Sugita, S. (2018). Crucial Role of Postsynaptic Syntaxin 4 in Mediating Basal Neurotransmission and Synaptic Plasticity in Hippocampal CA1 Neurons. *Cell Reports*, 23(10), 2955–2966.
- Binz, T., Sikorra, S., & Mahrhold, S. (2010). Clostridial neurotoxins: mechanism of SNARE cleavage and outlook on potential substrate specificity reengineering. *Toxins*, 2(4), 665–682.
- Bird, C. M., & Burgess, N. (2008). The hippocampus and memory: insights from spatial processing. *Nature Reviews Neuroscience*, 9(3), 182–194.
- Blasi, J., Chapman, E. R., Link, E., Binz, T., Yamasaki, S., Camilli, P. D., ... Jahn, R. (1993). Botulinum neurotoxin A selectively cleaves the synaptic protein SNAP-25. *Nature*, 365(6442), 160–163.
- Blasi, J., Chapman, E. R., Yamasaki, S., Binz, T., Niemann, H., & Jahn, R. (1993). Botulinum neurotoxin C1 blocks neurotransmitter release by means of cleaving HPC-1/syntaxin. *The EMBO journal*, 12(12), 4821–4828.

- Bliss, T. V., & Collingridge, G. L. (2013). Expression of NMDA receptor-dependent LTP in the hippocampus: bridging the divide. *Molecular Brain*, 6(1), 5.
- Bliss, T. V., & Lomo, T. (1973). Long-lasting potentiation of synaptic transmission in the dentate area of the anaesthetized rabbit following stimulation of the perforant path. *The Journal of physiology*, 232(2), 331–356.
- Borovac, J., Bosch, M., & Okamoto, K. (2018). Regulation of actin dynamics during structural plasticity of dendritic spines: Signaling messengers and actin-binding proteins. *Molecular and Cellular Neuroscience*.
- Bosch, M., & Hayashi, Y. (2012). Structural plasticity of dendritic spines. *Current opinion in neurobiology*, 22(3), 383–388.
- Bosch, M., Castro, J., Saneyoshi, T., Matsuno, H., Sur, M., & Hayashi, Y. (2014). Structural and molecular remodeling of dendritic spine substructures during long-term potentiation. *Neuron*, 82(2), 444–459.
- Bradley, C. A., Peineau, S., Taghibiglou, C., Nicolas, C. S., Whitcomb, D. J., Bortolotto, Z. A., Kaang, B. K., Cho, K., Wang, Y. T., & Collingridge, G. L. (2012). A pivotal role of GSK-3 in synaptic plasticity. *Frontiers in molecular neuroscience*, 5, 13.
- Brandhorst, D., Zwilling, D., Rizzoli, S. O., Lippert, U., Lang, T., & Jahn, R. (2006). Homotypic fusion of early endosomes: SNAREs do not determine fusion specificity. *Proceedings of the National Academy of Sciences of the United States of America*, 103(8), 2701–2706.
- Brandon, E. P., Zhuo, M., Huang, Y. Y., Qi, M., Gerhold, K. A., Burton, K. A., Kandel, E. R., McKnight, G. S., & Idzerda, R. L. (1995). Hippocampal long-term depression and depotentiation are defective in mice carrying a targeted disruption of the gene encoding the RI beta subunit of cAMP-dependent protein kinase. *Proceedings of the National Academy of Sciences of the United States of America*, 92(19), 8851–8855.
- Brown, T. C., Correia, S. S., Petrok, C. N., & Esteban, J. A. (2007). Functional compartmentalization of endosomal trafficking for the synaptic delivery of AMPA receptors during long-term potentiation. *The Journal of neuroscience: the official journal of the Society for Neuroscience*, 27(48), 13311–13315.

- Brunger, A. T., Choi, U. B., Lai, Y., Leitz, J., White, K. I., & Zhou, Q. (2019). The pre-synaptic fusion machinery. *Current opinion in structural biology*, 54, 179–188.
- Brunger, A. T., Leitz, J., Zhou, Q., Choi, U. B., & Lai, Y. (2018). Ca<sup>2+</sup>-Triggered Synaptic Vesicle Fusion Initiated by Release of Inhibition. *Trends in cell biology*, 28(8), 631–645.
- Brunt, J., Carter, A. T., Stringer, S. C., & Peck, M. W. (2018). Identification of a novel botulinum neurotoxin gene cluster in *Enterococcus*. *FEBS letters*, 592(3), 310–317.
- Bucci, C., Parton, R. G., Mather, I. H., Stunnenberg, H., Simons, K., Hoflack, B., & Zerial, M. (1992). The small GTPase rab5 functions as a regulatory factor in the early endocytic pathway. *Cell*, 70(5), 715–728.
- Bukharaeva, E. A. (2015). Synchronous and asynchronous quantal release at synapses. *Biochemistry (Moscow) Supplement Series A: Membrane and Cell Biology*, 9(4), 263–269.
- Burkhardt, P., Hattendorf, D. A., Weis, W. I., & Fasshauer, D. (2008). Munc18a controls SNARE assembly through its interaction with the syntaxin N-peptide. *The EMBO journal*, 27(7), 923–933.
- Castillo, P. E., Chiu, C. Q., & Carroll, R. C. (2011). Long-term plasticity at inhibitory synapses. *Current opinion in neurobiology*, 21(2), 328–338.
- Chanaday, N. L., & Kavalali, E. T. (2018). Optical detection of three modes of endocytosis at hippocampal synapses. *eLife*, 7, e36097.
- Chanaday, N. L., Cousin, M. A., Milosevic, I., Watanabe, S., & Morgan, J. R. (2019). The Synaptic Vesicle Cycle Revisited: New Insights into the Modes and Mechanisms. *The Journal of Neuroscience*, 39(42), 8209–8216.
- Chen, C.-C., Lu, J., & Zuo, Y. (2014). Spatiotemporal dynamics of dendritic spines in the living brain. *Frontiers in Neuroanatomy*, 8.
- Chevaleyre, V., & Siegelbaum, S. A. (2010). Strong CA2 pyramidal neuron synapses define a powerful disinaptic cortico-hippocampal loop. *Neuron*, 66(4), 560–572.
- Cho, E., Kim, D.-H., Hur, Y.-N., Whitcomb, D. J., Regan, P., Hong, J.-H., ... Park, M. (2015). Cyclin Y inhibits plasticity-induced AMPA receptor exocytosis and LTP. *Scientific Reports*, 5(1).

- Choquet D. (2018). Linking Nanoscale Dynamics of AMPA Receptor Organization to Plasticity of Excitatory Synapses and Learning. *The Journal of neuroscience: the official journal of the Society for Neuroscience*, 38(44), 9318–9329.
- Citri, A., & Malenka, R.C. (2008). Synaptic Plasticity: Multiple Forms, Functions, and Mechanisms. *Neuropsychopharmacology*, 33, 18-41.
- Collingridge, G. L., Isaac, J. T. R., & Wang, Y. T. (2004). Receptor trafficking and synaptic plasticity. *Nature Reviews Neuroscience*, 5(12), 952–962.
- Collingridge, G. L., Peineau, S., Howland, J. G., & Wang, Y. T. (2010). Long-term depression in the CNS. *Nature Reviews Neuroscience*, 11(7), 459–473.
- Crupi, R., Impellizzeri, D., & Cuzzocrea, S. (2019). Role of Metabotropic Glutamate Receptors in Neurological Disorders. *Frontiers in molecular neuroscience*, 12, 20.
- Curti, S., & O'Brien, J. (2016). Characteristics and plasticity of electrical synaptic transmission. *BMC cell biology*, 17 Suppl 1(Suppl 1), 13.
- Daro, E., van der Sluijs, P., Galli, T., & Mellman, I. (1996). Rab4 and cellubrevin define different early endosome populations on the pathway of transferrin receptor recycling. *Proceedings of the National Academy of Sciences of the United States of America*, 93(18), 9559–9564.
- Darsow, T., Rieder, S. E., & Emr, S. D. (1997). A Multispecificity Syntaxin Homologue, Vam3p, Essential for Autophagic and Biosynthetic Protein Transport to the Vacuole. *The Journal of Cell Biology*, 138(3), 517–529.
- Deak, F., Shin, O.-H., Kavalali, E. T., & Sudhof, T. C. (2006). Structural Determinants of Synaptobrevin 2 Function in Synaptic Vesicle Fusion. *Journal of Neuroscience*, 26(25), 6668–6676.
- Denker, A., & Rizzoli, S. O. (2010). Synaptic vesicle pools: an update. *Frontiers in synaptic neuroscience*, 2, 135.
- Derkach, V. A., Oh, M. C., Guire, E. S., & Soderling, T. R. (2007). Regulatory mechanisms of AMPA receptors in synaptic plasticity. *Nature Reviews Neuroscience*, 8(2), 101–113.
- Díaz, E., Schimmöller, F., & Pfeffer, S. R. (1997). A novel Rab9 effector required for endosome-to-TGN transport. *The Journal of cell biology*, 138(2), 283–290.

- Diekmann, Y., Seixas, E., Gouw, M., Tavares-Cadete, F., Seabra, M. C., & Pereira-Leal, J. B. (2011). Thousands of rab GTPases for the cell biologist. *PLoS computational biology*, 7(10), e1002217.
- Dolly, J. O., Black, J., Williams, R. S., & Melling, J. (1984). Acceptors for botulinum neurotoxin reside on motor nerve terminals and mediate its internalization. *Nature*, 307(5950), 457–460.
- Dong, M., Liu, H., Tepp, W. H., Johnson, E. A., Janz, R., & Chapman, E. R. (2008). Glycosylated SV2A and SV2B mediate the entry of botulinum neurotoxin E into neurons. *Molecular biology of the cell*, 19(12), 5226–5237.
- Dong, M., Richards, D. A., Goodnough, M. C., Tepp, W. H., Johnson, E. A., & Chapman, E. R. (2003). Synaptotagmins I and II mediate entry of botulinum neurotoxin B into cells. *The Journal of cell biology*, 162(7), 1293–1303.
- Dong, M., Tepp, W. H., Liu, H., Johnson, E. A., & Chapman, E. R. (2007). Mechanism of botulinum neurotoxin B and G entry into hippocampal neurons. *The Journal of cell biology*, 179(7), 1511–1522.
- Dunwiddie, T., & Lynch, G. (1978). Long-term potentiation and depression of synaptic responses in the rat hippocampus: localization and frequency dependency. *The Journal of physiology*, 276, 353–367.
- Edelmann, E., Cepeda-Prado, E., & Leßmann, V. (2017). Coexistence of Multiple Types of Synaptic Plasticity in Individual Hippocampal CA1 Pyramidal Neurons. *Frontiers in synaptic neuroscience*, 9, 7.
- Engert, F., & Bonhoeffer, T. (1999). Dendritic spine changes associated with hippocampal long-term synaptic plasticity. *Nature*, 399(6731), 66–70.
- Esteves da Silva, M., Adrian, M., Schätzle, P., Lipka, J., Watanabe, T., Cho, S., Futai, K., Wierenga, C. J., Kapitein, L. C., & Hoogenraad, C. C. (2015). Positioning of AMPA Receptor-Containing Endosomes Regulates Synapse Architecture. *Cell reports*, 13(5), 933–943.
- Fasshauer, D., Antonin, W., Margittai, M., Pabst, S., & Jahn, R. (1999). Mixed and Non-cognate SNARE Complexes. *Journal of Biological Chemistry*, 274(22), 15440–15446.
- Fasshauer, D., Sutton, R. B., Brunger, A. T., & Jahn, R. (1998). Conserved structural features of the synaptic fusion complex: SNARE proteins reclassified as Q- and R-SNAREs.

Proceedings of the National Academy of Sciences of the United States of America, 95(26), 15781–15786.

Feng, Y., Press, B., & Wandinger-Ness, A. (1995). Rab 7: an important regulator of late endocytic membrane traffic. *The Journal of cell biology*, 131(6 Pt 1), 1435–1452.

Ferro-Novick, S., & Novick, P. (1993). The Role of GTP-Binding Proteins in Transport along the Exocytic Pathway. *Annual Review of Cell Biology*, 9(1), 575–599.

Fifková, E., & Anderson, C. L. (1981). Stimulation-induced changes in dimensions of stalks of dendritic spines in the dentate molecular layer. *Experimental Neurology*, 74(2), 621–627.

Fifková, E., & Van Harreveld, A. (1977). Long-lasting morphological changes in dendritic spines of dentate granular cells following stimulation of the entorhinal area. *Journal of Neurocytology*, 6(2), 211–230.

Fox-Loe, A. M., Henderson, B. J., & Richards, C. I. (2017). Utilizing pHluorin-tagged Receptors to Monitor Subcellular Localization and Trafficking. *Journal of visualized experiments: JoVE*, (121), 55466.

Friedman, H. V., Bresler, T., Garner, C. C., & Ziv, N. E. (2000). Assembly of New Individual Excitatory Synapses. *Neuron*, 27(1), 57–69.

Fu, Z., Chen, C., Barbieri, J. T., Kim, J.-J. P., & Baldwin, M. R. (2009). Glycosylated SV2 and Gangliosides as Dual Receptors for Botulinum Neurotoxin Serotype F. *Biochemistry*, 48(24), 5631–5641.

Fukuda, R., McNew, J. A., Weber, T., Parlati, F., Engel, T., Nickel, W., ... Söllner, T. H. (2000). Functional architecture of an intracellular membrane t-SNARE. *Nature*, 407(6801), 198–202.

Gallwitz, D., Donath, C., & Sander, C. (1983). A yeast gene encoding a protein homologous to the human c-has/bas proto-oncogene product. *Nature*, 306(5944), 704–707.

Ganley, I. G., Carroll, K., Bittova, L., & Pfeffer, S. (2004). Rab9 GTPase regulates late endosome size and requires effector interaction for its stability. *Molecular biology of the cell*, 15(12), 5420–5430.

Gardner, A., & Barbieri, J. (2018). Light Chain Diversity among the Botulinum Neurotoxins. *Toxins*, 10(7), 268.

- Geinisman, Y., Berry, R. W., Disterhoft, J. F., Power, J. M., & Van der Zee, E. A. (2001). Associative learning elicits the formation of multiple-synapse boutons. *The Journal of neuroscience : the official journal of the Society for Neuroscience*, 21(15), 5568–5573.
- Gerges, N. Z., Backos, D. S., & Esteban, J. A. (2004). Local Control of AMPA Receptor Trafficking at the Postsynaptic Terminal by a Small GTPase of the Rab Family. *Journal of Biological Chemistry*, 279(42), 43870–43878.
- Gill D. M. (1982). Bacterial toxins: a table of lethal amounts. *Microbiological reviews*, 46(1), 86–94.
- Goody, R. S., Müller, M. P., & Wu, Y.-W. (2017). Mechanisms of action of Rab proteins, key regulators of intracellular vesicular transport. *Biological Chemistry*, 398(5-6).
- Götte, M., & Gallwitz, D. (1997). High expression of the yeast syntaxin-related Vam3 protein suppresses the protein transport defects of *apep12null* mutant. *FEBS Letters*, 411(1), 48–52.
- Greger, I. H., Watson, J. F., & Cull-Candy, S. G. (2017). Structural and Functional Architecture of AMPA-Type Glutamate Receptors and Their Auxiliary Proteins. *Neuron*, 94(4), 713–730.
- Grosshans, B. L., Ortiz, D., & Novick, P. (2006). Rabs and their effectors: achieving specificity in membrane traffic. *Proceedings of the National Academy of Sciences of the United States of America*, 103(32), 11821–11827.
- Gu, Y., & Huganir, R. L. (2016). Identification of the SNARE complex mediating the exocytosis of NMDA receptors. *Proceedings of the National Academy of Sciences*, 113(43), 12280–12285.
- Gundersen C. B. (2017). A Membrane-Fusion Model That Exploits a  $\beta$ -to- $\alpha$  Transition in the Hydrophobic Domains of Syntaxin 1A and Synaptobrevin 2. *International journal of molecular sciences*, 18(7), 1582.
- Gundersen, C. B. (2019). Fast, synchronous neurotransmitter release: past, present and future. *Neuroscience*.
- Hammarlund, M., Palfreyman, M. T., Watanabe, S., Olsen, S., & Jorgensen, E. M. (2007). Open syntaxin docks synaptic vesicles. *PLoS biology*, 5(8), e198.
- Han, J., Pluhackova, K., & Böckmann, R. A. (2017). The Multifaceted Role of SNARE Proteins in Membrane Fusion. *Frontiers in Physiology*, 8.

- Han, K., Kim, M. H., Seeburg, D., Seo, J., Verpelli, C., Han, S., Chung, H. S., Ko, J., Lee, H. W., Kim, K., Heo, W. D., Meyer, T., Kim, H., Sala, C., Choi, S. Y., Sheng, M., & Kim, E. (2009). Regulated RalBP1 binding to RalA and PSD-95 controls AMPA receptor endocytosis and LTD. *PLoS biology*, 7(9), e1000187.
- Harris, K. M., Jensen, F. E., & Tsao, B. (1992). Three-dimensional structure of dendritic spines and synapses in rat hippocampus (CA1) at postnatal day 15 and adult ages: implications for the maturation of synaptic physiology and long-term potentiation. *The Journal of neuroscience: the official journal of the Society for Neuroscience*, 12(7), 2685–2705.
- Hasan, N., Corbin, D., & Hu, C. (2010). Fusogenic Pairings of Vesicle-Associated Membrane Proteins (VAMPs) and Plasma Membrane t-SNAREs – VAMP5 as the Exception. *PLoS ONE*, 5(12), e14238.
- Hayashi, T., McMahon, H., Yamasaki, S., Binz, T., Hata, Y., Südhof, T. C., & Niemann, H. (1994). Synaptic vesicle membrane fusion complex: action of clostridial neurotoxins on assembly. *The EMBO journal*, 13(21), 5051–5061.
- Hayashi, Y. (2000). Driving AMPA Receptors into Synapses by LTP and CaMKII: Requirement for GluR1 and PDZ Domain Interaction. *Science*, 287(5461), 2262–2267. doi:10.1126/science.287.5461.2262
- Hebb D. 1949. *The organisation of behaviour*. New York, NY: John Wiley and Sons.
- Herculano-Houzel S. (2009). The human brain in numbers: a linearly scaled-up primate brain. *Frontiers in human neuroscience*, 3, 31.
- Hering, H., & Sheng, M. (2001). Dendritic spines : structure, dynamics and regulation. *Nature Reviews Neuroscience*, 2(12), 880–888.
- Hong, W. (2005). SNAREs and traffic. *Biochimica et Biophysica Acta (BBA) - Molecular Cell Research*, 1744(2), 120–144.
- Hoogstraaten, R. I., van Keimpema, L., Toonen, R. F., & Verhage, M. (2020). Tetanus insensitive VAMP2 differentially restores synaptic and dense core vesicle fusion in tetanus neurotoxin treated neurons. *Scientific reports*, 10(1), 10913.
- Hua, Z., Leal-Ortiz, S., Foss, S. M., Waites, C. L., Garner, C. C., Voglmaier, S. M., & Edwards, R. H. (2011). v-SNARE composition distinguishes synaptic vesicle pools. *Neuron*, 71(3), 474–487.

- Humeau, Y., Doussau, F., Grant, N. J., & Poulain, B. (2000). How botulinum and tetanus neurotoxins block neurotransmitter release\*\*This paper is dedicated to the memory of Heiner Niemann. *Biochimie*, 82(5), 427–446.
- Huotari, J., & Helenius, A. (2011). Endosome maturation. *The EMBO Journal*, 30(17), 3481–3500.
- Hutagalung, A. H., & Novick, P. J. (2011). Role of Rab GTPases in membrane traffic and cell physiology. *Physiological reviews*, 91(1), 119–149.
- Jabeen, S., & Thirumalai, V. (2018). The interplay between electrical and chemical synaptogenesis. *Journal of neurophysiology*, 120(4), 1914–1922.
- Jackman, S. L., Turecek, J., Belinsky, J. E., & Regehr, W. G. (2016). The calcium sensor synaptotagmin 7 is required for synaptic facilitation. *Nature*, 529(7584), 88–91.
- Jahn, R., & Scheller, R. H. (2006). SNAREs — engines for membrane fusion. *Nature Reviews Molecular Cell Biology*, 7(9), 631–643.
- Jahn, R., & Südhof, T. C. (1999). Membrane Fusion and Exocytosis. *Annual Review of Biochemistry*, 68(1), 863–911.
- Johnson, E. A., & Bradshaw, M. (2001). Clostridium botulinum and its neurotoxins: a metabolic and cellular perspective. *Toxicon*, 39(11), 1703–1722.
- Jurado, S., Goswami, D., Zhang, Y., Molina, A. J., Südhof, T. C., & Malenka, R. C. (2013). LTP requires a unique postsynaptic SNARE fusion machinery. *Neuron*, 77(3), 542–558.
- Kádková, A., Radecke, J., & Sørensen, J. B. (2019). The SNAP-25 Protein Family. *Neuroscience*, 420, 50–71.
- Kaesler, P. S., & Regehr, W. G. (2014). Molecular mechanisms for synchronous, asynchronous, and spontaneous neurotransmitter release. *Annual review of physiology*, 76, 333–363.
- Kelly, E. E., Horgan, C. P., McCaffrey, M. W., & Young, P. (2010). The role of endosomal-recycling in long-term potentiation. *Cellular and Molecular Life Sciences*, 68(2), 185–194.
- Kennedy, M. J., & Ehlers, M. D. (2006). Organelles and trafficking machinery for postsynaptic plasticity. *Annual review of neuroscience*, 29, 325–362.
- Kennedy, M. J., Davison, I. G., Robinson, C. G., & Ehlers, M. D. (2010). Syntaxin-4 Defines a Domain for Activity-Dependent Exocytosis in Dendritic Spines. *Cell*, 141(3), 524–535.

- Kim CH, Lee J, Lee JY, Roche KW. Metabotropic glutamate receptors: phosphorylation and receptor signaling. *J Neurosci Res.* 2008;86:1–10.
- Kim, C. H., Chung, H. J., Lee, H. K., & Huganir, R. L. (2001). Interaction of the AMPA receptor subunit GluR2/3 with PDZ domains regulates hippocampal long-term depression. *Proceedings of the National Academy of Sciences of the United States of America*, 98(20), 11725–11730.
- Kirchhausen, T. (2000). Clathrin. *Annual Review of Biochemistry*, 69(1), 699–727.
- Kleim, J. A., Freeman, J. H., Bruneau, R., Nolan, B. C., Cooper, N. R., Zook, A., & Walters, D. (2002). Synapse formation is associated with memory storage in the cerebellum. *Proceedings of the National Academy of Sciences*, 99(20), 13228–13231.
- Kloepper, T. H., Kienle, C. N., & Fasshauer, D. (2007). An elaborate classification of SNARE proteins sheds light on the conservation of the eukaryotic endomembrane system. *Molecular biology of the cell*, 18(9), 3463–3471.
- Klöpffer, T. H., Kienle, N., Fasshauer, D., & Munro, S. (2012). Untangling the evolution of Rab G proteins: implications of a comprehensive genomic analysis. *BMC biology*, 10, 71.
- Knafo, S., Ariav, G., Barkai, E., & Libersat, F. (2004). Olfactory learning-induced increase in spine density along the apical dendrites of CA1 hippocampal neurons. *Hippocampus*, 14(7), 819–825.
- Koike, S., & Jahn, R. (2019). SNAREs define targeting specificity of trafficking vesicles by combinatorial interaction with tethering factors. *Nature communications*, 10(1), 1608.
- Kopec, C. D. (2006). Glutamate Receptor Exocytosis and Spine Enlargement during Chemically Induced Long-Term Potentiation. *Journal of Neuroscience*, 26(7), 2000–2009.
- Kopec, C. D., Kessels, H. W. H. G., Bush, D. E. A., Cain, C. K., LeDoux, J. E., & Malinow, R. (2007). A robust automated method to analyze rodent motion during fear conditioning. *Neuropharmacology*, 52(1), 228–233.
- Korizova, L. K., & Montal, M. (2002). Translocation of botulinum neurotoxin light chain protease through the heavy chain channel. *Nature Structural Biology*, 10(1), 13–18.

- Kouranti, I., Sachse, M., Arouche, N., Goud, B., & Echard, A. (2006). Rab35 Regulates an Endocytic Recycling Pathway Essential for the Terminal Steps of Cytokinesis. *Current Biology*, 16(17), 1719–1725.
- Kümmel, D., Krishnakumar, S. S., Radoff, D. T., Li, F., Giraud, C. G., Pincet, F., Rothman, J. E., & Reinisch, K. M. (2011). Complexin cross-links prefusion SNAREs into a zigzag array. *Nature structural & molecular biology*, 18(8), 927–933.
- Kweon, D. H., Kong, B., & Shin, Y. K. (2017). Hemifusion in Synaptic Vesicle Cycle. *Frontiers in molecular neuroscience*, 10, 65.
- Lai, K.-O., & Ip, N. Y. (2013). Structural plasticity of dendritic spines: The underlying mechanisms and its dysregulation in brain disorders. *Biochimica et Biophysica Acta (BBA) - Molecular Basis of Disease*, 1832(12), 2257–2263.
- Lai, Y., Choi, U. B., Leitz, J., Rhee, H. J., Lee, C., Altas, B., Zhao, M., Pfuetzner, R. A., Wang, A. L., Brose, N., Rhee, J., & Brunger, A. T. (2017). Molecular Mechanisms of Synaptic Vesicle Priming by Munc13 and Munc18. *Neuron*, 95(3), 591–607.e10.
- Langille, J. J., & Brown, R. E. (2018). The Synaptic Theory of Memory: A Historical Survey and Reconciliation of Recent Opposition. *Frontiers in systems neuroscience*, 12, 52.
- Lasiecka, Z. M., & Winckler, B. (2011). Mechanisms of polarized membrane trafficking in neurons -- focusing in on endosomes. *Molecular and cellular neurosciences*, 48(4), 278–287.
- Lee S, Zhang H, Webb D. (2015). Dendritic spine morphology and dynamics in health and disease. *Cell Health and Cytoskeleton*. 7:121-131.
- Leto, D., & Saltiel, A. R. (2012). Regulation of glucose transport by insulin: traffic control of GLUT4. *Nature reviews. Molecular cell biology*, 13(6), 383–396.
- Leuner, B., Falduto, J., & Shors, T. J. (2003). Associative memory formation increases the observation of dendritic spines in the hippocampus. *The Journal of neuroscience : the official journal of the Society for Neuroscience*, 23(2), 659–665.
- Li, D. T., Habtemichael, E. N., Julca, O., Sales, C. I., Westergaard, X. O., DeVries, S. G., Ruiz, D., Sayal, B., & Bogan, J. S. (2019). GLUT4 Storage Vesicles: Specialized Organelles for Regulated Trafficking. *The Yale journal of biology and medicine*, 92(3), 453–470.

- Li, Z., & Sheng, M. (2003). Some assembly required: the development of neuronal synapses. *Nature Reviews Molecular Cell Biology*, 4(11), 833–841.
- Lin, D.-T., Makino, Y., Sharma, K., Hayashi, T., Neve, R., Takamiya, K., & Huganir, R. L. (2009). Regulation of AMPA receptor extrasynaptic insertion by 4.1N, phosphorylation and palmitoylation. *Nature Neuroscience*, 12(7), 879–887.
- Lin, H., Huganir, R., & Liao, D. (2004). Temporal dynamics of NMDA receptor-induced changes in spine morphology and AMPA receptor recruitment to spines. *Biochemical and Biophysical Research Communications*, 316(2), 501–511.
- Lin, J. W., Ju, W., Foster, K., Lee, S. H., Ahmadian, G., Wyszynski, M., Wang, Y. T., & Sheng, M. (2000). Distinct molecular mechanisms and divergent endocytotic pathways of AMPA receptor internalization. *Nature neuroscience*, 3(12), 1282–1290.
- Linden, D. J., & Connor, J. A. (1995). Long-Term Synaptic Depression. *Annual Review of Neuroscience*, 18(1), 319–357.
- Link, E., Edelmann, L., Chou, J. H., Binz, T., Yamasaki, S., Eisel, U., ... Jahn, R. (1992). Tetanus toxin action: Inhibition of neurotransmitter release linked to synaptobrevin proteolysis. *Biochemical and Biophysical Research Communications*, 189(2), 1017–1023.
- Lisman, J., Yasuda, R., & Raghavachari, S. (2012). Mechanisms of CaMKII action in long-term potentiation. *Nature reviews. Neuroscience*, 13(3), 169–182.
- Liu, Y., & Barlowe, C. (2002). Analysis of Sec22p in Endoplasmic Reticulum/Golgi Transport Reveals Cellular Redundancy in SNARE Protein Function. *Molecular Biology of the Cell*, 13(9), 3314–3324.
- Lledo, P. (1998). Postsynaptic Membrane Fusion and Long-Term Potentiation. *Science*, 279(5349), 399–403.
- Lu, W.-Y., Man, H.-Y., Ju, W., Trimble, W. S., MacDonald, J. F., & Wang, Y. T. (2001). Activation of Synaptic NMDA Receptors Induces Membrane Insertion of New AMPA Receptors and LTP in Cultured Hippocampal Neurons. *Neuron*, 29(1), 243–254.
- Lüscher, C., & Malenka, R. C. (2012). NMDA receptor-dependent long-term potentiation and long-term depression (LTP/LTD). *Cold Spring Harbor perspectives in biology*, 4(6), a005710.

- Lüscher, C., Xia, H., Beattie, E. C., Carroll, R. C., von Zastrow, M., Malenka, R. C., & Nicoll, R. A. (1999). Role of AMPA receptor cycling in synaptic transmission and plasticity. *Neuron*, 24(3), 649–658.
- Mahrhold, S., Rummel, A., Bigalke, H., Davletov, B., & Binz, T. (2006). The synaptic vesicle protein 2C mediates the uptake of botulinum neurotoxin A into phrenic nerves. *FEBS Letters*, 580(8), 2011–2014.
- Makino, H., & Malinow, R. (2009). AMPA receptor incorporation into synapses during LTP: the role of lateral movement and exocytosis. *Neuron*, 64(3), 381–390.
- Malenka, R. C. (2003). Synaptic Plasticity and AMPA Receptor Trafficking. *Annals of the New York Academy of Sciences*, 1003(1), 1–11.
- Maletic-Savatic, M. (1999). Rapid Dendritic Morphogenesis in CA1 Hippocampal Dendrites Induced by Synaptic Activity. *Science*, 283(5409), 1923–1927.
- Matsuzaki, M., Honkura, N., Ellis-Davies, G. C., & Kasai, H. (2004). Structural basis of long-term potentiation in single dendritic spines. *Nature*, 429(6993), 761–766.
- McBride, H. M., Rybin, V., Murphy, C., Giner, A., Teasdale, R., & Zerial, M. (1999). Oligomeric Complexes Link Rab5 Effectors with NSF and Drive Membrane Fusion via Interactions between EEA1 and Syntaxin 13. *Cell*, 98(3), 377–386.
- McMahon, H. T., Missler, M., Li, C., & Südhof, T. C. (1995). Complexins: Cytosolic proteins that regulate SNAP receptor function. *Cell*, 83(1), 111–119.
- McNew, J. A., Parlati, F., Fukuda, R., Johnston, R. J., Paz, K., Paumet, F., ... Rothman, J. E. (2000). Compartmental specificity of cellular membrane fusion encoded in SNARE proteins. *Nature*, 407(6801), 153–159.
- Meldrum, B. S. (2000). Glutamate as a Neurotransmitter in the Brain: Review of Physiology and Pathology. *The Journal of Nutrition*, 130(4), 1007S–1015S.
- Mercer, A., Trigg, H. L., & Thomson, A. M. (2007). Characterization of neurons in the CA2 subfield of the adult rat hippocampus. *The Journal of neuroscience: the official journal of the Society for Neuroscience*, 27(27), 7329–7338.
- Mettlen, M., Chen, P. H., Srinivasan, S., Danuser, G., & Schmid, S. L. (2018). Regulation of Clathrin-Mediated Endocytosis. *Annual review of biochemistry*, 87, 871–896.

- Misura, K. M. S., Scheller, R. H., & Weis, W. I. (2000). Three-dimensional structure of the neuronal-Sec1–syntaxin 1a complex. *Nature*, 404(6776), 355–362.
- Munafò, D. B., & Colombo, M. I. (2002). Induction of Autophagy Causes Dramatic Changes in the Subcellular Distribution of GFP-Rab24. *Traffic*, 3(7), 472–482.
- Münchau, A., & Bhatia, K. P. (2000). Uses of botulinum toxin injection in medicine today. *BMJ (Clinical research ed.)*, 320(7228), 161–165.
- Neves G., Cooke, S. F., Bliss T. V. P. (2008). Synaptic plasticity, memory and the hippocampus: a neural network approach to causality, *Nature Reviews Neuroscience*, 9, 65–75.
- Niciu, M. J., Kelmendi, B., & Sanacora, G. (2012). Overview of glutamatergic neurotransmission in the nervous system. *Pharmacology, biochemistry, and behavior*, 100(4), 656–664.
- Nicoll, R. A. (2017). A Brief History of Long-Term Potentiation. *Neuron*, 93(2), 281–290.
- Niemann, H., Blasi, J., & Jahn, R. (1994). Clostridial neurotoxins: new tools for dissecting exocytosis. *Trends in Cell Biology*, 4(5), 179–185.
- Nishiki T., Kamata Y., Nemoto Y., Omori A., Ito T., Takahashi M., Kozaki S. (1994). Identification of protein receptor for Clostridium botulinum type B neurotoxin in rat brain synaptosomes. *Jornal of Biological Chemistry*, 269(14), 10498–10503.
- Niswender, C. M., & Conn, P. J. (2010). Metabotropic glutamate receptors: physiology, pharmacology, and disease. *Annual review of pharmacology and toxicology*, 50, 295–322.
- Noguchi, J., Matsuzaki, M., Ellis-Davies, G. C., & Kasai, H. (2005). Spine-neck geometry determines NMDA receptor-dependent Ca<sup>2+</sup> signaling in dendrites. *Neuron*, 46(4), 609–622.
- Novick, P., & Zerial, M. (1997). The diversity of Rab proteins in vesicle transport. *Current Opinion in Cell Biology*, 9(4), 496–504.
- Novick, P., Field, C., & Schekman, R. (1980). Identification of 23 complementation groups required for post-translational events in the yeast secretory pathway. *Cell*, 21(1), 205–215.
- Oh, W. C., Hill, T. C., & Zito, K. (2013). Synapse-specific and size-dependent mechanisms of spine structural plasticity accompanying synaptic weakening. *Proceedings of the National Academy of Sciences of the United States of America*, 110(4), E305–E312.

- Ohshima, T., Ogura, H., Tomizawa, K., Hayashi, K., Suzuki, H., Saito, T., ... Mikoshiba, K. (2005). Impairment of hippocampal long-term depression and defective spatial learning and memory in p35<sup>-/-</sup> mice. *Journal of Neurochemistry*, 94(4), 917–925.
- Ohya, T., Miaczynska, M., Coskun, Ü., Lommer, B., Runge, A., Drechsel, D., ... Zerial, M. (2009). Reconstitution of Rab- and SNARE-dependent membrane fusion by synthetic endosomes. *Nature*, 459(7250), 1091–1097.
- Opazo, P., Labrecque, S., Tigaret, C. M., Frouin, A., Wiseman, P. W., De Koninck, P., & Choquet, D. (2010). CaMKII Triggers the Diffusional Trapping of Surface AMPARs through Phosphorylation of Stargazin. *Neuron*, 67(2), 239–252.
- Palmer, C. L., Lim, W., Hastie, P. G., Toward, M., Korolchuk, V. I., Burbidge, S. A., Banting, G., Collingridge, G. L., Isaac, J. T., & Henley, J. M. (2005). Hippocalcin functions as a calcium sensor in hippocampal LTD. *Neuron*, 47(4), 487–494.
- Park, M., Salgado, J. M., Ostroff, L., Helton, T. D., Robinson, C. G., Harris, K. M., & Ehlers, M. D. (2006). Plasticity-induced growth of dendritic spines by exocytic trafficking from recycling endosomes. *Neuron*, 52(5), 817–830.
- Parlati, F., McNew, J. A., Fukuda, R., Miller, R., Söllner, T. H., & Rothman, J. E. (2000). Topological restriction of SNARE-dependent membrane fusion. *Nature*, 407(6801), 194–198.
- Parlati, F., Varlamov, O., Paz, K., McNew, J. A., Hurtado, D., Sollner, T. H., & Rothman, J. E. (2002). Distinct SNARE complexes mediating membrane fusion in Golgi transport based on combinatorial specificity. *Proceedings of the National Academy of Sciences*, 99(8), 5424–5429.
- Patterson, M. A., Szatmari, E. M., & Yasuda, R. (2010). AMPA receptors are exocytosed in stimulated spines and adjacent dendrites in a Ras-ERK-dependent manner during long-term potentiation. *Proceedings of the National Academy of Sciences of the United States of America*, 107(36), 15951–15956.
- Peineau, S., Nicolas, C. S., Bortolotto, Z. A., Bhat, R. V., Ryves, W. J., Harwood, A. J., Dournaud, P., Fitzjohn, S. M., & Collingridge, G. L. (2009). A systematic investigation of the protein kinases involved in NMDA receptor-dependent LTD: evidence for a role of GSK-3 but not other serine/threonine kinases. *Molecular brain*, 2, 22.

- Peineau, S., Taghibiglou, C., Bradley, C., Wong, T. P., Liu, L., Lu, J., ... Collingridge, G. L. (2007). LTP Inhibits LTD in the Hippocampus via Regulation of GSK3 $\beta$ . *Neuron*, 53(5), 703–717.
- Penn, A. C., Zhang, C. L., Georges, F., Royer, L., Breillat, C., Hosy, E., ... Choquet, D. (2017). Hippocampal LTP and contextual learning require surface diffusion of AMPA receptors. *Nature*, 549(7672), 384–388.
- Perdigão, C., Barata, M. A., Araújo, M. N., Mirfakhar, F. S., Castanheira, J., & Guimas Almeida, C. (2020). Intracellular Trafficking Mechanisms of Synaptic Dysfunction in Alzheimer's Disease. *Frontiers in cellular neuroscience*, 14, 72.
- Pereda A. E. (2014). Electrical synapses and their functional interactions with chemical synapses. *Nature reviews. Neuroscience*, 15(4), 250–263.
- Pereira-Leal, J. B., & Seabra, M. C. (2001). Evolution of the rab family of small GTP-binding proteins. *Journal of Molecular Biology*, 313(4), 889–901.
- Perera, H. K., Clarke, M., Morris, N. J., Hong, W., Chamberlain, L. H., & Gould, G. W. (2003). Syntaxin 6 regulates Glut4 trafficking in 3T3-L1 adipocytes. *Molecular biology of the cell*, 14(7), 2946–2958.
- Perez, J. L., Khatri, L., Chang, C., Srivastava, S., Osten, P., & Ziff, E. B. (2001). PICK1 Targets Activated Protein Kinase  $\alpha$  to AMPA Receptor Clusters in Spines of Hippocampal Neurons and Reduces Surface Levels of the AMPA-Type Glutamate Receptor Subunit 2. *The Journal of Neuroscience*, 21(15), 5417–5428.
- Petrantonakis, P. C., & Poirazi, P. (2014). A compressed sensing perspective of hippocampal function. *Frontiers in systems neuroscience*, 8, 141.
- Petrini, E. M., Lu, J., Cognet, L., Lounis, B., Ehlers, M. D., & Choquet, D. (2009). Endocytic trafficking and recycling maintain a pool of mobile surface AMPA receptors required for synaptic potentiation. *Neuron*, 63(1), 92–105.
- Pfeffer, S. R. (2005). Structural Clues to Rab GTPase Functional Diversity. *Journal of Biological Chemistry*, 280(16), 15485–15488.
- Pylypenko, O., Hammich, H., Yu, I. M., & Houdusse, A. (2018). Rab GTPases and their interacting protein partners: Structural insights into Rab functional diversity. *Small GTPases*, 9(1-2), 22–48.

- Raingo, J., Khvotchev, M., Liu, P., Darios, F., Li, Y. C., Ramirez, D. M., Adachi, M., Lemieux, P., Toth, K., Davletov, B., & Kavalali, E. T. (2012). VAMP4 directs synaptic vesicles to a pool that selectively maintains asynchronous neurotransmission. *Nature neuroscience*, 15(5), 738–745.
- Raingo, J., Khvotchev, M., Liu, P., Darios, F., Li, Y. C., Ramirez, D. M., Adachi, M., Lemieux, P., Toth, K., Davletov, B., & Kavalali, E. T. (2012). VAMP4 directs synaptic vesicles to a pool that selectively maintains asynchronous neurotransmission. *Nature neuroscience*, 15(5), 738–745.
- Ramirez, D. M., Khvotchev, M., Trauterman, B., & Kavalali, E. T. (2012). Vti1a identifies a vesicle pool that preferentially recycles at rest and maintains spontaneous neurotransmission. *Neuron*, 73(1), 121–134.
- Rebola, N., Reva, M., Kirizs, T., Szoboszlai, M., Lőrincz, A., Moneron, G., ... DiGregorio, D. A. (2019). Distinct Nanoscale Calcium Channel and Synaptic Vesicle Topographies Contribute to the Diversity of Synaptic Function. *Neuron*. 104(4), 693-710.
- Reiner, A., & Levitz, J. (2018). Glutamatergic Signaling in the Central Nervous System: Ionotropic and Metabotropic Receptors in Concert. *Neuron*, 98(6), 1080–1098.
- Rossetto, O., Schiavo, G., Montecucco, C., Poulain, B., Deloye, F., Lozzi, L., & Shone, C. C. (1994). SNARE motif and neurotoxins. *Nature*, 372(6505), 415–416.
- Rost, B. R., Schneider, F., Grauel, M. K., Wozny, C., Bentz, C., Blessing, A., Rosenmund, T., Jentsch, T. J., Schmitz, D., Hegemann, P., & Rosenmund, C. (2015). Optogenetic acidification of synaptic vesicles and lysosomes. *Nature neuroscience*, 18(12), 1845–1852.
- Roth, R. H., Cudmore, R. H., Tan, H. L., Hong, I., Zhang, Y., & Huganir, R. L. (2019). Cortical Synaptic AMPA Receptor Plasticity during Motor Learning. *Neuron*.
- Royo, M., Gutiérrez, Y., Fernández-Monreal, M., Gutiérrez-Eisman, S., Jiménez, R., Jurado, S., & Esteban, J. A. (2019). A retention-release mechanism based on Rab11-FIP2 for AMPA receptor synaptic delivery during long-term potentiation. *Journal of Cell Science*, 132(24) : jcs234237.
- Rozov, A., Bolshakov, A. P., & Valiullina-Rakhmatullina, F. (2019). The Ever-Growing Puzzle of Asynchronous Release. *Frontiers in cellular neuroscience*, 13, 28.

- Rummel, A., Häfner, K., Mahrhold, S., Darashchonak, N., Holt, M., Jahn, R., ... Binz, T. (2009). Botulinum neurotoxins C, E and F bind gangliosides via a conserved binding site prior to stimulation-dependent uptake with botulinum neurotoxin F utilising the three isoforms of SV2 as second receptor. *Journal of Neurochemistry*, 110(6), 1942–1954.
- Rummel, A., Karnath, T., Henke, T., Bigalke, H., & Binz, T. (2004). Synaptotagmins I and II Act as Nerve Cell Receptors for Botulinum Neurotoxin G. *Journal of Biological Chemistry*, 279(29), 30865–30870.
- Salminen, A., & Novick, P. J. (1987). A ras-like protein is required for a post-Golgi event in yeast secretion. *Cell*, 49(4), 527–538.
- Sampo, B., Kaech, S., Kunz, S., & Banker, G. (2003). Two Distinct Mechanisms Target Membrane Proteins to the Axonal Surface. *Neuron*, 37(4), 611–624.
- Sanhueza, M., Fernandez-Villalobos, G., Stein, I. S., Kasumova, G., Zhang, P., Bayer, K. U., Otmakhov, N., Hell, J. W., & Lisman, J. (2011). Role of the CaMKII/NMDA receptor complex in the maintenance of synaptic strength. *The Journal of neuroscience: the official journal of the Society for Neuroscience*, 31(25), 9170–9178.
- Scales, S. J., Chen, Y. A., Yoo, B. Y., Patel, S. M., Doung, Y.-C., & Scheller, R. H. (2000). SNAREs Contribute to the Specificity of Membrane Fusion. *Neuron*, 26(2), 457–464.
- Schiavo, G. G., Benfenati, F., Poulain, B., Rossetto, O., de Laureto, P. P., DasGupta, B. R., & Montecucco, C. (1992). Tetanus and botulinum-B neurotoxins block neurotransmitter release by proteolytic cleavage of synaptobrevin. *Nature*, 359(6398), 832–835.
- Schiavo, G., Matteoli, M., & Montecucco, C. (2000). Neurotoxins Affecting Neuroexocytosis. *Physiological Reviews*, 80(2), 717–766.
- Schiavo, G., Rossetto, O., Santucci, A., DasGupta, B.R., Montecucco, C. (1992). Botulinum neurotoxins are zinc proteins. *The Journal of Biological Chemistry*, 267(33), 23479-83.
- Schmidt, M. R., & Haucke, V. (2007). Recycling endosomes in neuronal membrane traffic. *Biology of the Cell*, 99(6), 333–342.
- Schoch S., Deák F., Königstorfer A., Mozhayeva M., Sara Y., Südhof T.C., Kavalali E.T. (2001). SNARE Function Analyzed in Synaptobrevin/VAMP Knockout Mice. *Science*, 294(5544), 1117–1122.

Schoch, S. (2001). SNARE Function Analyzed in Synaptobrevin/VAMP Knockout Mice. *Science*, 294(5544), 1117–1122.

Scott A. B. (1981). Botulinum toxin injection of eye muscles to correct strabismus. *Transactions of the American Ophthalmological Society*, 79, 734–770.

Sherman S. M. (2014). The function of metabotropic glutamate receptors in thalamus and cortex. *The Neuroscientist: a review journal bringing neurobiology, neurology and psychiatry*, 20(2), 136–149.

Shi, L., Shen, Q. T., Kiel, A., Wang, J., Wang, H. W., Melia, T. J., Rothman, J. E., & Pincet, F. (2012). SNARE proteins: one to fuse and three to keep the nascent fusion pore open. *Science (New York, N.Y.)*, 335(6074), 1355–1359.

Shitara, A., Shibui, T., Okayama, M., Arakawa, T., Mizoguchi, I., Sakakura, Y., & Takuma, T. (2017). VAMP4 and its cognate SNAREs are required for maintaining the ribbon structure of the Golgi apparatus. *Journal of Oral Biosciences*, 59(4), 192–196.

Shitara, A., Shibui, T., Okayama, M., Arakawa, T., Mizoguchi, I., Sakakura, Y., & Takuma, T. (2013). VAMP4 is required to maintain the ribbon structure of the Golgi apparatus. *Molecular and cellular biochemistry*, 380(1-2), 11–21.

Shu, T., Jin, H., Rothman, J. E., & Zhang, Y. (2019). Munc13-1 MUN domain and Munc18-1 cooperatively chaperone SNARE assembly through a tetrameric complex. *Proceedings of the National Academy of Sciences*, 201914361.

Singh B.R., Kumar R., Cai S. (2014) Molecular Mechanism and Effects of Clostridial Neurotoxins. In: Kostrzewa R. (eds) *Handbook of Neurotoxicity*. Springer, New York, NY

Sinha, R., Ahmed, S., Jahn, R., & Klingauf, J. (2011). Two synaptobrevin molecules are sufficient for vesicle fusion in central nervous system synapses. *Proceedings of the National Academy of Sciences of the United States of America*, 108(34), 14318–14323.

Small, S. A., Simoes-Spassov, S., Mayeux, R., & Petsko, G. A. (2017). Endosomal Traffic Jams Represent a Pathogenic Hub and Therapeutic Target in Alzheimer's Disease. *Trends in neurosciences*, 40(10), 592–602.

Söllner, T., Bennett, M. K., Whiteheart, S. W., Scheller, R. H., & Rothman, J. E. (1993). A protein assembly-disassembly pathway in vitro that may correspond to sequential steps of synaptic vesicle docking, activation, and fusion. *Cell*, 75(3), 409–418.

- Sönnichsen, B., De Renzis, S., Nielsen, E., Rietdorf, J., & Zerial, M. (2000). Distinct membrane domains on endosomes in the recycling pathway visualized by multicolor imaging of Rab4, Rab5, and Rab11. *The Journal of cell biology*, 149(4), 901–914.
- Stanton, P. K., Winterer, J., Bailey, C. P., Kyrozis, A., Raginov, I., Laube, G., ... Müller, W. (2003). Long-Term Depression of Presynaptic Release from the Readily Releasable Vesicle Pool Induced by NMDA Receptor-Dependent Retrograde Nitric Oxide. *The Journal of Neuroscience*, 23(13), 5936–5944.
- Star, E. N., Kwiatkowski, D. J., & Murthy, V. N. (2002). Rapid turnover of actin in dendritic spines and its regulation by activity. *Nature Neuroscience*, 5(3), 239–246.
- Stegmaier, M., Klumperman, J., Foletti, D. L., Yoo, J. S., & Scheller, R. H. (1999). Vesicle-associated membrane protein 4 is implicated in trans-Golgi network vesicle trafficking. *Molecular biology of the cell*, 10(6), 1957–1972.
- Stein, A., Weber, G., Wahl, M. C., & Jahn, R. (2009). Helical extension of the neuronal SNARE complex into the membrane. *Nature*, 460(7254), 525–528.
- Stenmark, H. (2009). Rab GTPases as coordinators of vesicle traffic. *Nature Reviews Molecular Cell Biology*, 10(8), 513–525.
- Südhof T. C. (2012). Calcium control of neurotransmitter release. *Cold Spring Harbor perspectives in biology*, 4(1), a011353.
- Suh, Y. H., Terashima, A., Petralia, R. S., Wenthold, R. J., Isaac, J. T. R., Roche, K. W., & Roche, P. A. (2010). A neuronal role for SNAP-23 in postsynaptic glutamate receptor trafficking. *Nature Neuroscience*, 13(3), 338–343.
- Sun, J., & Roy, S. (2018). The physical approximation of APP and BACE-1: A key event in Alzheimer's disease pathogenesis. *Developmental neurobiology*, 78(3), 340–347.
- Sutton, R. B., Fasshauer, D., Jahn, R., & Brunger, A. T. (1998). Crystal structure of a SNARE complex involved in synaptic exocytosis at 2.4 Å resolution. *Nature*, 395(6700), 347–353.
- Tanaka, H., & Hirano, T. (2012). Visualization of subunit-specific delivery of glutamate receptors to postsynaptic membrane during hippocampal long-term potentiation. *Cell reports*, 1(4), 291–298.

- Tanaka, J., Horiike, Y., Matsuzaki, M., Miyazaki, T., Ellis-Davies, G. C., & Kasai, H. (2008). Protein synthesis and neurotrophin-dependent structural plasticity of single dendritic spines. *Science (New York, N.Y.)*, 319(5870), 1683–1687.
- Tansey, E.M. Chemical neurotransmission in the autonomic nervous system: Sir Henry Dale and acetylcholine. *Clinical Autonomic Research* 1, 63–72 (1991).
- Teng, F. Y., Wang, Y., & Tang, B. L. (2001). The syntaxins. *Genome biology*, 2(11), REVIEWS3012.
- Tisdale, E. J., Bourne, J. R., Khosravi-Far, R., Der, C. J., & Balch, W. E. (1992). GTP-binding mutants of rab1 and rab2 are potent inhibitors of vesicular transport from the endoplasmic reticulum to the Golgi complex. *The Journal of cell biology*, 119(4), 749–761.
- Todman D. (2008). Henry Dale and the discovery of chemical synaptic transmission. *European neurology*, 60(3), 162–164.
- Tran, T. H. T., Zeng, Q., & Hong, W. (2007). VAMP4 cycles from the cell surface to the trans-Golgi network via sorting and recycling endosomes. *Journal of Cell Science*, 120(6), 1028–1041.
- Traynelis, S. F., Wollmuth, L. P., McBain, C. J., Menniti, F. S., Vance, K. M., Ogden, K. K., ... Dingledine, R. (2010). Glutamate Receptor Ion Channels: Structure, Regulation, and Function. *Pharmacological Reviews*, 62(3), 405–496.
- Trimble, W. S., Cowan, D. M., & Scheller, R. H. (1988). VAMP-1: a synaptic vesicle-associated integral membrane protein. *Proceedings of the National Academy of Sciences*, 85(12), 4538–4542.
- Turton, K., Chaddock, J. A., & Acharya, K. R. (2002). Botulinum and tetanus neurotoxins: structure, function and therapeutic utility. *Trends in Biochemical Sciences*, 27(11), 552–558.
- Ullrich O., Stenmark H., Alexandrov K., Huber L.A., Kaibuchi K., Sasaki T., Takai Y., Zerial M. (1993). Rab GDP dissociation inhibitor as a general regulator for the membrane association of rab proteins. *The journal of biological chemistry*, 268(24), 18143-50.
- Ullrich, O., Reinsch, S., Urbé, S., Zerial, M., & Parton, R. G. (1996). Rab11 regulates recycling through the pericentriolar recycling endosome. *The Journal of cell biology*, 135(4), 913–924.

- Ungar, D., & Hughson, F. M. (2003). SNARE Protein Structure and Function. *Annual Review of Cell and Developmental Biology*, 19(1), 493–517.
- Van der Sluijs, P., Hull, M., Webster, P., Mâle, P., Goud, B., & Mellman, I. (1992). The small GTP-binding protein rab4 controls an early sorting event on the endocytic pathway. *Cell*, 70(5), 729–740.
- Van Harreveld, A., & Fifkova, E. (1975). Swelling of dendritic spines in the fascia dentata after stimulation of the perforant fibers as a mechanism of post-tetanic potentiation. *Experimental Neurology*, 49(3), 736–749.
- Veca, A., & Dreisbach, J. H. (1988). Classical neurotransmitters and their significance within the nervous system. *Journal of Chemical Education*, 65(2), 108.
- Verdú, M. P. M., Portalés, A., SanJuan, M. P., & Jurado, S. (2018). Postsynaptic SNARE proteins: Role in synaptic transmission and plasticity. *Neuroscience*.
- Verhage, M., Maia A.S., Plomp J.J., Brussaard A.B., Heeroma J.H., Vermeer H., Toonen R.F., Hammer R.E., van den Berg T.K., Missler M. et al. (2000). Synaptic Assembly of the Brain in the Absence of Neurotransmitter Secretion. *Science*, 287(5454), 864–869.
- Vilinsky, I., Stewart, B. A., Drummond, J., Robinson, I., & Deitcher, D. L. (2002). A *Drosophila* SNAP-25 null mutant reveals context-dependent redundancy with SNAP-24 in neurotransmission. *Genetics*, 162(1), 259–271.
- Wandinger-Ness, A., & Zerial, M. (2014). Rab proteins and the compartmentalization of the endosomal system. *Cold Spring Harbor perspectives in biology*, 6(11), a022616.
- Wang, C.-C., Ng, C. P., Lu, L., Atlashkin, V., Zhang, W., Seet, L.-F., & Hong, W. (2004). A Role of VAMP8/Endobrevin in Regulated Exocytosis of Pancreatic Acinar Cells. *Developmental Cell*, 7(3), 359–371.
- Wang, S., Li, Y., Gong, J., Ye, S., Yang, X., Zhang, R., & Ma, C. (2019). Munc18 and Munc13 serve as a functional template to orchestrate neuronal SNARE complex assembly. *Nature Communications*, 10(1).
- Wang, T., Li, L., & Hong, W. (2017). SNARE proteins in membrane trafficking. *Traffic*, 18(12), 767–775.

- Wang, Z., Edwards, J. G., Riley, N., Provance, D. W., Jr, Karcher, R., Li, X. D., Davison, I. G., Ikebe, M., Mercer, J. A., Kauer, J. A., & Ehlers, M. D. (2008). Myosin Vb mobilizes recycling endosomes and AMPA receptors for postsynaptic plasticity. *Cell*, 135(3), 535–548.
- Weimbs, T., Low, S. H., Chapin, S. J., Mostov, K. E., Bucher, P., & Hofmann, K. (1997). A conserved domain is present in different families of vesicular fusion proteins: a new superfamily. *Proceedings of the National Academy of Sciences of the United States of America*, 94(7), 3046–3051.
- Wilcke, M., Johannes, L., Galli, T., Mayau, V., Goud, B., & Salamero, J. (2000). Rab11 regulates the compartmentalization of early endosomes required for efficient transport from early endosomes to the trans-golgi network. *The Journal of cell biology*, 151(6), 1207–1220.
- Wilson, A. L., Erdman, R. A., & Maltese, W. A. (1996). Association of Rab1B with GDP-dissociation Inhibitor (GDI) Is Required for Recycling but Not Initial Membrane Targeting of the Rab Protein. *Journal of Biological Chemistry*, 271(18), 10932–10940.
- Wilson, T. (2010). *Spinning-Disk Microscopy Systems*. *Cold Spring Harbor Protocols*, 2010(11), pdb.top88–pdb.top88.
- Wurmser, A. E., Sato, T. K., & Emr, S. D. (2000). New component of the vacuolar class C-Vps complex couples nucleotide exchange on the Ypt7 GTPase to SNARE-dependent docking and fusion. *The Journal of cell biology*, 151(3), 551–562.
- Xu, T., Yu, X., Perlik, A. J., Tobin, W. F., Zweig, J. A., Tennant, K., Jones, T., & Zuo, Y. (2009). Rapid formation and selective stabilization of synapses for enduring motor memories. *Nature*, 462(7275), 915–919.
- Xue, M., & Zhang, B. (2002). Do SNARE proteins confer specificity for vesicle fusion?. *Proceedings of the National Academy of Sciences of the United States of America*, 99(21), 13359–13361.
- Xue, M., Craig, T. K., Xu, J., Chao, H. T., Rizo, J., & Rosenmund, C. (2010). Binding of the complexin N terminus to the SNARE complex potentiates synaptic-vesicle fusogenicity. *Nature structural & molecular biology*, 17(5), 568–575.
- Yang, B., Gonzalez, L., Prekeris, R., Steegmaier, M., Advani, R. J., & Scheller, R. H. (1999). SNARE Interactions Are Not Selective. *Journal of Biological Chemistry*, 274(9), 5649–5653.

- Yang, B., Gonzalez, L., Prekeris, R., Steegmaier, M., Advani, R. J., & Scheller, R. H. (1999). SNARE Interactions Are Not Selective. *Journal of Biological Chemistry*, 274(9), 5649–5653.
- Yang, G., Pan, F., & Gan, W. B. (2009). Stably maintained dendritic spines are associated with lifelong memories. *Nature*, 462(7275), 920–924.
- Yang, Y., Wang, X. B., Frerking, M., & Zhou, Q. (2008). Delivery of AMPA receptors to perisynaptic sites precedes the full expression of long-term potentiation. *Proceedings of the National Academy of Sciences of the United States of America*, 105(32), 11388–11393.
- Yap, C. C., & Winckler, B. (2012). Harnessing the power of the endosome to regulate neural development. *Neuron*, 74(3), 440–451.
- Yudowski, G. A., Puthenveedu, M. A., Leonoudakis, D., Panicker, S., Thorn, K. S., Beattie, E. C., & von Zastrow, M. (2007). Real-time imaging of discrete exocytic events mediating surface delivery of AMPA receptors. *The Journal of neuroscience: the official journal of the Society for Neuroscience*, 27(41), 11112–11121.
- Zerial, M., & Stenmark, H. (1993). Rab GTPases in vesicular transport. *Current Opinion in Cell Biology*, 5(4), 613–620.
- Zhang, S., Lebreton, F., Mansfield, M. J., Miyashita, S. I., Zhang, J., Schwartzman, J. A., Tao, L., Masuyer, G., Martínez-Carranza, M., Stenmark, P., Gilmore, M. S., Doxey, A. C., & Dong, M. (2018). Identification of a Botulinum Neurotoxin-like Toxin in a Commensal Strain of *Enterococcus faecium*. *Cell host & microbe*, 23(2), 169–176.e6.
- Zhang, S., Masuyer, G., Zhang, J., Shen, Y., Lundin, D., Henriksson, L., ... Stenmark, P. (2017). Identification and characterization of a novel botulinum neurotoxin. *Nature Communications*, 8, 14130.
- Zhao, W. D., Hamid, E., Shin, W., Wen, P. J., Krystofiak, E. S., Villarreal, S. A., Chiang, H. C., Kachar, B., & Wu, L. G. (2016). Hemi-fused structure mediates and controls fusion and fission in live cells. *Nature*, 534(7608), 548–552.
- Zheng, N., Jeyifous, O., Munro, C., Montgomery, J. M., & Green, W. N. (2015). Synaptic activity regulates AMPA receptor trafficking through different recycling pathways. *eLife*, 4, e06878.
- Zhu, Y., Pak, D., Qin, Y., McCormack, S. G., Kim, M. J., Baumgart, J. P., ... Zhu, J. J. (2005). Rap2-JNK Removes Synaptic AMPA Receptors during Depotentiation. *Neuron*, 47(2), 321.

Zornetta, I., Azarnia Tehran, D., Arrigoni, G., Anniballi, F., Bano, L., Leka, O., Zanotti, G., Binz, T., & Montecucco, C. (2016). The first non Clostridial botulinum-like toxin cleaves VAMP within the juxtamembrane domain. *Scientific reports*, 6, 30257.

Zucker, R. S., & Regehr, W. G. (2002). Short-Term Synaptic Plasticity. *Annual Review of Physiology*, 64(1), 355–405.